PB-226 956

INCINERATOR PROCESSES AND EMISSIONS. MIXING STUDIES IN ISOTHERMAL MODELS OF INCINERATOR COMBUSTION CHAMBERS

T. R. S. Rao, et al

Pennsylvania State University
University Park, Pennsylvania

June 1970

DISTRIBUTED BY:

NTIS
National Technical Information Service
U. S. DEPARTMENT OF COMMERCE
5285 Port Royal Road, Springfield Va. 22151

PB 226 956

INCINERATOR PROCESSES AND EMISSIONS

Mixing Studies in Isothermal Models of Incinerator Combustion Chambers

Technical Report FS/PHS 6/70-1

by

T. R. S. Rao and R. H. Essenhigh

June 1970

Prepared for the
Department of Health, Education, and Welfare
Under Contract No. 5R01 AP00397

Reproduced by
NATIONAL TECHNICAL
INFORMATION SERVICE
U S Department of Commerce
Springfield VA 22151

Combustion Laboratory
Fuel Science Section
Department of Materials Science
The Pennsylvania State University
University Park, Pennsylvania 16802

226

PREFACE

This report describes the progress of research on a subprogram which is part of a general program of research on behavior of incinerators, with special reference to incinerator processes and emissions, a project sponsored by the Department of Health, Education, and Welfare (Public Health Service) under Grant No. 5R01 AP00397. This subprogram is concerned with aerodynamic factors in incinerator combustion chambers, and particularly with mixing. The period covered by this progress report is the forty-five months from September 1966, when this subprogram was initiated, to June 1970. This report provided the basis for the doctoral thesis submitted by Satyanarayana T. R. Rao at The Pennsylvania State University.

ACKNOWLEDGMENTS

The author wishes to thank Professor Robert H. Essenhigh, thesis adviser, for the initial presentation of the thesis problem and his guidance and support. Mr. E. Dale Simpson, Mr. Robert A. Frank, and Mr. Carl J. Martin have helped to a large extent in building the equipment. The author also wishes to thank Dr. Gideon Gelernter, Mr. James P. Stumbar, and fellow graduate students for their help.

The author thanks the Department of Health, Education, and Welfare for providing a half-time graduate assistantship during the period covering this thesis study.

TABLE OF CONTENTS

Page

ACKNOWLEDGMENTS ii

LIST OF TABLES vii

LIST OF FIGURES viii

1. INTRODUCTION 1

2. BACKGROUND 6

  2.1. Similarity and Modelling 6

    2.1.1. Categories of Similarity 7

    2.1.2. Methods of Establishing Similarity . . 9

    2.1.3. Complete and Partial Similarity 11

    2.1.4. Similarity Rules That Can Be Neglected in the Modelling of Flows in Combustion Chambers 12

    2.1.5. The Regime Concept 13

    2.1.6. General Use of the Models and the Principles of Isothermal Modelling of the Flow Patterns in Combustion Chambers 15

    2.1.7. Further Experimental Details 16

  2.2. Mixing Studies Related to Furnaces 18

    2.2.1. Isothermal Free Jets 19

    2.2.2. Nonisothermal Free Jets 24

    2.2.3. Enclosed Jets and Recirculation Phenomena 26

    2.2.4. Swirled Jets 31

    2.2.5. Stirred Reactor Approaches to Mixing Problems in Combustion Chambers 34

Page

2.2.6. Residence Time Distribution (R.T.D.) 37

2.2.7. Summary of Mixing Studies in Furnaces 39

2.3. Incinerators 40

2.4. Relation of the Above Summary to This Thesis Study 43

3. STATEMENT OF THE PROBLEM 45

4. EXPERIMENTAL 47

4.1. General Considerations of Approach 47

4.2. Basis of Method 48

4.3. Equipment 50

4.3.1. Incinerator Model 50

4.3.2. Furnace Simulation Model - Fig. 3 . . . 56

4.3.3. Gas Sampling System - Fig. 5 61

4.3.4. Tracer Gas Supply System - Fig. 6 . . . 68

4.3.5. Carrier Gas (Air) Supply System 70

4.3.6. Ancillary Equipment 72

4.4. Procedure 75

5. THEORY 82

5.1. Physical Model 82

5.2. Mathematical Model 85

6. RESULTS 92

6.1. General Behavior 92

6.1.1. Instrument Effect on the General Behavior 95

6.1.2. Transit Time Determination and Allowance for Its Effects 100

Page

6.2. Summary of the Behavior of Opposed Vortex Flow 102

6.2.1. Exit Sampling with Variation of the Offset Angle 103

6.2.2. Internal Sampling 105

6.2.3. Stirring Factor Variation with Offset Angle 108

6.2.4. Variation of Stirring Factor with Jet Array Spacing 110

6.2.5. Variation of Stirring Factor with Momentum Ratio 113

6.2.6. Other Results 117

6.3. Mixing Behavior of Straight and Swirling Jets 119

6.3.1. General Behavior with Straight and Swirled Jets 122

6.3.2. Variation of Combined Plug Flow Time with Distance 123

6.3.3. Stirring Factors at High Swirl 129

6.3.4. Behavior at Zero Swirl 133

6.3.5. Effect of Increasing Swirl 135

6.3.6. Backmix Experiments 136

6.4. Tracer Jet Dissipation and Turbulence Effects 140

6.5. Error Analysis 141

7. DISCUSSION, CONCLUSIONS, AND SUGGESTIONS FOR FUTURE WORK 145

7.1. Incinerator Model Results 145

7.2. Application of the Incinerator Model Results 146

7.3. Swirling and Straight Jets 147

Page

7.4. Suggestions for Future Work 152

NOMENCLATURE 153

REFERENCES 154

APPENDIX A. Derivation of the Equation for the Correction of the Instrument Effect 159

APPENDIX B. Data for the Incinerator-Model Tests 167

APPENDIX C. Data for Tests on the Straight, Tangential Entry and Vane-Swirled Jets 196

LIST OF TABLES

Table Page

1. Raw and Corrected Data for a Straight Jet 98

2. Variation of Stirring Factor with Momentum Ratio at an Offset Angle, 20° 116

LIST OF FIGURES

Figure Page

1. Schematic Layout of the Equipment for the Study of Mixing Effectiveness in the Incinerator and the Furnace Models 52

2. A Half-Scale Box Built to Model the Incinerator in the Subprogramme (9) 54

3. The Furnace Simulation Model with Arrangement for Fitting Various Jets at the Inlet 57

4. Sketches of Straight, Tangential Entry and Vane-Swirled Burners 59

5. Schematic Layout of the Tracer Supply System 62

6. Layout of the Gas Sampling System 69

7. Layout of the Electronic Equipment 74

8. Schematic Representation of the Bragg's Idealized Approximation to the Desired Flow Pattern in a Combustion Chamber 83

9. Schematic Representation of the Modified Bragg Model 84

10. Typical Experimental Curve for the Decay of the Tracer with Time after Helium is Cut-Off at the Injection Point 94

11. Variation of the Uncorrected and the Corrected Concentrations with Three Instrument Factors for a Straight Jet (4 in. dia.) Flowing into the Box at Re = 41250 97

12. Tracer Cut-Off Experiment on the Analyzer to Determine the Instrument Factor, τ_i, and the Transit Time in the Capillary Tube 101

13. Tracer Concentration Decay in the Exit Stream of the Air Model as a Function of Time Plotted for Various Offset Angles 104

14. Variation of the Combined Plug Flow Time with Distance from the Inlet 107

Figure Page

15. Variation of Various Time Ratios with the Offset Angles for the Opposed Vortex Flow 109

16. Variation of the Stirring Factor with the Offset Angle of the Jets 111

17. Variation of Various Time Ratios with Spacing Between the Jet Arrays 112

18. Variation of the Stirring Factor with the Spacing . . . 114

19. Variation of the Combined Plug Flow Time with Distance at a Spacing of 26 Inches 115

20. Helium Concentrations (Output) Reached at Three Inches from the Inlet Due to the Injection of Equal Helium Flows at Various Distances from the Inlet 121

21. Variation of the Combined Plug Flow Time with Distance from the Inlet for Two Levels of Secondary Vane Angles 124

22. Variation of the Combined Plug Flow Time with Distance from the Inlet for the Tangential Entry Jet 126

23. Variation of the Combined Plug Flow Time with Distance from the Inlet for a Straight Jet (4 in. dia.) 128

24. Variation of Various Residence Times with Reynolds Number for the Vane Swirled Jet 131

25. Variation of Various Time Ratios with Reynolds Number for the Vane Swirled Jet 132

26. Variation of the Amount of Backmix with the Distance of the Tracer Injection Point from the Inlet for Tangential Entry Jet at Three Levels of Swirl 138

27. Variation of the Amount of Backmix with the Stirring Factor 139

28. Variation of the Steady State Concentration of Helium Across the Box at a Distance of Two Inches from the Inlet 143

29. Variation of the Instrument Factor with the Instrument (Bridge) Current at a Fixed Flow Rate 164

Figure Page

30. Variation of Instrument (Gow-Mac Analyzer) Output with Helium Concentration in the Sample Gases 165

1. INTRODUCTION

An incinerator is a steel or a refractory chamber whose purpose is to destroy domestic and industrial wastes by burning. → p 6 In incinerators, mixing occurs in the overbed combustion space, between overfire or secondary air and smoke plus gasification products generated by incomplete combustion or gasification of the solid fuel bed. The primary purpose of the overfire air is, of course, to burn up the smoke and gasification products, and there is here, first, a problem of mixing and, second, a problem of flame holding. If mixing is poor, the air and combustible gases can be striated with the result that, as discussed by Essenhigh (1), the flame may approximate to a diffusion flame, with some regions so air rich there is no combustion, other flaming regions where mixing is adequate, but other regions can be again hot but fuel rich so that cracking and smoke formation will occur. Even good mixing, however, will not necessarily guarantee combustion of smoke and gases, since this by itself is no adequate guarantee for ignition and flame holding. If the flame is not held, there is no combustion at all and the unit emits smoke and this results in undesirable air pollution.

Satisfactory flame holding combined with adequate mixing should therefore guarantee smoke-free combustion, and if the temperatures are maintained above an appropriate level this should also destroy odor. For example, a flame can be held if the gas and flame speeds match and this principle of matching of speeds holds good in premixed bunsen type flames; however this does not hold good for large industrial flames because of two reasons. One is, even if the firing method uses premixed gases, the firing velocities in industrial operations are much larger than the maximum flame velocity for the gas mixture. On the other hand if the firing is such that it produces a diffusion flame, the concept of velocity balancing does not exist because flame speed is undefined for a diffusion flame. A flame can also be held by using a mechanical flame holder such as a rod, grille, plate, etc. However, mechanical flame holders are unsatisfactory because they are subjected to high temperatures and thus will disintegrate. Therefore attention has been given to the development of an aerodynamic flame holder as described in this thesis. The principles on which an effective aerodynamic flame holder can be created in combustion chambers were stated by Bragg (2) about 17 years ago in jet-engine studies, and these led to what is known as the Bragg criterion or the Bragg model. According to this the first section of a combustion chamber should be one in which the gases are stirred in such a way that substantial backmixing should take place; and this section should be followed by a region where the gases revert to plug-flow. Ignition and flame holding occur in the stirred section which then acts as a flame holder; and burn-out is optimized in the plug flow region. Such a system obviously solves both mixing and the flame holding problem simultaneously.

Such a stirred section has been found to be generated by two standard burner designs, which is why they work, and these generate swirl (3,4). However two problems exist. First, it is obvious, in general, that even with reasonably "good" mixing, differences in the degree or quality or effectiveness of mixing must exist. Since experience and existing analyses (5,6) suggest that the effectiveness of mixing affects ignition and flame holding, the first problem is how to quantify the effectiveness of mixing. The second is how to apply these concepts to an incinerator, and how to optimize effectiveness of mixing in incinerators.

To solve the first problem, we introduced the concept of a stirring factor to characterize the degree of stirring in the initial stirred section, following Essenhigh (6); and developed a technique, to measure stirring factors generated by the systems of interest using a modified tracer cut-off technique used by Beer and Lee (3). The basis of the method is measurement of unsteady state concentration of a tracer gas in a carrier gas flowing through an isothermal model of a combustion chamber and will be described in greater detail in Sec. 4.

For solving the second problem, experience suggested that an overfire jet configuration generating a counter-vortex flow above the bed should be adequate. This configuration has been tested by Biswas (7,8) and is found to be effective in stabilizing flames in smoke. The configuration has also been used by Shieh (9) in a test incinerator for combustion tests. Therefore the counter-vortex flow pattern has been used to study and to optimize the effectiveness of mixing (maximum W) in an isothermal model of the test incinerator.

The problem of flame holding and mixing exists in all combustion chambers, such as furnaces, kilns, and even jet engine combustors. To solve these problems many attempts have been made to design burners, and to study the flow patterns and mixing produced by them. Such studies have generated a large amount of significant and useful data on velocity, pressure and concentration profiles. However since the data obtained are mechanistic in nature, they hold good for the particular system in which they were obtained, and it becomes very difficult to compare the effectiveness of different burners. However in a recent paper Essenhigh (6) has shown that useful comparison can be made by studying how closely the various burners generate flows approximating to the Bragg pattern. However, except for the limited studies of Beer and Lee (3) and Drake and Hubbard (4), not many other studies have been reported. Therefore straight and swirling jets, which are largely used in conventional furnaces, have been selected for studies and also for comparison with the opposed-vortex pattern. Another reason for choosing these jets is that these are very simple to manufacture and were to be used to develop and check experimental techniques, because of the simpler flow patterns they create, before moving onto the much more complex opposed vortex burner. Also a large amount of information is available on these jets which can be used for providing any necessary mechanistic interpretation of the flow patterns producing stirring in the stirred sections.

Specifically, investigation of the stirring effect of swirled and unswirled jets has been carried out: (i) to compare the mixing behavior of the opposed vortex burner, proposed for the incinerator, with those of straight and swirling jets; and (ii) to study whether the countervortex system itself was an "optimum" method, or whether some other jet configuration might be more effective. Clearly, a comparative standard was called for, and this provided the incentive to study the effectiveness of mixing (W) created by straight and swirling jets.

The highlights of the results obtained are: (i) the effectiveness of mixing (W) could be optimized in the incinerator model and this optimum mixing was slightly smaller than that of a swirled jet; and (ii) the straight jets do not create an effective stirred section where a stirring factor could be measured; however, half-angles of 6.7° were obtained for different sized straight jets.

In addition to the above results information was generated on the relation between the backmix process and the effectiveness of mixing.

2. BACKGROUND

the report

In this section a summary is presented of: (i) the modelling and similarity principles and their application to the modelling of combustion chambers; and (ii) the mixing studies whose results can explain the mixing behavior of jets in furnaces and incinerators. No attempt has been made to give the history of development of the two areas, but the stress has been to emphasize the underlying physical phenomena and principles.

2.1. Similarity and Modelling

Solution of problems of applied science and engineering requires understanding of the physical and chemical processes involved so that formulation of a theory or sets of theories describing these processes is possible. One means of formulating the theories can be by induction and elimination, which leads to the prediction of the phenomena accurately. The theories are usually checked against experiments carried out in a well-designed, fully determined system. Processes to which rigorous theory can be applied are, however, still generally very simple and cannot always provide the quantitative knowledge required for design and development.

Another approach that is possible is direct experimentation on full scale systems; however, this has its own disadvantages. Usually experimentation on the full scale system is expensive and time consuming. The choice and range of variables is very limited and the results obtained are valid strictly for the experimental system investigated and thus cannot be generalized.

A compromise between the theoretical approach, on the one hand, and experiment on the full scale system on the other hand, can be, and has been achieved by model studies. These tools of analysis are comparatively inexpensive and provide useful and yet general information in the quickest possible time.

The term modelling can be used to cover experimental techniques which are aimed at simulating certain aspects of the full scale or prototype-process. These are not just limited to geometrically similar small scale systems, but also include anologues in which physical and chemical processes could be different from those in the prototype.

The success of modelling depends mainly on the similarity between the process investigated in the model and the prototype. There are various similarities that are used widely; for our purposes a brief summary pertinent to combustion chamber modelling has been included below. A fuller discussion of various aspects of modelling and similarity can be found in Langhaar (10), and Johnstone and Thring (11).

2.1.1. Categories of Similarity

The various broad categories of similarity that are usually used in modelling of combustion chambers are: (i) geometric similarity, (ii) mechanical similarity, and (iii) thermal similarity.

(i) Geometric similarity is the simplest of model laws. It implies that every linear dimension of the model is scaled to a constant ratio of the corresponding linear dimension of the full scale chamber, the prototype; alternatively, two bodies are geometrically similar when to every point in one body there exists a corresponding point in the other. Sometimes this has to be abandoned for one or more dimensions, which gives rise to distorted models. Distorted modelling becomes necessary in non-isothermal systems or when chemical reaction plays an important role in the process investigated.

(ii) Mechanical similarity comprises static similarity, kinematic similarity and dynamic similarity. Static similarity requires that the model and the prototype system undergo similar elastic or plastic deformation when corresponding stress is applied. This is usually important in studies on structural members and unimportant in combustion studies.

Kinematic similarity is concerned with solid or fluids in motion and it implies that, in the two systems, fluid or solid particles follow geometrically similar paths in corresponding intervals of time, which is the same as saying that the stream line pattern in the prototype and the model are geometrically similar. This means that there is a velocity scale ratio maintained constant between corresponding points of the prototype and the model.

Dynamic similarity requires that the force ratios causing acceleration of the masses in the corresponding systems be maintained constant. It also implies that the systems are kinematically similar (11).

(iii) Thermal similarity has to be followed when modelling flow of heat by conduction, radiation, natural and forced convection where there is bulk movement of matter. For the first three processes, a temperature difference is necessary and the last one depends additionally on the form of motion or flow pattern. Hence, in moving systems thermal similarity necessitates kinematic similarity. Therefore, thermal similarity requires, in addition to kinematic similarity, that the ratio of temperature differences between any two points in the prototype and the corresponding points in the model be maintained constant.

2.1.2. Methods of Establishing Similarity

There are generally two methods of establishing similarity. One is the method of dimensional analysis and the other one is the method of differential equations.

(i) Method of dimensional analysis: This method uses either the Buckingham Pi (Π) theorem or the Rayleigh method to establish dimensionless numbers on which the physical phenomena depend. The selection of the variables requires intuition and experience, otherwise unwanted and meaningless variables can creep in. The method has another drawback in that it is so mechanical that one can set up dimensionless groups with an existing probability that he has lost grasp of the physical phenomena involved. However, the advantage of the method is that when governing differential equations are so complex and cannot be easily written down, then dimensional analysis provides a useful framework for the possible relationships between the various variables governing the phenomena. Another advantage is that it vastly reduces the number of experiments to be performed so that instead of varying all the variables individually, it becomes necessary to vary the Pi groups. One of the examples that can be cited is the well-known relationship between Reynolds number, Prandtl number, Nusselt number in forced convection heat transfer, where, by applying the method of dimensional analysis to the physical variables, one can get:

$$\text{Nusselt number} = f(\text{Reynolds number, Prandtl number})$$

(The method of derivation of these numbers is quite straight forward (11) and is not therefore shown.) The above equation can be written as

$$\Pi_1 = f(\Pi_2, \Pi_3)$$

Then similarity between prototype and model will be established if the various Pi groups are held the same in the prototype and model. This is usually called complete similarity and further discussion is given below, in Sec. 2.1.3.

(ii) Method of differential equations: If the differential equation or equations are known or can be established for the phenomena of interest, then we can derive dimensionless groups out of these equations. The equations will usually be balance equations describing conservation of mass, energy or the balance of forces. Such equations should be dimensionally uniform or homogeneous (10) and by a division of a characteristic mass, energy or force, any of these equations can be transformed into a relationship between dimensionless groups. Such dimensionless groups have the advantage over the Pi groups derived by Pi theorem that these groups are derived by the differential equations that give quantitative relationship between the physical and chemical variables involved. However, it is not always necessary to write differential equations to set up the similarity laws, which can also be done by the Pi theorem.

2.1.3. Complete and Partial Similarity

Complete similarity, as discussed under Sec. 2.1.2, is said to be achieved when all the Pi groups, derived by either the differential equations or the Pi theorem, are held constant between the prototype and the model. In most cases it is either impossible or unnecessary to obtain complete similarity. For example, if one has to allow equal residence times, then, it becomes impossible to have equal Reynolds numbers in the model and prototype. Consequently, some of the dimensionless variables, which are believed to have secondary influences or which affect the phenomenon in a known manner, are allowed to deviate between the model and the prototype, and this is called the art of partial modelling. For example in modelling of furnaces, it is shown by Fryling (12) that the Reynolds number may vary considerably as long as the flow remains in the turbulent range; the maintenance of turbulent flows is necessary since all industrial combustion chambers operate in the turbulent range. Anson (13) has suggested, in the course of large boiler investigations, that reduction in Reynolds number by a factor of 50 will yield realistic results as long as the flow remains turbulent.

Therefore, it is the responsibility of the experimentalist to select the groups, if any, that need to be maintained constant for the process; and this requires an insight and intuition which requires a good knowledge of the process involved. Therefore, the technique of partial modelling becomes an art and a science.

2.1.4. Similarity Rules That Can Be Neglected in the Modelling of Flows in Combustion Chambers

The Pi groups, one can reject, or which need not be held the same as explained in Sec. 2.1.3 , depend on the questions the experimentalist expects his model to answer. Therefore, it is rather a judgement than a rule, hence an art. The following have been listed by Beer (14) as some of the principles that have been generally found successful in partial modelling of combustion chambers.

(a) If the Reynolds number is large and the process investigated depends on turbulent mixing, the molecular transport properties can be neglected in such cases and so there is no necessity to maintain equal Prandtl and Schmidt numbers between the prototype and the model.

(b) If the Reynolds number is large and we are interested in jet mixing in an enclosure, then it is not necessary to maintain the same Reynolds number in the model and the prototype. This applies to the region before the jet expands to fill the box. This is in addition to the discussions of Sec. 2.1.3.

(c) If the Froude number is sufficiently large (that is, inertial forces are large compared to buoyancy forces), then it will be unnecessary to maintain the same Froude numbers. But in some industrial furnaces where flame contour is changed due to buoyancy, one may have to include buoyancy effects.

(d) If the settling velocity of oil drops or coal particles is not comparable to the bulk flow velocity, then two phase flow effects need not be simulated; i.e., phase separation is negligible and the flow may be treated as homogeneous.

(e) However, when the drop size of oil drops is scaled, it becomes necessary to scale down by using the ratio of residence times, since the burning time of a droplet is proportional to its diameter.

(f) When nonisothermal conditions are to be simulated with isothermal flow in the model, the geometrical similarity should be modified so as to maintain the mass flow and velocity ratio, but distort the nozzle diameter according to the "Thring-Newby criterion." The Thring-Newby criterion is discussed in Johnstone and Thring (11) and by Thring and Newby (15) and will be discussed further below, for completeness. The Thring-Newby criterion is one of the most important and simplest of the model laws.

2.1.5. The Regime Concept

Broadly similarity can be classified as static, dynamic, thermal, chemical, etc., as explained above. Any real system may come under one or more than one of these headings according to the particular aspect of its behavior that is being considered. However, of all the processes that may be occurring in series or in parallel, one process may be rate determining with the rest of the processes not determining the rate. Here a concept of regime has been generally introduced (11). The regime is generally used to mean the rate-determining process in a system in which several other processes in series or in parallel may be occurring. For example, the gas phase burning in an incinerator will be mostly subjected to a mixing regime until mixing is relatively close to perfect; but after the mixing reaches a certain closeness to perfectness, both mixing and chemical reaction rate control the rate of burning, and this can be called a mixed regime. When either mixing controls the reaction rate, or the chemical kinetics controls the reaction rate at perfect mixing, the regimes can be called pure regimes. For reliable modelling two conditions become necessary. 1) The regime should be relatively pure, i.e., the process should depend chiefly on a single dimensionless group. 2) The regime should be of the same type on the small and the large scale. In modelling an incinerator, as discussed in Sec. 1, the process is controlled by mixing and this is relatively a pure regime controlled by the fluid dynamics of the system and the fluid dynamics of the system is usually subject to a dynamic regime and so dynamic similarity is the most important of all similarities, as far as mixing and fluid flow modelling of the incinerator are concerned. However, if the results of a hot incinerator model like Shieh's (9) test incinerator, where combustion goes on, are to be used to predict the behavior of a much larger practical incinerator, then the regime may become possibly a mixed one because mixing and/or chemical kinetics, and/or heat transfer rates may play a combined role in the process of combustion. And then similarity laws will be subject to a mixed regime. For further discussions and reading one can refer to Johnstone and Thring (11). However, combustion in practical furnaces and incinerators is subject usually to a pure regime, the dynamic regime, as discussed above, and, therefore, isothermal models have been successfully used to study the flow patterns.

2.1.6. General Use of the Models and the Principles of Isothermal Modelling of the Flow Patterns in Combustion Chambers

Isothermal air and water models have been used extensively in research and development of the combustion chambers. Models have been widely used to study mixing and flow patterns inside the open hearth furnaces in the steel industry and glass melting tanks in the glass industry; to study the pressure drops and fluid flow in ducts; to study the effects of design changes of large furnaces and in the design of ships, harbours, and aircraft.

It has been found by Hottel (16) that combustion does not affect greatly the flow patterns in highly turbulent systems. This means that chemical reactions can be viewed to produce temperature changes which in turn change the physical properties of the gases. This will reflect in only numerical value changes of the dimensionless group which control the physical processes of mixing and fluid flow. Therefore, successful modelling of mixing and fluid flow can be achieved if certain dimensionless groups are kept constant between the prototype and the model. As has already been explained, Reynolds number can be generally reduced, which leads to certain advantages in modelling in that the flow rates through the model can be comparatively reduced. This means that smaller pumps and blowers will be needed which leads to economy. Another consequence is that since the flow rate can be reduced, the residence time increases and this leads to better flow visualization in water modelling. Some of the techniques and their brief descriptions used in modelling are described further below.

2.1.7. Further Experimental Details

Some pioneering work in experimenting with cold models or isothermal models were made by Groume-Grjimailo (17) using oil or kerosene and water to simulate buoyancy effects and this work was mostly qualitative. However, they performed the experiments with fluid velocities far below those required for dynamic similarity and consequently they failed to simulate the effects of turbulence. Rosin (18) developed a water model for the study of the flow distribution in complex combustion systems, such as furnaces, and maintained dynamic similarity in order to ensure equivalent turbulence in the model. More recent workers, cited by Johnstone and Thring (11), are Chesters (19) in the investigation of the open-hearth furnace using water models, Newby (20) in the investigation of the Bessemer Converter, and in the gas turbine field Watson and Clarke (21).

A recent worker using hydrochloric acid and caustic soda for mixing studies in water models of the glass tanks is Inman (22).

A cold model is capable of giving both qualitative and quantitative information. Quantitative data can be obtained on the pressure drops and the velocity profiles in the different parts of the furnace. Qualitative information that is usually obtained is on the turbulence patterns in the furnace gases and the regions in which flame impingement or excessive erosion of refractories may occur.

As explained above, cold models are operated with either water or air as the working fluid. The kinematic viscosity of the hot furnace gases is of the order of 12 times that of cold air and 130 times that of water. Hence for maintaining equal Reynolds numbers, for dynamic similarity, in a one-twelfth scale model, the cold air velocity should be equal to that in the prototype, whereas with water as the working fluid the velocity is required to be one-tenth as great. Owing to their lower corresponding velocities, water models are more suitable for visual observation of the flow patterns, e.g., by the injection of air bubbles a pulse of dye, fine balsa dust, polysterin particles, or aluminum powder. Air models are easier to construct and are mostly used for quantitative measurements using probes. However, air models can also be used for visualization using some smoke like titanium-tetrachloride or some other smoke like kerosene smoke, and oil fogs.

The flow in water models built of transparent plastic is usually made visible in a cross-section by a high-intensity, narrow plane beam of light cutting a slice across the model and can be viewed or photographed at right angles to the plane beam.

In air models, tracers like CO_2, nitrous oxide, helium or radioactive gases are used for the study of mixing of the jet flows and the surrounding fluid, and the mixing is determined from the analysis of samples withdrawn from various points in the model. The tracer may also be temperature (e.g., the jet fluid can be preheated) and local mixedness is determined by measuring the temperature at that point. In three component mixing, which happens when double concentric jets are fed into a box, between primary fluid, secondary fluid, and recirculated fluid, two tracers are used, one being temperature and the other may be a tracer gas. In a study of this nature by Beer, Chigier and Lee (23) primary fluid was preheated to 80°C and secondary fluid was tagged with CO_2 tracer. The local concentrations in terms of primary, secondary and recirculation fluid were then determined from the measurements of temperatures and CO_2 concentration analyses of samples.

"Transient" tracer techniques can be used for residence time distribution studies (11) both in the isothermal models and in the prototypes. This type of technique has been used by Beer and Lee (3) with salt solution as the tracer in a water model and with argon tracer in the prototype furnace. Transient tracer technique using helium tracer in an air model has been used in our studies and will be described in greater detail in Sec. 4.

2.2. Mixing Studies Related to Furnaces

A large number of experimental and theoretical studies have been performed to study and to improve mixing rates in furnaces. Some studies are purely empirical with detailed measurements of velocity, pressure and concentration measurements using various types of burners as the promoters of mixing in both the presence and the absence of the walls. When the walls are absent, the burners produce what can be called the free-jets and the nature of the jets that emerge from the burners depend on the burner design. For example, burners have been designed to produce swirl in the fluid emerging from the burner and also to produce concentric primary and secondary streams of fluids emerging at different rates with different swirl in each stream. Generally, the two streams have been swirled in the same sense, i.e., the direction of rotation is the same; the reason for this is, as has been found, mixing effectiveness will be reduced by opposite swirling of the two streams. The information that is obtained in the absence of the walls is found to hold good when the furnace is much larger than the size of the burner. When the furnace size is not much larger than the size of the burner, the free jet behavior does not simulate the behavior in the furnace because the recirculation which affects the flow pattern in the furnace does not exist in the free jet. However, information on the free jets is found useful to the furnace designers, when the furnace is large compared to the burner size, for calculating the combustion rates (in so far as these are governed by the mixing rates of the fuel and the oxidizer, air) and for theoretical physicists for comparing the different theories of turbulent mixing. Therefore, certain information on the free-jets has been included below.

2.2.1. Isothermal Free Jets

Although circular, rectangular, square, and free jets have been studied and summarized (24,25), the case of most interest to us is a cylindrical free jet since most burners used in the industry are cylindrical. Certain facts can be concluded about this type of jet from symmetry and fundamental laws of fluid mechanics before any assumptions are introduced as to the nature of the mixing process. The approach followed is the same as the one used in summarizing by Thring (26). Let u be the velocity parallel to the main flow of the jet at any distance x from the jet mouth measured along the jet axis and at a distance y from the jet axis. The diameter d of the jet pipe mouth is assumed to be very small compared to x. The momentum G is conserved because there is assumed to be no pressure drop along the jet.

Therefore $$G = \rho \int_0^\infty 2\Pi u^2 y \, dy \qquad (2.1)$$

If the jet is assumed to be of conical shape, the velocities at any two points on a line through the jet mouth must have the same ratio to the velocities at the same values of x on the axis; hence, u must be of the form

$$u = f(x) \cdot \phi\ (y/x) \tag{2.2}$$

By writing $= (y/x)$, Eqn. (2.1) becomes

$$G = [f(x)]^2\ \rho \int_0^\infty 2\Pi[\phi(\zeta)]^2 \zeta x^2 \cdot d\zeta$$

and the right hand side can only be constant for all x if

$$f(x) = 1/x$$

Therefore $$u = (1/x)\ \phi\ (\zeta) \tag{2.3}$$

It follows at once that on the axis where $y = 0$ or at points on a line through the jet orifice for which y/x = constant, u varies inversely with x, the distance from the orifice on the axis.

Thring (26) summarizes that the point which has been of interest to the theoretical physicists is the form of the function $\phi(\zeta)$. This has been determined experimentally by many workers, Reichardt (27), Corrsin (28), and has been calculated by:

(i) Tollmien (29) using Prandtl hypothesis that the shearing forces in the jet are resisted by the transport of momentum by eddies which move a distance L (the mixing length) before losing their identity. He assumed L is proportional to $x (L=Cx)$. From these assumptions it is possible to calculate $\phi(\zeta)$ with C as the only unknown parameter. By fitting the curve for (u/u_m) where u_m is the velocity on the axis, Tollmien found C = 0.0158 and the radius of the jet outside which the fluid has no forward velocity was $y_o = 0.214x$, giving the jet half-angle of 12°.

(ii) Howarth (30) applied the Taylor hypothesis that it is the vorticity which is transported by a distance L unchanged and provides the resistance to shear. This theory gives a function for (u/u_m) which fits the experimental results slightly worse than the case considered by Tollmien, above, particularly at the edges of the jet.

(iii) In one of the recent papers, Hinze and Van der Hegge Zijnen (31) give further detailed experimental measurements and show the assumption, that there is an effective turbulent kinematic viscosity which remains constant in the jet, gives better fit than the assumptions of Tollmien and Howarth as described above. Hinze and Van der Hegge Zijnen then give

$$G = 0.0164 \ u_m^2 \ x^2 \tag{2.4}$$

while the mass of the jet and entrained air flowing at any distance x is given as

$$M = 0.38 \ x \ (G \cdot \rho)^{1/2} \tag{2.5}$$

While the numerical constant in this equation is likely to be in error especially when the temperature variations and the density differences between the jet and entrained fluid exist, the fact that M is directly proportional to x is likely to be approximately true in all cases. This means that the amount of gas entrained by the jet increases linearly along the jet so long as the gas available is in excess of that needed by Eqn. (2.5). Values of the numerical constant vary for isothermal air jets from 0.22 to 0.404 according to various investigators (26,27,28); but Ricou and Spalding (32) have developed a technique to measure M which enabled them to obtain a value of 0.282 for the constant and have found that Eqn. (2.5) applies only after a Reynolds number (based on the nozzle dia.) of 2.5×10^4. The numerical constant was found to be independent of the ambient fluid (propane, CO_2, H_2, air) entrained by the air jet. However, when the jet was burning, it was found that the entrainment rate was down by 30 percent which was explained to be due to the buoyancy effects.

In applying the Eqn. (2.5) it is always necessary to remember that the entrained gas is not fully mixed with the jet at the time of entrainment as the jet has a central core containing a high proportion of the jet fluid and an outer portion with a high proportion of the entrained gas. Empirically it has been found that the gaussian error curve gives the distribution of velocity across the free turbulent jet to a very good approximation. Also Davis (33) using a round nozzle of diameter d_o gives the following empirical equation for the axial velocity of a turbulent jet as:

$$u_m = (8.4\ d_o u_o)/(x + 2d_o) \tag{2.6}$$

where u_o is the average velocity of the jet as it emerges from the nozzle. This formula is found to apply for all distances, $x > 8d_o$, where the velocity profiles are fully developed and remain constant, and the jet is said to be self-preserving. For regions of $x < 4.5d_o$, the jet has a potential core where the velocity is uniform until $x = 4.5d_o$, and for a length $4.5d_o < x < 8d_o$, the region is transition (34). Comparison of the Eqn. (2.6) with the Eqn. (2.3) means that the jet issuing from an orifice of diameter d_o, is equivalent to a very small jet issuing from a point $2d_o$ farther back. This agrees with the results of straight jets in our studies. In applying the Eqn. (2.5) it was stated above that although the surrounding fluid may have been entrained by a jet, this does not mean that it is fully mixed. It follows that the time average concentration of nozzle fluid varies across the jet, and, moreover, the instantaneous concentration values at a given point will also vary with time. This latter effect is usually referred to as "unmixedness" (35).

Apart from the effects of the unmixedness, the maximum concentration of the nozzle fluid has been found to be on the jet axis. Experimental results of the concentration of jet fluid along the axis can be expressed by the formula of Sunavala, Hulse and Thring (36)

$$1/c_m = 0.22\ (x/d) - 1.5 \qquad (2.7)$$

Again the gaussian error curve is found to fit the concentration variation across the jet. However, it has been found by Forstall and Shapiro (37) in a slightly different situation of two concentric jets, that, in problems of turbulence, mass and temperature diffuse at equal rates which is about 1.5 times the diffusion rate of momentum. Another important result they obtained was that the turbulent diffusion coefficients are substantially independent of the laminar coefficients. This means that, in turbulent mixing, the molecular properties are not important and hence do not control the rates. In fact, they showed that because of the above reason any tracer can be used to study mixing without much change in the results.

2.2.2. Nonisothermal Free Jets

This arises when the jet fluid is of a different temperature from the surrounding fluid which the jet will entrain. It has been found by Sunavala (36) that when the temperature of the jet fluid is higher than that of the surrounding fluid t_a, the rate of decay of the velocity on the jet axis is greater than the rate of decay for an isothermal jet. However, the rate of decay can be made to coincide with that of the isothermal jet if the orifice diameter d_o is replaced by an "equivalent diameter" (d_e) given by:

$$d_e = d_o \, (t_a/t_o)^{1/2} = d_o \, (\rho_o/\rho_a)^{1/2} \tag{2.8}$$

This concept of the equivalent diameter is based on the assumption that the development of the jet is determined by the conservation of the total jet momentum. The total momentum for a single jet can be written as:

$$G_x = 2\Pi \int_o^\infty \rho \, u^2 r dr \tag{2.9}$$

where G_x is total momentum across the jet at a distance x from the orifice, and u,ρ are the velocity and the density at a radius r from the axis of the jet. The initial momentum in the jet, G_o, at x = o is:

$$G_o = (\Pi/4) \, d_o^2 \, \rho_o \, V_o^2 \tag{2.10}$$

where d_o = diameter of the orifice, ρ_o = density of nozzle fluid, and V_o = average velocity of nozzle fluid.

It can be argued that the jet fluid mixes with the ambient fluid and attains a density of the ambient fluid. For example, in a combustion chamber of large size compared to the jet size (d_o) the reactants mix with the reaction products and attain the temperature and the density of the combustion gases. This was in fact studied originally in greater detail by Thring and Newby (15) in a theoretical way and their derivations give the same conclusion as will be given by this somewhat more simplified approach.

Since the final density of the jet (ρ_a) is the same as that of the ambient gases, a jet of fluid with density ρ_a with velocity V_o may be considered an equivalent jet if this jet emerges with the same momentum as before in the nonisothermal jet. If the diameter of this equivalent jet is d_e, then

$$G_e = (\Pi/4)\ d_e^2\ \rho_a\ V_o^2 \tag{2.11}$$

where G_e is the momentum emerging from the equivalent jet. But $G_e = G_o$. Therefore, from Eqns. (2.10) and (2.11)

$$(\Pi/4)\ d_o^2\ \rho_o\ V_o^2 = (\Pi/4)\ (d_e)^2\ \rho_a\ V_o^2$$

The above equation can be simplified to give:

$$d_e = d_o(\rho_o/\rho_a)^{1/2} \tag{2.12}$$

It has been shown by Thring and Newby (15) that this Eqn. (2.12) can be effectively used as a similarity criterion for isothermal model studies of mixing in furnaces, and therefore is called the "Thring-Newby criterion." This essentially means that when a scaled down isothermal model of a furnace is used, the burner diameter is a larger fraction of the combustion chamber size in the model than in the prototype, i.e., the model is geometrically distorted. By using this criterion and a cold model reduced by a scale of 10, Thring and Newby were able to predict the combustion gas compositions along the length of an oil fired furnace.

In their model, methane was used as a tracer gas and was analyzed by using the infrared absorption. The above discussion has been shown to be good for the gas jets; however, suspensions of pulverized fuel and atomized liquid fuel in air or steam can be treated as gases, at least as an approximation; then the above discussion holds good to these cases also. This concept of equivalent diameter has also been found to be useful to reduce data on entrainment rates of H_2, CO_2, propane, air into the air jet into one single equation by Ricou and Spalding (32). They state that the above idea of equivalent diameter was also surmised by Squire and Trouncer (38). The Thring-Newby criterion holds good only when the nozzle size is very small compared to the chamber size. The case when the burner diameter is not small in relation to the chamber size is discussed below.

2.2.3. Enclosed Jets and Recirculation Phenomena

When a jet flows into a space bounded by walls it is called an enclosed jet. For an enclosed jet issuing from a nozzle into a duct, two extreme cases can be considered.

(a) There is ample supply of secondary fluid surrounding the jet so that the jet can freely entrain it until it expands to reach the walls of the duct. This is the case considered under the free-jet theory above.

(b) The surrounding secondary fluid is less than that the jet can entrain. Then a convective flow of gases occurs from downstream of the jet and mixes with the jet upstream and this is referred to as recirculation. The existence of recirculation has been known for many years (39) and aerodynamicists involved in the furnace design were well aware of this phenomenon about fifteen years ago (19). Large scale mechanical recirculation is now used in certain power station boilers, mainly to control the heat transfer to steam superheaters and water-cooled walls in the chambers. This is accomplished by transporting flue gases from the vicinity of the air-heater through ducts back into the combustion chamber. Bluff body recirculation (40) is also used to stabilize flames in systems where the velocity of the fuel/air mixture is greater than the flame speed in the mixture. In a survey paper on recirculation, Hedley and Jackson (41) gave a summary of the various studies on the effects of recirculation. They were able to argue that there exists a critical amoung of the recirculated gases at which the stability of the system would be a minimum, and on either side of this critical amount the stability would be higher. However, no definite reasons have been established for the existence of this critical limit. Hedley and Jackson (41) state that in a study by Putnam and Karr (42) using propane air flames, they were able to show that the blow-off velocity was lower with recirculation and thus detrimental until the recirculation was 22 percent of the inlet flow. Also, the stability was minimum when recirculation was 10 percent. Recirculation beyond 22 percent was found to increase the stability of the system. Recirculation has also been used as a source of heat for rapid ignition of the incoming fuel-air mixture. Longwell and Weiss (43) showed experimentally that recirculation of four parts by weight of combustion products to one part of the incoming fuel-air mixture produced the maximum combustion rate. Higher ratios produced blow-off at much lower combustion rates due to excessive dilution by the inert combustion products. The chamber used by Longwell is one, in which mixing is found close to perfect and therefore called a well-mixed reactor, in which the heat release rate is controlled more by chemical kinetics rather than by the physical rate of mixing. The studies applying the "stirred-reactor" concept to combustion chambers will be covered later under residence time distribution (R.T.D.) studies.

Additionally, the beneficial effects of recirculation in coal fired systems have been reported, according to Hedley and Jackson (41), by various investigators (44,45,46). It has generally been reported that flame speeds increase by a factor of three to ten in coal-air mixtures when recirculation is introduced into a previously non-recirculating flame (41).

Studies, using both theory and isothermal water models, on the enclosed jets, have been performed by Craya and Curtet (47), and Curtet and Barchillon (48) to study flow patterns and turbulence levels in the enclosed jets. Curtet used Reynolds equations and two dimensional and axisymmetric cases, assuming nonviscous assumptions in the recirculation eddy; he found that a universal velocity profile for a confined jet cannot be obtained since the experimental profiles did not fit either the cosine or the gaussian curve. However, he introduced a similarity parameter for the enclosed jet; the similarity parameter is called Craya-Curtet number and is discussed later. Craya also showed experimentally that a straight jet oscillates under certain conditions when the inlet flow surrounding the central jet falls short of some minimum value. He was also able to calculate the recirculation discharge along the centre line in terms of entrance velocities and showed that the experimental values checked with the theoretical calculations. He was also able to locate its centre or eye, recirculation boundary, and velocity distributions. He also observed experimentally that the flow in a water model chamber with a straight jet is essentially a jet flow super-imposed on which is a recirculation eddy and the recirculation flow starts as far downstream as the exit and flows only nearer the walls.

The work of Barchillon and Curtet (48) experimentally mapped the flow field in the mixing zone when the ratio of nozzle fluid to the surrounding fluid was varied, by velocity and pressure measurements and by photographic techniques using water models. Also they found that the turbulence intensity in the axial direction was much higher for confined jets compared to straight jets, and the turbulence intensity increased further downstream to about 80 percent of the mean axial velocity. In the recirculation eddy they found very high levels of turbulence, the fluctuating velocity was greater than the mean velocity in the downstream region of the centre recirculation eddy.

In a somewhat similar study on the coaxial gas jets, Squire and Trouncer (38), and Forstall and Shapiro (37) had shown before Curtet that the principal independent variable affecting the mixing region is the velocity ratio of the nozzle fluid and the surrounding fluid. However, since Craya and Curtet were the first to develop a rigorous theory for the confined jets, the mixing parameter is named after them as the Craya-Curtet number by Becker, *et al.* (49). In the study by Becker, Hottel and Williams (49), they used an oil-fog technique to study the flow field consisting of a jet-region and a recirculation eddy for various values of the Craya-Curtet numbers. They found that the similarity of geometrically similar ducted flow systems with a jet flow super-imposed on a ground uniform flow requires constancy of the ratio of the initial strengths of the ground stream and the jet, and this is the ratio defined as the Craya-Curtet number. At low values of this ratio, the ground stream falls short of the entrainment capacity of the jet and a recirculation eddy was found to be set up. They found that, with recirculation and when the ratio of the nozzle size to the duct size is very small, the parameters of Craya and Curtet and of Thring and Newby are essentially equivalent, but under other conditions the latter parameter was found quite inadequate.

When combustion is going on in the above situation of confined jets, Thring and Newby (15) have established a modelling parameter ϕ, given by:

$$\phi = [(m_a + m_o)d_e/m_oL]_{model} = [(m_a + m_o)d/m_oL]_{hot\ system}$$

where m_a = mass of the secondary flow, m_o = mass of the jet flow, d = dia. of the nozzle in the prototype, d_e = dia. of equivalent nozzle in the model, L = length dimension used for geometrical scaling.

The values of ϕ for usual zone of industrial furnace operation is given by Barchillon and Curtet (48) as 0.1 to 0.3. A range, for ϕ of 0.07 to 0.941 was covered by Barchillon and Curtet (48) in their experiments, and Becker, et al. (49) covered 0.05 to 1.2 in their studies.

Additionally half-angles of confined jets have been found to remain at about the same as for a free-jet. Usually a concentration half-angle has a range of 5.45° to 8.9° and an average value of 6.36° for fifteen studies listed by Field, et al. (34). The velocity half-angle has an average of 4.95° with a range of 4.6° to 5.4°. These values can be compared with a value of 6.7° obtained for the confined straight jets during our investigations.

2.2.4. Swirled Jets

The practice of imparting rotation about the axis of the burner jets has long been used for increasing stability and intensity of combustion. The increase in ignition stability is due to an axial recirculation vortex, which causes hot burnt gases to travel back towards the burner where they are entrained by the inlet cold fluid and cause ignition.

Some work on flames by Kerr and Fraser (50,51) has shown that there is a relation between the level of swirl imparted to the gases and the combustion efficiency obtained. In fact, it has been generally found there is an optimum level of swirl for maximum combustion efficiency, beyond which any increase in swirl results in a reduction in efficiency. It has also been generally found that the length of the flame varies inversely with the swirl. The reason has been found to be due to the higher mixing rates obtained with swirl. Higher mixing is achieved due to the internal recirculation which will be set up in addition to the external recirculation. In swirled jets it has been found by Kerr and Fraser (50,51) that angular component of momentum is conserved in addition to the axial component of the momentum. Therefore, the ratio of angular to axial momentum has provided a useful modelling parameter in the modelling of swirled flows in combustion chambers (3).

According to Field, et al. (34), theoretical studies of swirled jets were made by Loitsyanskii (52) and Gortler (53), but their studies are only applicable to fully developed weak swirling jets with no axial reversal of the flow at any point. Field, et al. (34) report that experimental studies on swirling jet flames produced by introducing air through tangential ports have been reported by Cude (54), who found that the flame length was considerably reduced by swirl. Hottel and Pearson (55) have studied swirling jets, but again their system did not induce significant central or inner recirculation. Recently Beer and Chigier (56) at the International Flame Research Foundation, IJmuiden, have studied swirling jets, issuing from a swirl generator having tangential air entries, into stagnant air. They found that comparatively large subatmospheric pressures in the central region of the jet lead to the onset of reverse flow and a closed internal vortex ring is set up. The size and strength of this ring was proportional to the degree of swirl, and the flow behaved like a solid body rotation with maximum tangential velocity at larger radius. In a study by Mathur (57) it was found that the axial velocity profiles do not follow the error curve relationship and the free swirling jet suddenly experienced an expansion on emerging--the rate of expansion increasing with swirl. After a distance of two to four times the nozzle diameter, the angle of spread remains the same for a particular vane angle. He found the tangent of the vane angle gives a good measure of swirl and the enclosed jets spread faster than the free jets. The central recirculation which was obtained after 30° vane angle was found to be stronger in the enclosed jets than in the free jets. The minima in upstream and downstream wall static pressure coincided with the region of maximum reverse velocity in the outer and the inner recirculation regions respectively, and the maxima coincided with the impingement point. He also found that, in order to obtain significant internal recirculation in double concentric jets, it is necessary to swirl both the streams. For example, a combination of 45° vane angle swirlers in both the streams gives large central recirculation. Kerr (51), however, found that if the two fluids were swirled in the opposite sense smoke formation increased, and vice versa. Kerr and Fraser (50) found that the entrainment rate, jet angle, and the reciprocal of the axial velocity all vary linearly with swirl which was found to alter the above by several hundred percent. The decay of axial velocity and concentration was found to increase with swirl by Chigier and Beer (56). Since all the swirling jets studied have tendencies to spread faster than unswirled jets, it seems the behavior of swirled jets is produced by the forced vortices, i.e., those in which angular velocity is constant, or tangential velocity increases with distance (like in a solid body rotation). Compared to this, in a free vortex the tangential velocity varies inversely with radius and the pressure field balances the centrifugal force, and the jet does not show a characteristic tendency to spread faster than a nonswirling jet. Also, no inner recirculation eddy develops in the free-vortex.

For more information on the swirling jets, annular jets, cross flowing jets, effects of buoyancy, and particle laden jet behavior, the work by Field, *et al.* (34) can be referred.

2.2.5. Stirred Reactor Approaches to Mixing Problems in Combustion Chambers

A combustion chamber should consist of a backmix reactor section (equivalent to Perfectly Stirred Reactor, P.S.R.) followed by a plug flow reactor section for maximum efficiency of burn-out. This has been shown by Levenspiel (58) for the case of a combustion chamber in which autothermal reactions are occurring. Autothermal reactions are those where heat is produced as a byproduct of the reaction and the reaction in turn increases with the temperature. However, the temperature jump that is necessary for ignition and flameholding is not considered there. This temperature jump is the most critical phenomenon which is highly desirable in the satisfactory operation of the combustion chambers. This jump is considered in detail by Vulis (5) and also the dependence of this temperature jump on the stirred reactor parameters like residense time, heat loss, and mixing effectiveness are treated in great detail in that book, and, according to the preface by Williams in Vulis (5), the most complete treatment to date on stirred reactors as applied to combustion is given by Vulis (5). However, Bragg (2), in the course of jet engine studies, postulated the flow pattern should be a P.S.R. section followed by a plug flow section for maximum efficiency. P.S.R. is one where the inlet gases distribute instantaneously and uniformly and the outgoing flow has the same concentration as that inside the reactor. Since this is only an ideal reactor, a mixing delay or similar reason should exist in a real system (5). Therefore, the perfectly stirred reactor can be replaced by a Well Stirred Reactor (W.S.R.). The Well Stirred Reactor definition is then similar to the P.S.R. with the addition of the mixing delay.

As shown by Longwell (40), in his spherical reactor, very high reaction rates and near perfect mixing can be achieved. His experiments are the closest approach yet made to the direct measurement of chemical reaction rates in flame processes unhindered by the physical rate of mixing of the gases and they show that the chemical-limit of heat release is extremely high. The experiments were repeated by others (59,60) with essentially the same results, although they concluded that it was better to consider the reactor as "well-mixed" rather than "perfectly-mixed." Bragg and Holiday (61) working on the theory of perfectly stirred reactors showed that, if excess air is used, a slower reaction rate is always obtained due to its cooling effect. They found justification for introducing excess air only in the last stages of combustion. Hottel (62) postulated not just one stirred reactor volume but several, connected in various theoretical series/parallel flow combinations. According to Hedley and Jackson (41), a similar model was conceived by Spalding (63) in which he analyzed pressure-drop requirements for high combustion intensities. He considered two sections of a combustor, one where the fresh feed was mixed with recirculated gases and another where part of the mixture was recirculated, the balance leaving the chamber as burnt gases. He showed that mixing with recirculated gases produced good combustion performance at the expense of a high pressure drop, but this was better than relying on random turbulence to produce a given combustion intensity. Thring and Masdin (64) have also used similar theoretical models utilizing recirculation to predict high combustion intensities.

Although stirred reactors can achieve very high combustion intensities, they cannot be expected to achieve complete burn-out of the reactants due to the following reason. If complete burn-out has to occur, the outgoing stream has zero concentration. Because of the definition of the P.S.R., the concentration inside the reactor volume is also zero; and, hence, there can be no reaction. This can happen only in an infinitely large reactor and, therefore, finite sized reactors (P.S.R.) cannot complete the burn-out of reactants. In addition, Hedley (41) and Avery (65) have shown that beyond a certain burn-out the heat release rates begin to go down in a P.S.R. until at 100 percent burn-out the heat release is zero. This is another fact to substantiate that complete burn-out cannot occur in a finite sized P.S.R. This same point was also established by Longwell (43) when he showed that blow-off occurred beyond 80 percent efficiency. Therefore, to burn-out the rest of the gases, a plug flow reactor is usually necessary. In a plug flow reactor, mixing between adjacent volumes of fluid does not occur. This enhances burn-out because further dilution with the products of combustion is eliminated and the temperature is high. A theoretical analysis by Essenhigh (66) shows that the size of the stirred section should be enough to bring about ignition and then the gases should flow into a plug flow region for optimized burn-out. He divided the chamber into a series of small P.S.R. sections and then showed that before ignition the P.S.R. sections have to be lumped into a larger one, and after ignition the P.S.R. sections have to be further divided which results in a plug flow. Beer and Lee (3) showed theoretically, by using reaction rate equation for pulverized coal and stirred reactor assumptions, the volume for burn-out is smaller, if it consists of a P.S.R. and plug-flow combination, than, if it consists either one of the stirred or the plug flow. This gives further substantiation for Bragg's hypothesis.

However, although Longwell showed that very high mixing rates, and thus high combustion intensities, can be achieved, his method of stirring using two concentric spheres with a large number of holes was not applicable to practical applications until Beer and Lee (3), about six years ago, showed that a swirl burner produces a flow pattern approximating the Bragg pattern. However, as explained before, perfect stirring is not feasible and only well-stirring is possible and this study then aims at measuring stirring factors, which will characterize well-stirring, generated by some burner systems of interest described in Sec. 4. The method used for characterizing stirring in stirred sections of combustion chambers is to study the residence time distribution in combustion chambers. Explanation of the residence time distribution is given below.

2.2.6. Residence Time Distribution (R.T.D.)

The time taken by an element of feed to pass through a combustion chamber will be dependent on the particular path that the element has followed in its passage through the chamber. The possible flow paths depend on the flow pattern within the chamber. Hence observation of the residence time distribution can give some information about the type of flow pattern. The measurement of residence time distribution cannot be made directly, but can be made by indirect methods. Usually a tracer is injected into the inlet stream and then the tracer is recorded at the outlet. The various types of signals, like a pulse signal or a step signal, that can be used and the method of analyzing the responses to plug flow, P.S.R., and mixed models using combinations of P.S.R., plug flow, bypass, dead space, recycle flow, etc., has been given by Levenspiel (58). However, he also discusses the fact that a particular combination of two or more of these can be used to fit any experimental residence time distribution, and such a mixed model may have very little correspondence with the true flow, and suggests the use of the simplest model which fits the residence time distribution and whose regions can be found by experiments. This is the approach followed by us to set-up only two models (W.S.R. and recycle model) to explain the behavior of highly swirled and straight jets.

The problem of the residence time distributions in continuous flow systems has received considerable attention. An introduction to the study of the residence time distributions has been given by Danckwerts (67). Danckwerts shows that the knowledge of the residence time distribution alone is enough to predict reactor performance if the reaction order is unity; however, if it is not unity, then in addition to the residence time distribution, knowledge of micromixing or "mixing on molecular" scale becomes necessary. He introduced the concept of the "degree of segregation" and described how this can be measured experimentally. However, the effect of segregation does not appear to be too large and the knowledge of the residence time distribution can serve as a very useful measure.

Residence time distribution studies have been performed by using a salt tracer cut-off technique in a 1/10 scale water model of a furnace by Beer and Lee (3), and the similarity laws they used were the equivalent diameter concept, and the degree of swirl was maintained constant between the furnace and the water model. Drake and Hubbard (4) have used radioactive krypton as a tracer in the air, which was swirled, and with a similar cut-off technique used by Beer and Lee, they studied residence time distribution in an oil fired furnace. Hottel, *et al.* (68) used an oil-fog cut-off technique to study the residence time distrubution, in the well-mixed bomb used by Longwell, as affected by changes in size and the number of injection holes, etc. A similar cut-off technique using helium as tracer has been used by us to perform studies of flow pattern in furnaces and incinerators. We also used carbon-dioxide, but for reasons to be explained later, replaced helium for carbon-dioxide.

Residence-time-distribution studies have enabled us to characterize mixing effectiveness in a W.S.R., without really measuring detailed velocity, pressure, concentration profiles, as has been done by previous workers, to study mixing.

2.2.7. Summary of Mixing Studies in Furnaces

Furnaces are usually chambers, built to be refractory, of course, into which fuel and air are injected in the form of jets for mixing and eventual heat release. Effectiveness of mixing, luminosity, flame length and thickness, temperature of the flame, and radiation from the flame depend largely on the type of jet used, size of the jet to the size of the chamber, momentum of the jet, excess air, etc. The types of jets used vary depending on the purpose of using them. However, understanding the behavior of various jets helps in understanding their influence in the furnaces. Therefore, various investigators have studied the jets and their behavior. The results of some of these investigations were summarized. It can also be said that in double concentric jets, annular jets, and highly swirled jets a central recirculation eddy will be set up in addition to the external recirculation eddy found in the straight jets and jets with small swirl imparted into them. The swirled jets have been generally found to produce faster mixing than the unswirled jets.

However, most of the studies are of a detailed nature where velocity, pressure, and concentration fields are measured with a large amount of equipment and time. An alternative, but simpler and more useful approach, is to study the residence time distribution in the furnaces. As has been discussed, information on the residence time distribution should be sufficient, at least as a beginning, to predict the combustor performance reasonably well. The approach in our studies is, therefore, to use the residence time distribution studies to compare the effects of changes in the burner design to promote mixing.

2.3. Incinerators

Incinerators are refractory chambers into which refuse material is fed for the primary purpose of burning the material, thereby either eliminating the refuse or reducing its size. However, even under favorable conditions, the bed, especially if it is overfired, creates air-pollution by large amounts of smoke and pyrolysis products. In the past, air-pollution was not considered an unhealthy process; however, with the increase of stringent air-pollution laws coming into existence, it becomes necessary that the smoke and gasification products have to be eliminated from the gases before they escape to the atmosphere. One method of achieving this is to burn them up in the overbed space of the incinerator. Up to this time this problem has been solved on a trial and error basis which leads to a large amount of know-how without generating any knowledge of know-why. Based on these purely empirical studies, certain empirical equations have been developed in the past for the design of the incinerators. However, these studies are limited by the system variables like the method of firing, the method of injecting the air, etc. Therefore, they may or may not result in an optimum method of waste elimination. From the above studies even certain fundamentals like the dependence of the mixing rates on the jet momentum, jet angle and the number of jets are left out, and even when they are specified it is done so that the necessary air is supplied with minimum pressure losses. However, if air is supplied there is no guarantee of mixing the air with the combustibles since the air and gases can flow as separate streams under extreme conditions and even if there is some mixing, it may still not be satisfactory as explained in Sec. 1. In practical incinerators, bends, walls, and baffles are used as promoters of mixing; however, the mixing produced by these may be only marginal and not substantial. Therefore, it seems, it becomes necessary to have large combustion volume for sufficient mixing and burn-out. Therefore, in our studies a system of jets generating countervortex flows have been used as promoters of mixing, and the system has been found by us to produce such good mixing that it can be characterized by a W.S.R.

In general, both in incinerators and furnaces, mixing itself is thought to be sufficient for combustion. However, a flame has to be held for ignition of cold reactants and this point is generally not considered, although it might have been implicitly considered combustion will occur if there is mixing, which is not true. Therefore, in addition to proper mixing a flame has to be held and, as explained before, this becomes possible if ignition is achieved. Usually additional torches using oil or gas are used in the overbed space for igniting the gases, but this is unnecessary if large amount of hot products flow upstream and mix with the relatively cold incoming gases and rise their temperature to ignition.

Steam jets and air jets are generally suggested for creating turbulence and mixing in incinerators by the Bituminous Coal Research (B.C.R.) (69). It was found that smoke formation was reduced when overfire air jets were used and overfire steam jets were found to reduce smoke by increasing turbulence and mixing. This study (69) gave certain design criteria for overfire jets as to the sizes and the numbers of jets. However, the results seem to have been less effective in increasing the knowledge of their effects on improving the performance because of the empirism involved in the B.C.R. approach. Although many big incinerators use overfire jets for the purpose of eliminating smoke, it has been reported by Woodruff (70) that generally the overfire air and the gases do not mix and very heterogeneous mixtures are produced, leading to insufficient combustion due to poor air and temperature distributions. Sternitzke (71) has studied air and temperature distributions in incinerators and has suggested uniform air and temperature distribution should eliminate the pollution problem. However, his studies do not suggest any criteria for studying the effects of positioning the air nozzles to create good mixing. Analyses by Essenhigh (72,73,74) has led to a research program on incinerators at the Combustion Laboratory of The Pennsylvania State University. The above analysis led this research program to study four problems in incinerators. Namely: (i) flame spread rates; (ii) methods of overfire air injection for optimum mixing; (iii) kinetics of smoke combustion; and (iv) reactivity data on incinerator materials. And the results of these four sub-programs have been used to check the operation of a test incinerator (9). The subject of this thesis corresponds to the sub-program on the methods of overfire air injection for optimum mixing conditions. Some of the results of this sub-program have been published (75,76). These results will be included in this thesis, of course.

The results of the above research program under the direction of Essenhigh have given kinetic constants for smoke combustion, optimum methods of mixing and flame holding, effectiveness of mixing achieved, methods of estimating flame spread, and knowledge on mechanisms of flame spread. These results are applicable to the design of incinerators, and methods of setting up mathematical equations to predict performance of an incinerator using the results has been explained by Essenhigh (74).

2.4. Relation of the Above Summary to This Thesis Study

The above summary on furnaces and incinerators has been included to provide any mechanistic interpretation to the gross results obtained in this thesis study, and, as such, no data exist for direct comparison with the results of this study. The summary on modelling laws is included to cover the necessary background on the modelling of the incinerator and the furnace combustion chambers.

3. STATEMENT OF THE PROBLEM

The main objective of this thesis study was to determine the optimum arrangement for the overfire air jets in a test incinerator to create an effective aerodynamic flameholder to burn-out smoke. Therefore creation of a well stirred reactor section, followed by a plug-flow section was set as the prime objective of the incinerator model experiments. This is to satisfy the Bragg criterion as discussed in Sec. 1. The degree of mixing (W) in the W.S.R. then has to be optimized for optimum conditions of mixing and flameholding.

At the inception of the smoke combustion program, however, a number of difficulties were foreseen, notably how best to create the necessary stirred section. Lacking time to develop the optimum method by modelling or other suitable means a "countervortex" method of stirring was adopted (76) using some intuitive concepts partly based on previous experience, with support from some preliminary water model experiments (73). Suitable combustion tests performed in parallel with these studies (76) have now established that the countervortex is, indeed, effective in stabilizing flames. The objective, then, was to investigate this configuration to determine whether it creates a W.S.R. and plug flow combination to satisfy the Bragg criterion, and if so, how to optimize its mixing effectiveness.

It was not known, however, whether the countervortex flow provides the optimum mixing, or whether some other jet configuration is better. Clearly, a comparative standard was called for, and the logical choice was to investigate straight and swirling jets for the comparative studies; since jet burners are used extensively in many industrial furnaces and combustion chambers and substantial information on their behavior already exists (3,4,24,25,26,34).

The following are then the questions that needed to be answered in the present thesis studies:

(i) Can a flow pattern, approximating to the ideal Bragg model, W.S.R. followed by plug flow, be generated by the opposed-vortex system of overfire air jets in a test incinerator?

(ii) If a W.S.R. is created, then can the degree of stirring in the W.S.R. be characterized by a stirring factor?

(iii) Can the mixing effectiveness (W) of the overfire air system be optimized?

(iv) How does the optimum mixing (maximum W) of the overfire air system compare with that of the swirling and the straight jets?

In the course of the investigations to provide answers to the above questions, answers to the following additional questions were also found:

(v) Can the size of the W.S.R. be varied? This information is necessary to generate knowledge on the control of the size of the W.S.R. to satisfy the requirement, that its size should be just enough to bring about ignition (66).

(vi) What is the effect on mixing, of reducing underfire air and increasing overfire air, on mixing in an incinerator?

(vii) What is the effect of Reynolds number variation on mixing effectiveness?

(viii) What are the effects of changes of the jet size, vane angles, and swirl levels in producing mixing?

4. EXPERIMENTAL

4.1. General Considerations of Approach

As explained above, to study the effectiveness of flameholding in incinerators and furnaces it becomes necessary to measure the effectiveness of mixing. This can be done in either a large prototype as has been done by Beer (3), and Drake (4), but it is more convenient and economical to study in scaled down isothermal models of the systems; however if one uses scaled down models, certain similarity criteria such as geometrical similarity, dynamic similarity, Thring-Newby criterion have to be established. Since the mixing is affected mostly by the hydrodynamic conditions inside the furnace and the incinerators, it can be considered a pure regime, and similarity laws become simpler. Purely theoretical or experimental approaches to mixing problems are of little direct applicability; on the one hand purely theoretical approaches are extremely complicated and thus inapplicable. The equations that are obtained are coupled, non-linear equations with very complex boundary conditions and, therefore, they cannot be easily solved. Purely experimental measurements of concentration, velocity, pressure profiles, although valuable, lack general applicability. The results are mechanistic in nature, applicable only to the particular system in which the measurements are made and thus do not lend themselves to a generalization for application to other systems. However, residence time distributions (58) can be measured, and mixing effectiveness can be characterized by a stirring factor. The study of residence time distributions requires a method of measurement of a tracer gas, such as helium, in a carrier gas.

4.2. Basis of Method

The method of cold-modelling to determine probable flow patterns in a combustion chamber or furnace, by study of behavior in an isothermal, modified-scale model, is a standard technique adequately described in the relevant literature (e.g., Johnstone and Thring (11)), and its validity depends on accurate matching of appropriate similarity criteria. General information about the gross behavior of the flows can then be obtained by measuring residence time distributions (58,77), and two standard methods of doing this are to inject either a pulse of a tracer into the "carrier" fluid flowing through the model and monitor the variation of concentration with time at the exit, or to impose a step function increase or decrease in the input carrier concentration and monitor at the exit as before. For operational and instrumental reasons as described in Sec. 4.4 the easiest technique is to establish an initial steady state flow of tracer in the carrier, and start the experiment by complete cut off of the tracer (at time zero) to impose a step function decrease. This is the technique used in these experiments, using air as carrier and helium as tracer.

Determination of the flow pattern then depends in part on interpretation of the tracer response at the exit. To consider two extreme cases: (1) If the flow is plug flow throughout the model from inlet to exit then the tracer response at the exit would be a similar step function drop in concentration, but at a time τ_p after input cutoff (time zero) where τ_p is the time required for the carrier to travel from inlet to exit (plug-flow residence time). (2) If the flow is "perfectly stirred," the tracer response at the exit should start immediately on cutoff, the concentration then decaying exponentially with time (58,77).

In practice many systems show a combination of these two responses (3,4). Initially this was interpreted as implying the real existence of two regions, one perfectly stirred and the other in plug-flow, exactly as required to satisfy the Bragg criterion. Further analysis, however, indicated that this might be misleading, and the stirred region might only be "well stirred" instead of perfectly stirred. Adopting Vulis's (5) suggestion that a well-stirred region might be represented conceptually by combination of a mixing-delay region in plug flow, with a perfectly stirred region, the concept of a stirring factor (W) was developed (6), and this is the parameter mentioned in the Introduction as used to quantify the effectiveness of mixing.

Measurement of the stirring factor is not entirely straightforward; this introduces the modification to the standard tracer technique also mentioned in the Introduction. It requires repetition of the same experiment, but with the analysis probe moved from the exit, to a position inside the chamber. Where the pattern is plug flow, measurement (generally on the chamber axis) at points moving closer to the inlet end only reduces the plug flow time (τ_p); the subsequent exponential decay characterizing the stirred region remains unchanged. When the probe enters the stirred region the plug flow time becomes constant. This residual time is assumed to correspond to the mixing delay time, and the stirring factor can then be calculated.

4.3. Equipment

To study the effectiveness of mixing produced by the opposed vortex system in the test incinerator (9) and by straight and swirling jets in a furnace, the following equipment was used:

(i) A scaled down model of the incinerator incorporating the opposed vortex system;

(ii) A scaled down model of a furnace with provision for fitting the straight and swirling jets at the inlet;

(iii) A carrier gas, air, supply and measurement system;

(iv) A tracer gas supply and measurement system;

(v) A tracer gas sampling and recording system;

(vi) Some ancillary equipment, such as the one needed to record the moment of tracer cut-off to the models.

4.3.1. Incinerator Model

The layout of the equipment is shown in Fig. 1. This is a half scale model of the test incinerator being investigated in a separate subprogram (9). The incinerator model itself is illustrated in Fig. 2. The model has dimensions 1 ft. x 1 ft. x 4 1/2 ft., built of 1/2 in. thick plexiglass sheets. The underfire air is supplied by a 4 in. pipe. The bed is simulated by inserting a back-up plate 3/8 in. thick drilled with 1/8 in. holes at 3/16 in. intervals, between two flanges. The space (1/2 ft. long) between the plate and the 4 in. diameter inlet was partially filled with glass beads (1 in. diameter) to assure uniform distribution of the flow across the plate. The whole box, built of 6 in. long sections flanged together to form the box, is erected vertically with the inlet (back-up plate) at the top. On one

Fig. 1. Schematic Layout of the Equipment for the Study of Mixing Effectiveness in the Incinerator and the Furnace Models.

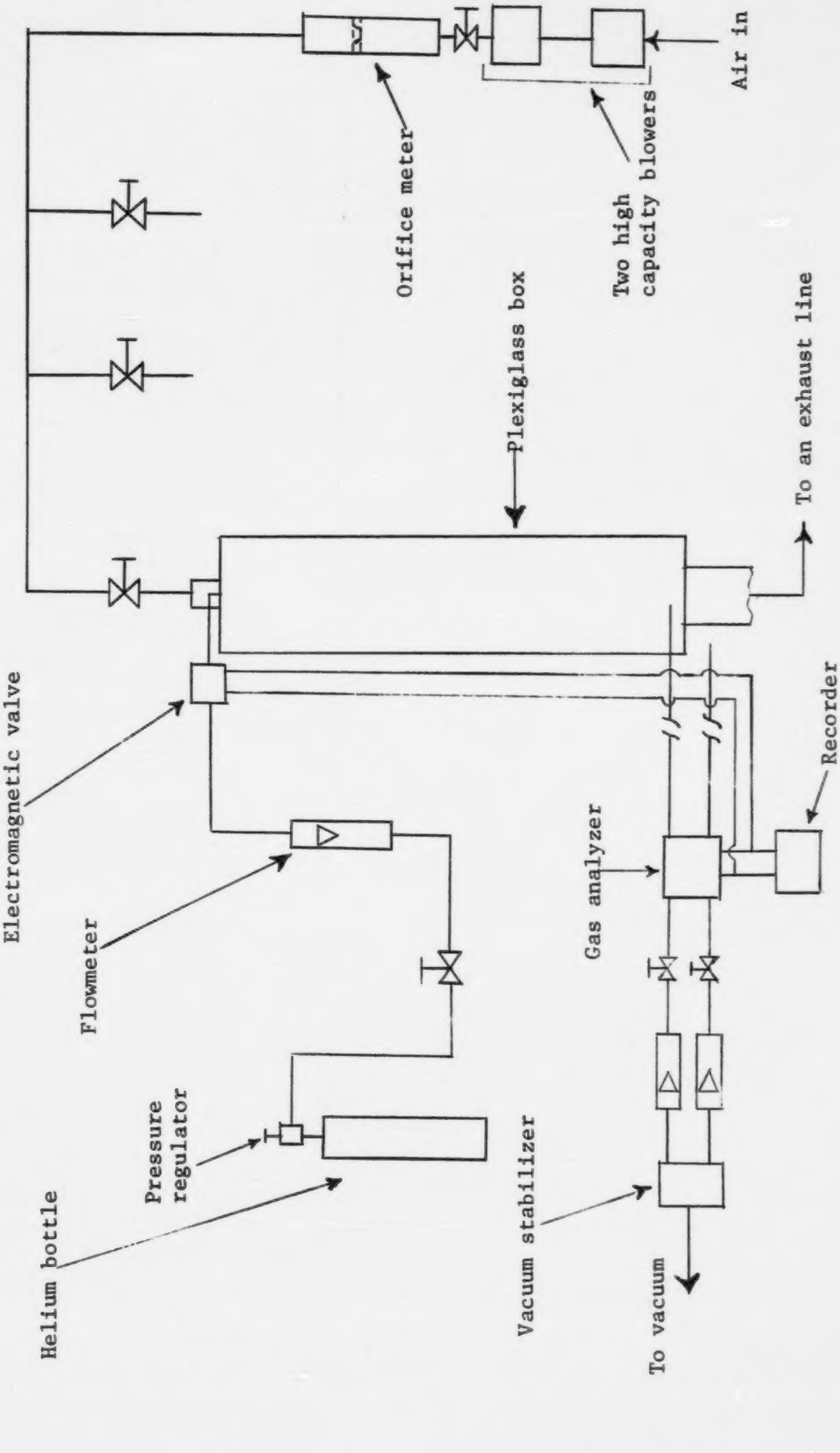
Helium bottle
Pressure regulator
Flowmeter
Electromagnetic valve
Vacuum stabilizer
To vacuum
Gas analyzer
Recorder
Plexiglass box
To an exhaust line
Orifice meter
Two high capacity blowers
Air in

Fig. 2. A Half-Scale Box Built to Model the Incinerator in the Subprogramme (9). (The box was built of 6 in. long sections with flanges and bolted together. This construction was adopted to vary the spacing. (See Sec. 4.1). The box was so designed that the offset angle could be varied from 0° to 70° in five steps.)

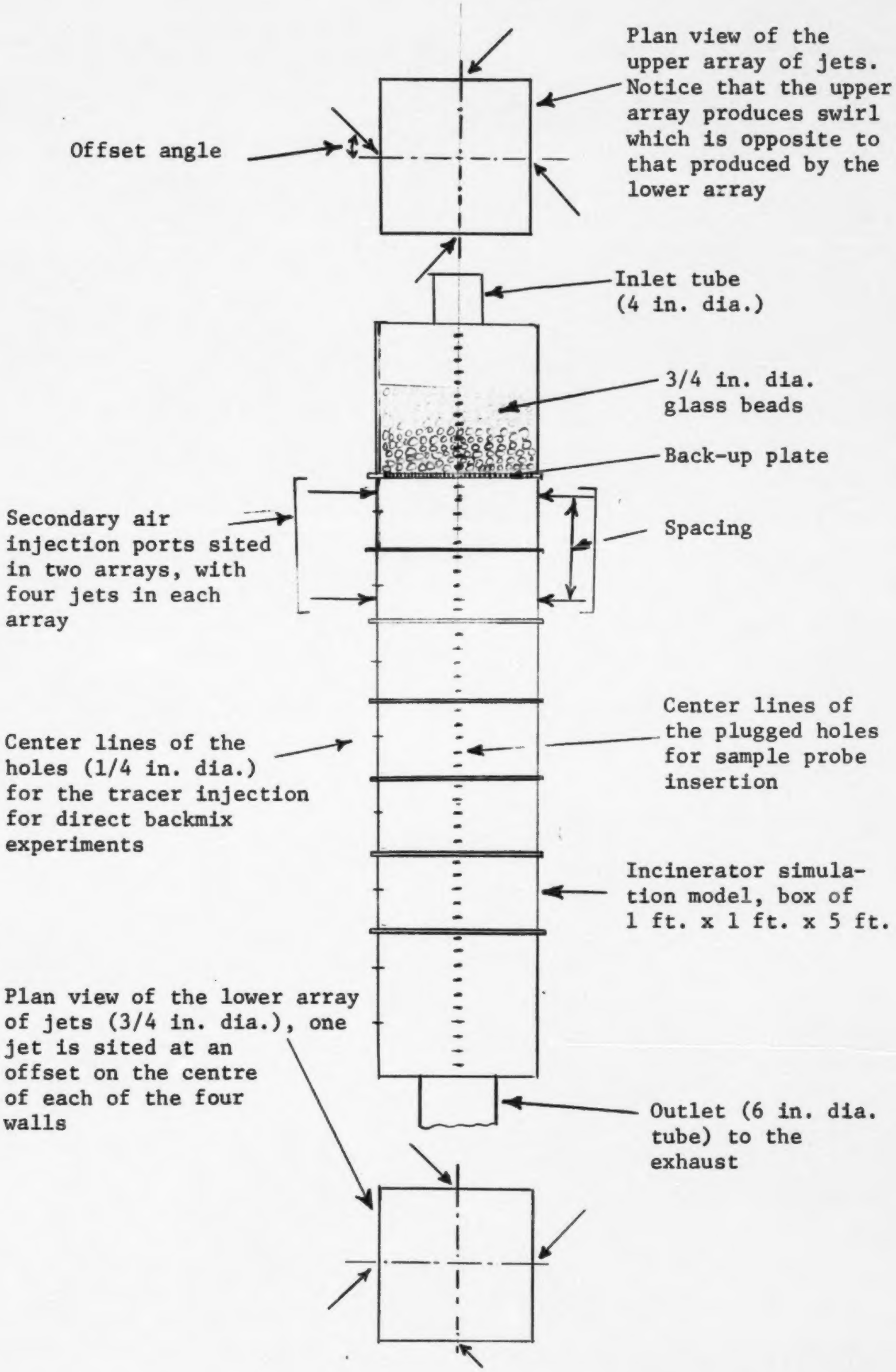
Plan view of the upper array of jets. Notice that the upper array produces swirl which is opposite to that produced by the lower array
Offset angle
Inlet tube (4 in. dia.)
3/4 in. dia. glass beads
Back-up plate
Secondary air injection ports sited in two arrays, with four jets in each array
Spacing
Center lines of the plugged holes for sample probe insertion
Center lines of the holes (1/4 in. dia.) for the tracer injection for direct backmix experiments
Incinerator simulation model, box of 1 ft. x 1 ft. x 5 ft.
Plan view of the lower array of jets (3/4 in. dia.), one jet is sited at an offset on the centre of each of the four walls
Outlet (6 in. dia. tube) to the exhaust

of the sides of the box sampling holes (forty-six in number), at 1 in. intervals, were provided for gas sampling at various distances as explained in Sec. 4.1. The holes were normally closed with 1/8 in. screws. In one of the screws a hole (1/20 in. dia.) was drilled through for the insertion of capillary gas sampling probe. This screw could be screwed into any one of the 46 holes for gas sampling at various distances from the inlet (the back-up plate). On another side of the box holes (3/8 in. dia.) were provided, normally closed by screws, for injection of the tracer gas (helium), for direct back-mix experiments. At the center of the back-up plate a 2 in. dia. helium injection tube is placed for the tracer injection as described in Sec. 4.1. (A 1/2 in. tube was used but it was found the helium velocity out of this tube was so large, much larger than the underfire air velocity through the back-up plate, that it flew as a separate stream in the model.) With the 2 in. tube the velocity of the tracer used at 2% to 4% of the air flow in the box comes down to underfire air velocity and is found to be suitable. (At the underfire air velocities used, no helium diffused up above the back-up plate.) The other end of the 2 in. tube is reduced to 1/2 in. which in turn is connected to a solenoid valve used for helium cut-off. In Fig. 2, two layers of jets are shown sited at two levels of the box. These are for overfire air injection and to study the effects of changes in offset angle, spacing, and momentum ratio of overfire to underfire air on mixing. The offset angle is defined as zero when the jets are directly opposed and 90° when the jets are tangential to the box. Five offset angles 0°, 15°, 30°, 50°, and 70° were used in these investigations. The offset angle could be changed by inserting new sections with a different offset angle already built in it. The box was built of sections, 6 in. long, as already indicated, for the above purpose and also for changing the spacing between the jet arrays. Spacing changes were accomplished by moving a section of the box, down the jet layers, to a region in between the jet arrays forming the countervortex burner. It can be seen from the arrangement of jets that the two layers swirl the fluid in opposite senses since the offset of the jets is opposite. The top jet array was always placed at 2 in. from the back-up plate since it is desirable to create the mixing region directly above the plate. The box has also got a 6 in. dia. outlet exhausting into a 6 in. line.

4.3.2. Furnace Simulation Model - Fig. 3

This is similar in construction to the above model except for the burner construction. The burners used are straight and swirling jets and these could be fitted at the center of the inlet plate. The box is then, 1 ft. x 1 ft. x 4 ft., built of 1/4 in. plexiglass sheets, erected vertically. The box has an outlet 6 in. in dia. exhausting into a 6 in. line. Forty-six sampling holes at 1 in. intervals, and the 3/8 in. holes on another side were constructed as in the incinerator model described above. However at the inlet to this box burners shown in Figs. 4A, 4B, 4C could be fitted to study the mixing effectiveness produced by the various burners, described below. Specifically three burners were used, all illustrated in Fig. 4.

(i) Straight jet - Fig. 4A: The jet body is a cylinder 6 in. long with a 1/2 in. coaxial tube for the helium supply. Three diameters were investigated: 2 in., 3 in., and 4 in. Using the 4 in. dia. jet, the box Reynolds number was varied in the experiments from

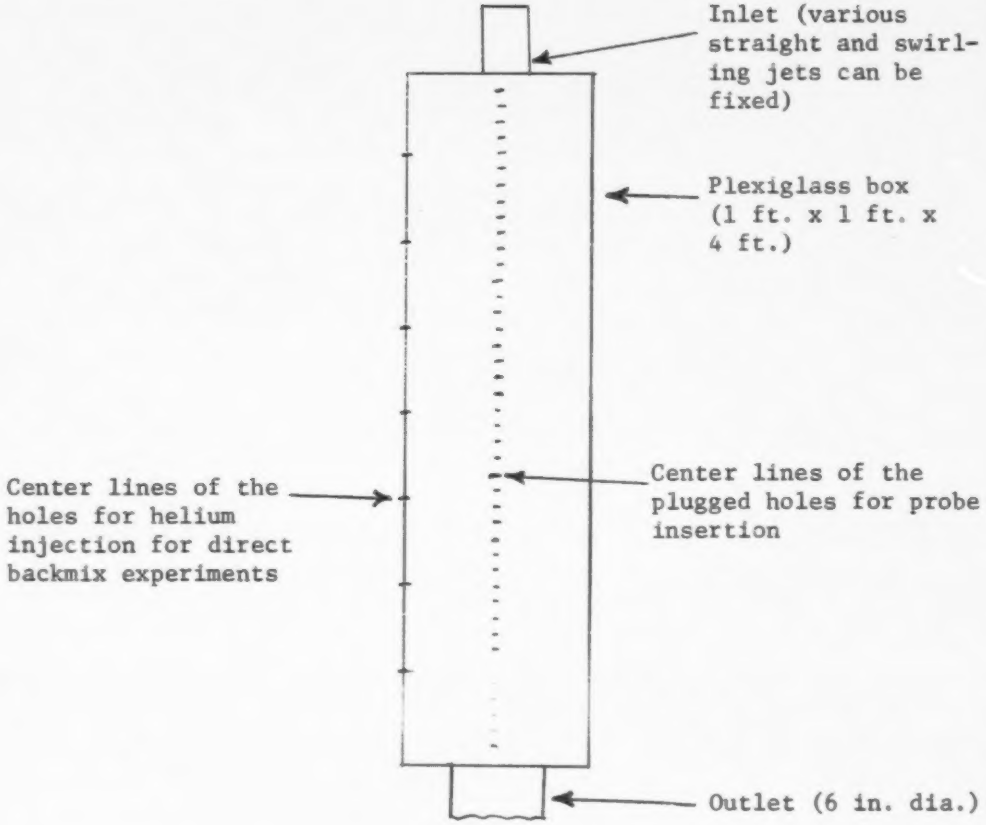
Inlet (various straight and swirling jets can be fixed)
Plexiglass box (1 ft. x 1 ft. x 4 ft.)
Center lines of the holes for helium injection for direct backmix experiments
Center lines of the plugged holes for probe insertion
Outlet (6 in. dia.)

Fig. 3. The Furnace Simulation Model with Arrangement for Fitting Various Jets at the Inlet.

Fig. 4. Sketches of Straight, Tangential Entry and Vane-Swirled Burners.

4A. Straight tubes (d = 2 in., 3 in., 4 in.) are used to study mixing created by unswirled, straight injection.

4B. Tangential entry jet, with axial unswirled and two tangential air inlets.

4C. Vane-swirled burner with secondary vanes capable of producing various levels of swirl, and primary vanes (fixed) and producing swirl in the axial air also.

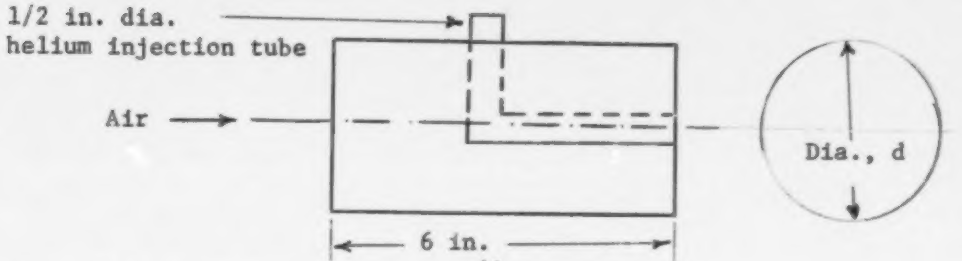
1/2 in. dia.
helium injection tube
Air
Dia., d
6 in.

4A

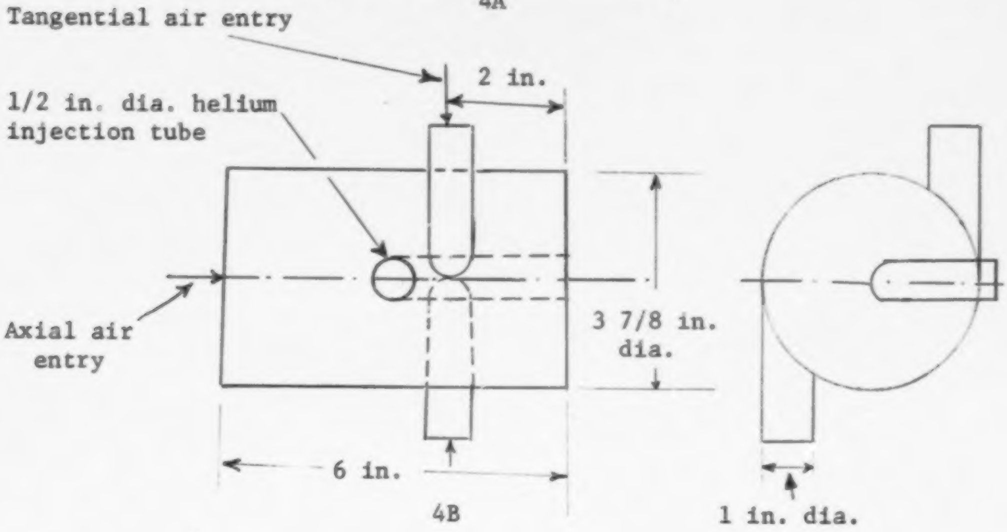
Tangential air entry
2 in.
1/2 in. dia. helium
injection tube
Axial air
entry
3 7/8 in.
dia.
6 in.
1 in. dia.

4B

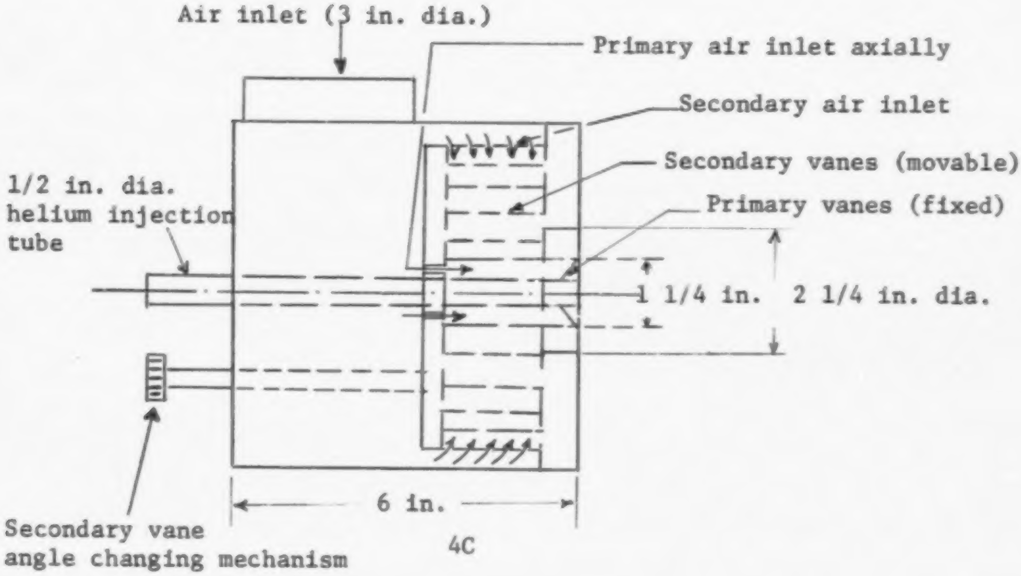
Air inlet (3 in. dia.)
Primary air inlet axially
Secondary air inlet
Secondary vanes (movable)
Primary vanes (fixed)
1/2 in. dia.
helium injection
tube
1 1/4 in.
2 1/4 in. dia.
6 in.
Secondary vane
angle changing mechanism

4C

2010 to 19200 in 10 steps. With the other two diameters, only experiments at Re_b = 12530 were carried out.

(ii) Tangential entry jet - Fig. 4B: In this unit the fluid jet can be swirled. The burner is substantially the same as the 4 in. dia. straight jet but for the addition of two 1 in. dia. tangential entry ports about 2 in. from the burner exit. The burner was always operated at the same (constant) total rate of air supply, generating a Reynolds number in the box of 8000, but with varying proportions of air supplied axially and tangentially. In the experiments the tangential percentage supplied was varied over the complete 0% to 100% range.

(iii) Vane swirled jet - Fig. 4C: This was a model of a standard burner used in a utility plant, kindly supplied by M. G. Malhouitre of the Electricite de France. It has a central 1 1/4 in. dia. primary pipe with 70° fixed vanes at the end, intended in the actual unit for fuel supply but fitted in the model with a helium supply pipe. Surrounding this, coaxially, is a cylinder of 2 1/4 in. dia. fitted with movable vanes capable of swirling the flow in the same direction as the primary vanes. The whole is surrounded by a 6 in. dia. wind box supplied through a 3 in. dia. pipe from the fans. The wind box supplies both primary and secondary air, with about 75% flowing through the secondary register (though there is some control of this). The secondary vane setting can be changed continuously from fully closed (0°) to fully open (90° - radial injection, zero swirl). In experiments with this burner, the effect of vane setting was first investigated, changing the setting from 10° to 90° in 3 steps, at a constant Re_b = 11900. At 10° vane setting the effect of flow velocity was then investigated for a box Reynolds number range of 7000 to 11500.

On test, all burners were fitted in the center of the upper end plate of the model, with the burner center-line on the model axis, and the end of the burner flush with the underside of the end plate.

Helium tracer could be supplied at the center of the burners by 1/2 in. tubes at about 2% to 4% of the carrier flow.

4.3.3. Gas Sampling System - Fig. 5

This consists of an analyzer, capillary tubes for gas suction, a power supply unit to the analyzer, two flow meters, and flow stabilizing and controlling equipment.

The analyzer is a (Gow-Mac) thermal conductivity analyzer with two thermal conductivity cells (with thermistor elements in the cells) connected into a wheatstone bridge. Through one of the cells atmospheric air is sucked as a reference gas and through the other sample gases from the box in which the mixing effectiveness is to be studied are sucked. When the box contains only air the bridge is balanced at any current through the cells. However when helium is present in the sample side, the bridge becomes unbalanced due to the higher thermal conductivity of helium in air, and the bridge was found to give an output which increases linearly proportional to the concentration of helium in the sample gases. This means the bridge output (mv) can be directly used as an indicator of concentrations, particularly when taking ratios of concentrations as is needed by the theory (Eqn. (5.16)). The thermistor used for filaments has a large negative temperature coefficient of resistance and thus gives large outputs for small changes in concentrations. Also this analyzer has a very fast response (small response time) and this is found to be

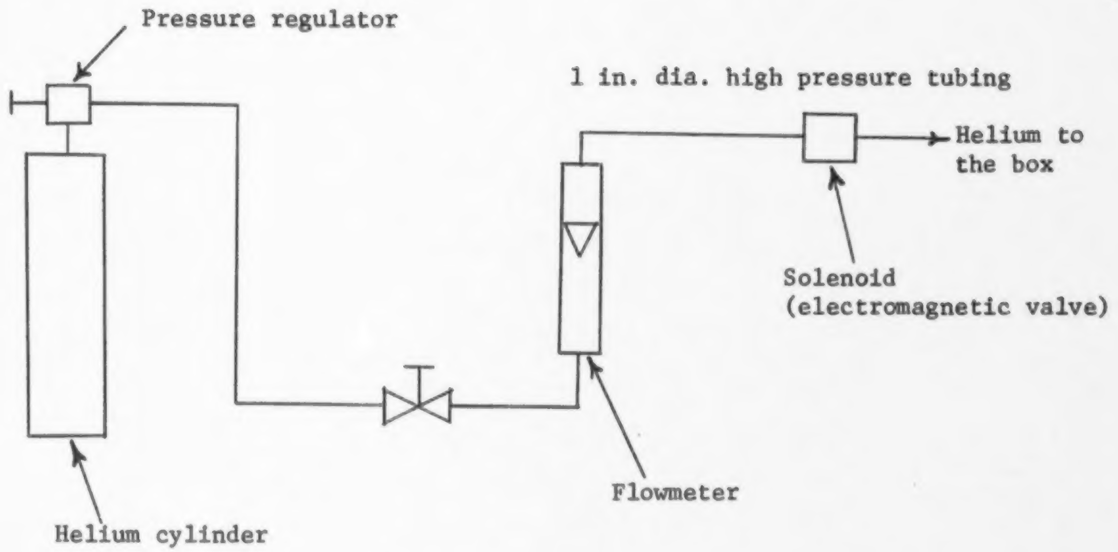
Pressure regulator
1 in. dia. high pressure tubing
Helium to
the box
Solenoid
(electromagnetic valve)
Helium cylinder
Flowmeter

Fig. 5. Schematic Layout of the Tracer Supply System.

extremely desirable for monitoring the unsteady state decay of the tracer gas after its cut-off. Fast response is necessary because, if the response is not fast, a distortion is produced by the instrument on the system response and this is called "instrumental effect" and explained in greater detail in Sec. 6. This type of fast responding, high sensitive analyzer was particularly found better suited for our studies where it is desirable to use small concentration levels and still be able to measure them accurately; larger tracer levels are undesirable, because when the tracer flow is cut-off, the flow rate will change and the analysis of the results becomes difficult and erroneous.

(Before using the Gow-Mac analyzer, a Lira analyzing CO_2 was used; but the Lira was so insensitive compared to the Gow-Mac analyzer, that CO_2 up to 10% of the total flow in the box had to be used to get measurable outputs. This used to consume large amounts of CO_2 and also found undesirable because of its possible effects in changing the flow conditions in the box after the tracer supply was cut-off. Therefore use of the Lira was stopped. However, there was another very important reason to discontinue the use of the Lira. This was due to its very slow response. For a step change in the input, the Lira had a response time of 10 seconds for a 63% change in output. (This response time used to be two to four times the residence time of the carrier air in the box.) The slow response was found to distort the system response so much that analysis of the results was made uncertain. The Lira also had a large initial time during which it would not respond to any step changes at the inlet. This made the analysis of the response still more uncertain; therefore further use of the Lira was abandoned and the Gow-Mac analyzer was bought and developed for our use as described below.)

The Gow-Mac analyzer, as manufactured and suggested for use by the manufacturer had a response time, 2.5 seconds, with much faster response than that of the Lira. However the instrument response time is found to be a function of the bridge currents, and the gas flow rates through the analyzer. When the bridge current and the flow rate was increased the response time could be brought down to about 8/10 second. Further increases were found to be detrimental to the instrument life and thus were abandoned. (See Appendix A for more details of this instrument behavior.) In fact there was a real instrumental problem before the technique using the Gow-Mac analyzer was developed.

Others who have used the above tracer technique have generally had much larger systems: e.g., both Beer and Lee (3), and Drake and Hubbard (4) used tracers (argon by Beer, radioactive krypton by Drake) in the full-sized furnace, so that the instrumental response was fast in relation to their residence times. Beer and Lee (3) also used water models, with salt tracer and an electrolytic detector which responds immediately. (We considered, but rejected water models because of the large quantities of water required.) When it became clear, working at the scale we had chosen, that the manufacturers information on the speed of response of the analyzers was misleading (when using the instruments to follow this type of transient behavior) we started inquiries about other systems. One that is quite promising involves a gaseous ionization detector, but this is as yet essentially undeveloped for commercial purchase (78). Another interesting possibility also depended on ionization but using a radioactive source. A third was to use an IR beam across the outlet of the box. The disadvantage of this is that it would be impossible to sample locally inside the box. The most promising alternative of all is a mass-spectrometer which was not provided for in the proposal to the sponsors and thus could not be bought because of the large amount of money involved. Also the Gow-Mac analyzer was found to be satisfactory and thus used in these studies. The output of the analyzer was recorded on a Honeywell strip chart recorder (Electronic 19). This recorder has a maximum chart speed of 1 in./sec., which was the speed used in our studies. The recorder also had spans ranging from 0.1 mv to 100 v in 20 steps; however, spans of 100 mv, 200 mv, and 500 mv were commonly used to increase the resolution of the outputs recorded. Also the recorder had provision for zero adjustment which is ± 10 times the span used. This was a big advantage since the Gow-Mac gives a zero-output of the order of 50 to 100 millivolts which has to be suppressed using the recorder zero adjustment since the analyzer had no suppression arrangements. The analyzer was contained in a temperature controlled box whose temperature could be controlled to ± 1/10°C. As explained above the operation of the analyzer depends on the D.C. current supplied to the analyzer. For this purpose a balanced power supply unit was used to supply the analyzer with constant D.C. voltage and current at the required levels. This unit of course plugs into an A.C. line.

For analysis, gases had to be sucked from the analyzer. Therefore a 1/16 in. dia. rubber tube was used. However the flow rates through the instrument, according to the manufacturer, had to be only 0.25 cc/sec. and at this flow rate the transit time through the tubes was 6 sec., which was more than the residence time in the plexiglass box, which made analysis of the results uncertain. Therefore capillary stainless tubings of various diameters were tried ranging from 0.01 in. to 0.05 in. and a capillary with an I.D. of 0.015 in. was found to have a transit time of 0.55 sec. at a flow rate of 15 cc/min. But at this flow rate the response time was about 2 sec., and hence it was found necessary to increase the flow rates further to bring down the response time. But with the existing suction pump, through the 0.015 in. I.D. tube, enough gases could not be sucked because of the large pressure drop; therefore a 0.03 in. I.D. tube was tried and found to be satisfactory. It gives a transit time of 0.8 sec. at 50 cc/min. and the response time of the instrument was then found to be about 0.75 sec. at 50 cc/min. and 8 ma bridge current. With this flow rate the experimental value of the transit time in the capillary tube checks very well with a value calculated by dividing the volume of the capillary tube by the flow rate through the tube. Since this transit time was small and also could be accurately determined by the tracer cut-off experiment on the analyzer itself, two capillary tubes of 5 ft. long were silver soldered to the inlet end of the instrument, one on the reference and the other on the sample side; (certain necessary changes to the cells at the inlet, like plugging the 2 in. x 1/8 in. dia. holes through the blocks, etc., had to be done which is not included here. When the reference side tube was not included, the zero output of the instrument was so large that it could not be completely offset. This was solved when two capillary tubes of equal lengths were used on sample and reference sides.) The length of the tubes at 5 ft. was selected as a compromise between pressure drop and the length necessary to reach all the holes in the box from a platform, 30 in. above the floor, on which the analyzer was mounted. To increase the capacity of the pump another pump was connected in series with the existing pump, which increased the flow rates.

Other parts of the gas sampling equipment are the vacuum stabilizers that were found to stabilize the flows through the reference and sample sides and gave a steady, unfluctuating output. Before the stabilizers were used, large fluctuations in output were felt even though the sample gas concentrations were steady. The problem was traced to the fluctuations in the flows through the instrument caused by the suction pump. This could be seen by the fluctuations in the readings of the rotameters used in the reference and sample lines for measurement of flow and large fluctuations of the mercury-column of a manometer. Even when the above centrifugal type pump was changed over to a reciprocating pump or an aspirator sucking gases, the fluctuations did not die down. Then when two separate pumps were used, one on the reference side and another on the sample side, out of phase fluctuations increased the fluctuations in the output. Therefore the use of two separate pumps was abandoned. Finally, two 5 gallon bottles were filled partially with rashig rings and made vacuum tight. Then the suction pump sucked air from the space over the rashig rings of one bottle. A long tube was passed to reach the bottom of this bottle and this tube was connected to a tube in the other bottle to suck gases from the space above the rashig rings in the other bottle. Another long tube was passed to reach the bottom of the other bottle. This tube was then connected to two calibrated rotameters, through two controlling needle valves, which were in turn connected to the analyzer outlet. Provision of the bottles coupled with the use of two, equally long (5 ft.), capillary tubes on the inlet side of the analyzer eliminated the fluctuations described above and the instrument could be used for analysis.

4.3.4. Tracer Gas Supply System - Fig. 6

Various tracers like helium, CO_2, N_2O, argon, radioactive krypton, smokes, oil-fogs, have been used in the past as tracers in the air models. However, helium was selected in these studies because of its large thermal conductivity and hence the sensitivity and accuracy of the Gow-Mac analyzer increases with helium. (As has already been shown by Forstall and Shapiro (37) the molecular properties of gases do not affect the turbulent mixing rates and therefore any tracer can be employed with little or negligible effect on the results.) Since large outputs are obtained with small concentration of helium, the tracer was supplied at 2% to 4% of the air flow rates and at this rate the helium supply velocities from the supply tubes were of the same order of magnitude as those in the burner (about 30 ft./sec.). To supply helium at these rates compressed helium bottles were used. Regulators on the bottle reduced the pressure from cylinder pressure to line pressure and maintained the flow rate constant although cylinder pressure decreased with time. The bottle was connected to a calibrated rotameter, for flow measurement, which in turn was connected to a solenoid valve through a controlling needle valve. The purpose of the solenoid valve was to cut-off helium supply abruptly to the model, and this is accomplished since the solenoid valve closes from the open position in a few microseconds. To record the moment of helium cut-off by the valve an electronic switch was built into the electrical supply line of

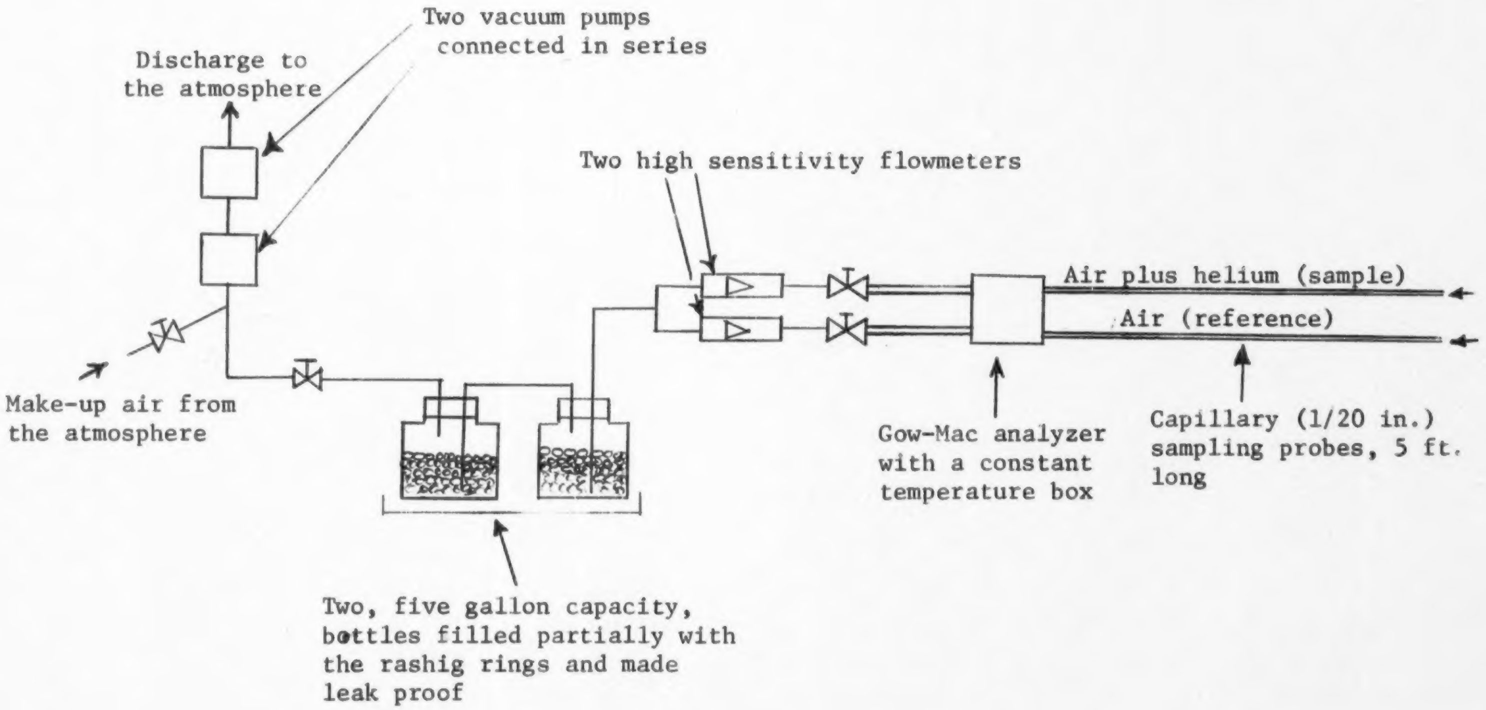
Two vacuum pumps connected in series
Discharge to the atmosphere
Two high sensitivity flowmeters
Air plus helium (sample)
Air (reference)
Make-up air from the atmosphere
Gow-Mac analyzer with a constant temperature box
Capillary (1/20 in.) sampling probes, 5 ft. long
Two, five gallon capacity, bottles filled partially with the rashig rings and made leak proof

Fig. 6. Layout of the Gas Sampling System.

the solenoid valve. (Details of the switch will be given below.) The outlet of the solenoid valve was connected to the helium supply tubes and the length of the tube between the valve and the box inlet was only a few inches so that any helium present downstream of the valve, after it is cut off, is negligible.

Sometimes titanium tetrachloride smoke was injected into the airstream for flow visualization; this smoke is found to be very toxic and to leave a coating on all the flow passages and the model and thus its use was only temporary and later abandoned.

4.3.5. Carrier Gas (Air) Supply System

This system has to be designed such that it can provide enough quantities of air into the box. As has already been explained the flow rates in actual furnaces and incinerators are such that the Reynolds numbers of the flow may be as high as 10^5. But sometimes the Reynolds number may be smaller and in at least one incinerator quoted by Fryling (12) the Reynolds number was 45000. To model these furnaces and incinerators, it is desirable to maintain equal Reynolds numbers between prototype and the model. However as already indicated in Sec. 2, certain similarity laws can be relaxed and Reynolds similarity is one such. Usually models are operated at reduced Reynolds numbers in the turbulent regime and the Reynolds numbers in the region of 10^4 are found satisfactory by many investigators in models. This reduced Reynolds number brings in economy and experimental convenience. Smaller flow rates will be needed and so smaller blowers, pumps and lines, valves, and flowmeters can be used. Smaller Reynolds numbers mean increased residence times and therefore increased instrumental response times can be allowed, and flow visualization becomes easier since velocities will be smaller.

The air-supply rates were then decided to give Reynolds numbers of 10^4 in the box. Two 3 in. and 4 in. lines were considered for supplying the necessary air flow and when pressure drops were calculated a 3 in. line was found satisfactory and hence was used. However two blowers (pyronics 16 oz., 250 cu.ft./min.), connected in series, were used to supply the air flow. This was necessary to overcome the rather high pressure drops in various bends and elbows. The layout of the air supply system is included in Fig. 1. An orifice meter (3 in. dia.) was used to measure the flow rates. Different orifices could be introduced to measure different ranges of flow rates for increased accuracy of measurement. The outlet of the orifice meter was branched into three outlets. One outlet was connected to the furnace model, the second was connected to the incinerator model and the last one supplied air to tangential ports of the tangential entry burner. All these three outlets have gate valves to cut-off or supply air flow to either one of the boxes. For example when the incinerator model was tested, airflow to the other two outlets was stopped. When the furnace model was operated, airflow to the incinerator model was cut off. When the incinerator model was operated, the air flow to the tangential jets was supplied by a third blower and measured by two rotameters, each rotameter measuring the air flow to one array or layer of jets. The flow was so adjusted that equal flows entered the two arrays of jets. The other air, underfire air, was supplied by the primary line as described before. When a tangential entry jet was used the axial flow was measured by the orifice meter and the tangential flow was measured by two rotameters.

This completes the description of the air supply and measurement system.

The rotameters and flowmeters were calibrated using a stop watch and a wet test meter.

4.3.6. Ancillary Equipment

This consists of an electronic switch built into the electrical supply line of the solenoid valve and three voltage-stabilized transformers.

As will be explained below the experimental technique or procedure is to set-up a steady state level of helium in air inside the model. Then the helium supply will be abruptly cut-off at the inlet, and from this moment analysis of tracer variation with time is needed. Then it becomes very important to know the exact time when the tracer supply was cut-off. For this purpose an electronic switch (Fig. 7) was built using electrical resistances, capacitances, and two solenoid switches (on-off type). One switch is normally closed type and the other is normally open type. Various magnitudes of resistances and capacitances were tried so that the pip produced by this switch on the recorder trace is about 5 millivolts and decays in less than 1/10th of a second. This was achieved when resistance was 1000 ohms and capacitance was two microfarads. When S_1 is closed to supply tracer gas, S_2 opens and S_3 closes. This charges the capacitor C. As soon as the switch S_1 is opened, the tracer supply is cut-off, S_2 closes and this makes the capacitor discharge a few millivolts into the recorder

Fig. 7. Layout of the Electronic Equipment. [This is built to produce a pip in the output of the analyzer when helium supply is stopped (S_1 is opened). Capsitor is charged when S_1 is closed and is discharged when S_1 is opened for the tracer cut-off.]

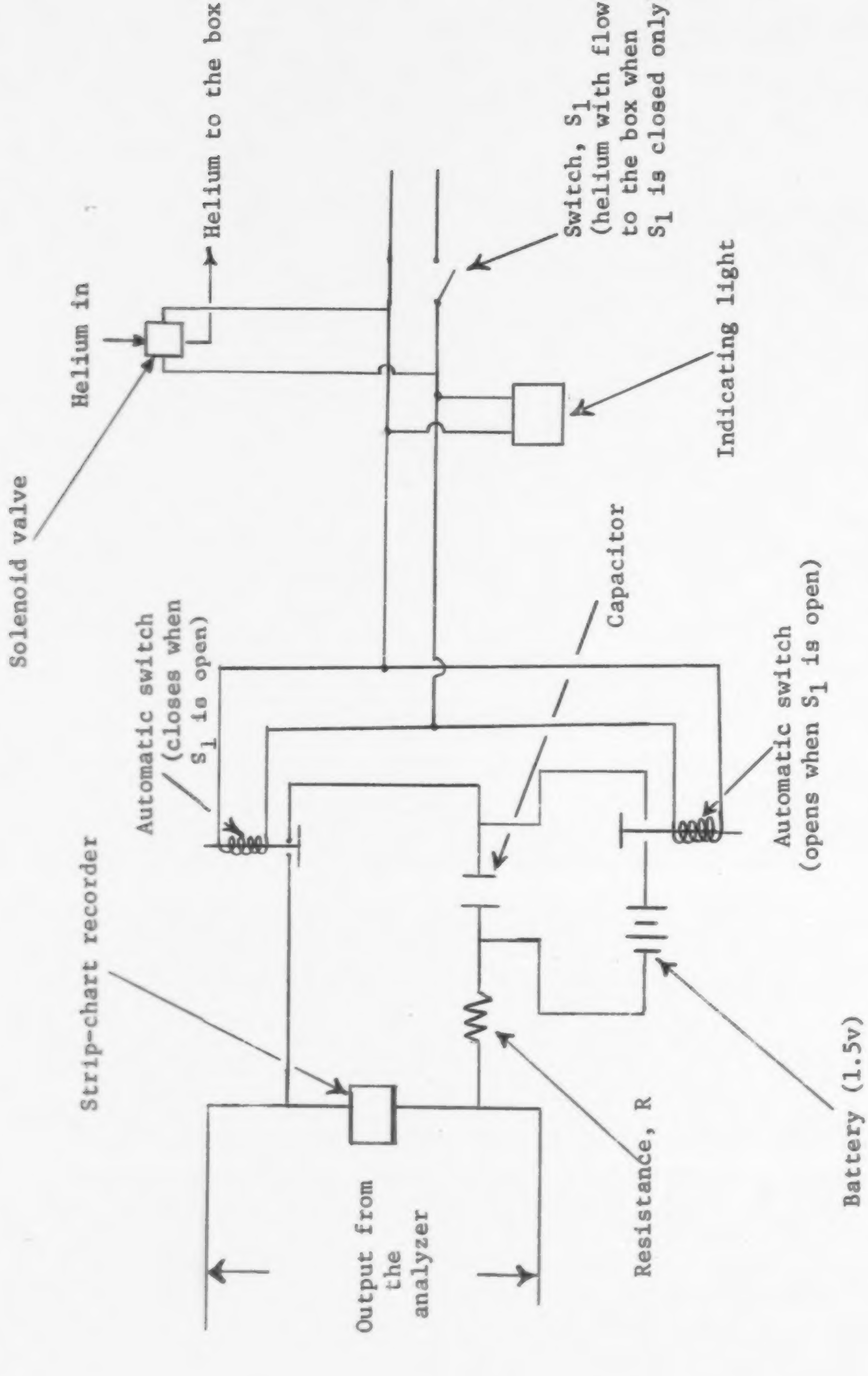
Helium to the box
Helium in
Solenoid valve
Switch, S_1 (helium with flow to the box when S_1 is closed only)
Indicating light
Automatic switch (closes when S_1 is open)
Capacitor
Automatic switch (opens when S_1 is open)
Strip-chart recorder
Battery (1.5v)
Resistance, R
Output from the analyzer

and the discharge rises fast and then decays. The rate of rise and decay is governed by the decay constant of the R-C circuit which is minimized to 1/10 sec. by matching the resistance and capacitance in the circuit. The rise and decay appears as a pip on the recorder trace.

The next ancillary equipment that needs mentioning is a group of three constant voltage transformers used to supply a stable output to the power-supply unit of the analyzer, the recorder, and the vacuum pumps. It was found that whenever other loads, like motors, were switched on in the building, the voltage to the analyzer was abruptly reduced and this used to appear as undesirable pips in the output and the pips appeared for long time. This was eliminated by using the above constant voltage transformers.

4.4. Procedure

The following typifies the procedure for all the experiments. Before an experiment can be run, the analyzer in its constant temperature box must be at a steady state. To reach this requires about four or five hours preheating, to 35°C (automatically controlled). At the end of this period the gas flow through the analyzer is started, and a further stabilization period of about 30 min. is required before the bridge is finally balanced. The cells can be run at higher temperatures, making the analyzer more sensitive, but the life of the thermistors drops sharply with increased temperature. At the steady state the cell pressure is about 72 in. Hg (absolute) (21.5 in. w.g. vacuum), at a flow rate of 50 cc/min. Measuring and controlling this very low flow rate caused considerable difficulty in setting up the analyzer in the first instance because of the high sensitivity of the accuracy of the response to variations in flow rate, but this problem was finally solved when sufficiently sensitive and accurate flowmeters (Brooks flowmeters) were installed in the two lines. The final bridge balance can be left till shortly before a run starts, after temperature stabilization inside the constant temperature box with flow is established. To make this final balance, the bridge voltage is applied (20 v) and the bridge current adjusted to 8 ma. This can be done about five minutes before the start of the first experiment; the balance is rechecked about every half hour during a sequence of several experiments and has been found to be quite stable.

The carrier air flow also has to be started sometime (generally about one hour) in advance of the start of the first experiment because the rather high frictional losses in the lines cause some degree of heating, and the thermal capacity of the pipelines requires about an hour for the air temperature and pressure to reach a steady state. The air flow rate to the model is adjusted by a gate valve in the air supply line. When the carrier air and analyzer have reached their steady states, an experimental run is started by switching on the helium supply. For technical reasons explained below, we follow the decay of the tracer concentration from a steady state, rather than its rise from zero. The helium flow rate is therefore adjusted to give roughly a concentration of 2% in the carrier air at the exit; when the flow system reaches steady state, this concentration generates a bridge output of about 75 mv. This takes about five minutes. A run is then started by closing the electromagnetic valve and recording the concentration changes as the tracer clears from the model. The reason for following the decay from a steady state rather than the rise from zero concentration is that the accuracy of measurement by the analyzer is much greater when measuring a small concentration difference (between two "high" values) than when measuring a small absolute concentration (from zero). It is particularly important that the initial changes should be measured accurately because they represent either accurate agreement with, or for important physical reasons, significant deviation from theoretical expectation, and we must be able to distinguish as accurately as possible between the two possibilities.

For recording the analyzer response the Honeywell fast pen recorder is used, generally set to 100 mv full scale, recording at 1 in./sec. Readout is continued till the pen trace drops below 5 mv, when the measurements become erratic, with low accuracy. The total duration of a typical run will range from 7 to 25 sec. depending on the carrier air flow rate. The run is completed by recording the following additional data: static pressure, temperature, and velocity-head drop across the orifice meter; barometric pressure and relative humidity in the laboratory.

During the run the sampling probe is, of course, kept in the same position. For a sequence of experiments on a given burner configuration at a given air rate, the first probe position is generally the model exit. When the first experiment and repeats are finished, the probe is repositioned, inside the model, a few inches upstream from its first station and generally still on the model axis, and the experiment is repeated. The experiments are then repeated with the probe moved progressively in steps up the chamber axis, till it is about 2 to 3 in. from the back-up plate in incinerator simulation and 2 in. from the inlet in the furnace model.

Because of scatter, each experiment is repeated between five and ten times at each probing station, and the results reported are based on about 5000 such measurements representing about 2000 measurements in the incinerator model and the rest on the behavior of jets in the furnace model. These included measurements for jet offset angles of 0°, 15°, 30°, 50°, and 70° for the incinerator model. The spacing was varied only for the 30° offset angle, but from zero to 26 in. in 5 steps (0, 4, 8, 14, 20, and 26 in.). The Reynolds number was also varied, by increasing the axial flow rate through the back-up plate whilst keeping the jet flow constant. This, alternatively, can be seen as changing the momentum ratio between the horizontal (jet) flow and the axial flow. Three levels of Reynolds number, or momentum ratio, were examined, for the 70° offset angle system. Another 50 experiments have also been performed with the helium injection downstream of the sampling point to determine the level of backmixing directly.

As reported above, about 3000 measurements were performed on the behavior of jets in the furnace simulation model. For the vane-swirled burner, the measurements included 10°, 35°, and the full open (90°) positions of secondary vanes. Also the box Reynolds number was varied from 7000 to 11200 in four steps. This can be alternatively viewed as variation in jet-momentum. With a swirled jet of the tangential entry type the swirl was varied in three steps: (i) all the flow entered axially with no tangential flow, this is zero swirl; (ii) 50% of the flow entered axially and the rest tangentially; and (iii) all the flow was introduced tangentially. In the above, the total flow was kept constant and the Reynolds number was 32000 based on the burner dia. of 3 7/8 in. and 8000 based on the box width of 12 in. With straight jets the diameter of the burners was varied over 2 in., 3 in., 4 in., and the flow rates into the box and the residence times in the box were kept constant with all the diameters. This provided a constant Reynolds number of 12700 (based on the box) but the Reynolds number of the jet varied due to the size difference between the jets. Also, with the 4 in. dia. jet, Reynolds number (Re_b) was varied in ten steps from 2010 to 19200. In addition, experiments have been performed, with the 4 in. jet, with helium injection downstream of the sampling point to determine the level of backmixing directly.

In free jets there is found always a potential core, where no mixing occurs, for about some distance (generally up to 4 1/2 nozzle diameters for straight jets (34)) downstream from the mouth of the nozzle. It is desirable to know whether such a behavior exists in the box; because if it exists, then it means that mixing cannot occur for some distance in the combustion chamber and thus some amount of chamber volume will not be utilized and this is undesirable. The most desirable thing is of course an instantaneous and uniform mixing of fuel with air and recirculated gases in the combustion chamber. Therefore in order to assess the extent of mixing, probing across the box was performed at 2 in. from the inlet and the profiles of the tracer concentration distribution were obtained for straight jets of 2 and 3 in. dia., "tangential-entry" jet, vane-swirled jet and the "opposed-vortex" incinerator simulation model. However it has been noticed that even with the straight jets, considerable mixing occurs just below the tracer injection tube, at 2 in. from the inlet; therefore no potential core exists in the enclosed jets tested in these studies.

As will be described in detail below in the results section, behavior of the flow approximates very well to a well stirred reactor followed by a modified plug flow. This was found out by exit and internal sampling conducted in the box as described above. However in the experiments where mixing delay times were measured the tracer was injected upstream and the probing was performed downstream. But in a well stirred reactor it should not matter where in the reactor the tracer is injected; in other words mixing delay time should not be altered by changing the injection point. To check this experimentally, helium was injected both upstream and at two different locations downstream of a probe placed in the stirred region; the mixing delay times were measured and compared. There was no significant difference due to changing the injection points in the opposed vortex system, the vane swirled, and the tangential entry jets.

These test experiments were in addition to about 100 initial setting-up experiments to establish the procedure, accuracy, repeatability, etc., and also to investigate the instrument behavior. As discussed in Appendix A, the (Gow-Mac) analyzer behaved like a stirred reactor with very close approximation to perfect stirring. At a (fixed) capillary flow rate through the analyzer of 50 cc/min. the calculated response time (instrument factor, τ_i) was 0.75 sec. This compared very well with an experimental value of 0.8 sec. determined by the helium cut-off experiments performed on the analyzer itself. This instrument behavior imposed a distortion on the output signal otherwise generated by the analysis of the gas flowing from the model. This will be discussed below in the results section. The method of determining the instrument behavior experimentally is also described below.

5. THEORY

5.1. Physical Model

Fig. 8 illustrates the typical schematic representation of an idealized, first-approximation to the desired flow patterns in a combustion chamber. This is the Bragg postulate or model, and it indicates a perfectly stirred reactor (P.S.R.) section followed by a plug flow. As mentioned above this has been used successfully in some previous investigations (3,4), but also as indicated above this is now known to be somewhat oversimplified even as a first approximation. The missing elements include: delayed mixing, which converts a P.S.R. to a "well stirred" reactor; by-pass, which results in a fraction of combustible mixture joining the reaction zone somewhat downstream (or even passing through the chamber unreacted); dead space, indicating incomplete utilization of the combustion volume. We may expect that most real combustion systems will exhibit these deviations from the ideal or Bragg model, to some degree or another, and our objective is to incorporate them in a suitable modification of the Bragg model equations. To do this (i.e., to construct the modified mathematical model) we first have to modify the Bragg model to include the above deviations. The modified model is schematically represented in Fig. 9. In this, the well stirred section is represented as an initial plug flow, to represent mixing delay, in series with a P.S.R. section following the suggestion of Vulis (5). Through the middle of the P.S.R. section, and running to the outlet is a by-pass section. This has been indicated down the axis of the chamber since this is most

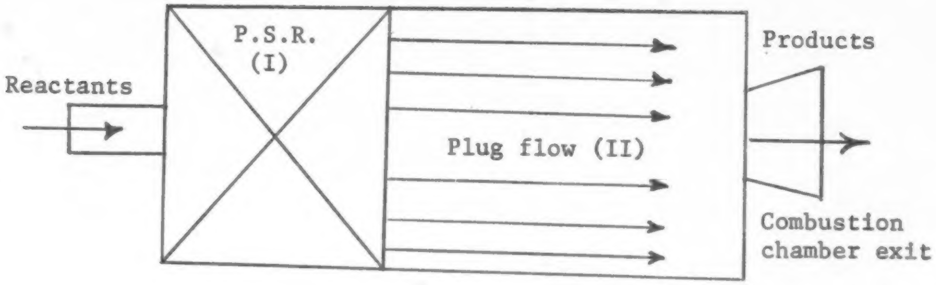
P.S.R.
(I)
Reactants
Plug flow (II)
Products
Combustion
chamber exit

Fig. 8. Schematic Representation of the Bragg's Idealized Approximation to the Desired Flow Pattern in a Combustion Chamber.

[It includes a perfectly stirred reactor (P.S.R.) section (I) to promote rapid ignition; followed by a plug flow section (II). Stirring is created by aerodynamic means.]

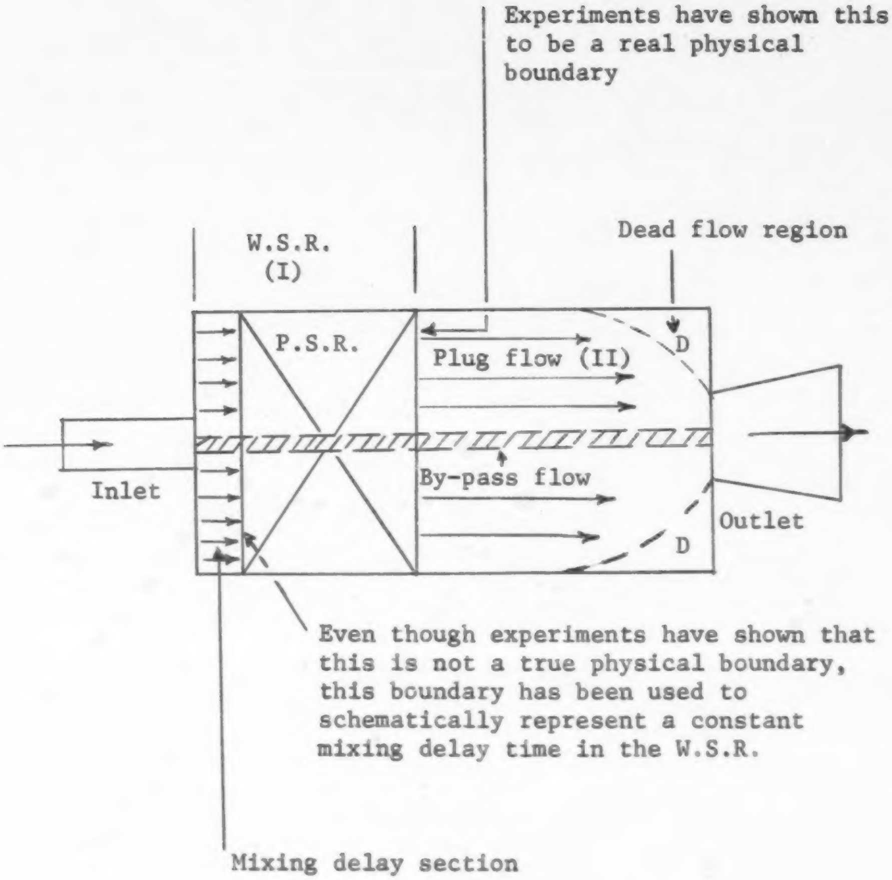
Experiments have shown this to be a real physical boundary
W.S.R. (I)
Dead flow region
P.S.R.
Plug flow (II)
D
Inlet
By-pass flow
Outlet
D
Even though experiments have shown that this is not a true physical boundary, this boundary has been used to schematically represent a constant mixing delay time in the W.S.R.
Mixing delay section

Fig. 9. Schematic Representation of the Modified Bragg Model.

[It includes the mixing delay, by-pass, and dead flow regions. Swirl burners (e.g., as found in oil firing) have been found to generate a W.S.R. and plug flow combination (3.4). Experiments on the isothermal air model, using the primary (plug) and secondary flows, have shown that the flows can be approximated by a W.S.R. and plug flow combination.]

likely to occur with a plane jet: it is not necessarily intended to represent expectations of physical reality. Also included are indications of dead flow or dead space, again representing a possible physically real location, but not necessarily so.

5.2. Mathematical Model

The mathematical model now to be constructed is intended as the mathematical representation of the physical model described above. The purpose of the model is to provide equations for experimental testing. The method of testing is the tracer technique described above; and the form of the mathematical equations we therefore need to derive is a description of the rate of decay of tracer concentration at the exit of the model.

In the derivation following, the effects of by-pass and dead space are not included; the analysis can be extended to include these but since no significant evidence of their effects has so far appeared in the experimental results, the theoretical extension has been left out.

In the model, assume an input flow rate of carrier air V cfm. In isothermal flow, the average residence time (τ_t) in the model, of volume V_o cu. ft., is

$$\tau_t = V_o/V \qquad (5.1)$$

This time is not significantly altered by starting or stopping the tracer gas (within limits of experimental measurement) so long as the tracer concentration is less than 1 or 2%.

(i) Consider first the limiting condition that the whole of the model volume is perfectly stirred, and suppose we are monitoring the decay of tracer concentration from an initial steady state value c_o ((cu.ft. x 100)/cu.ft.). This is a standard condition treated in many texts (13,82). At any time, t, after the input tracer supply is cut off, let the concentration in the model be, c, uniform throughout. In a further period of time, δt, assume that the average concentration in the model drops to $(c - \delta c)$. The drop in concentration for the whole model is $(V_o \delta c)$ which must equal the quantity leaving in the carrier flow, which is $(Vc\delta t)$. Hence

$$-V_o \delta c = Vc\delta t \qquad (5.2)$$

Substituting using Eqn. (5.1) and taking the limit we obtain the standard differential equation for the system (P.S.R.)

$$dc/dt = -(c/\tau_t) \qquad (5.3)$$

Integrating between limits $c = c_o$ at $t = 0$, and $c = c$ at $t = t$, gives

$$(c/c_o) = \exp(-t/\tau_t) \qquad (5.4)$$

This indicates that c is normalized by dividing by c_o, and t by τ_t.

(ii) Consider now the idealization represented by the Bragg model. In this the total residence time remains τ_t, given by Eqn. (5.1); but Eqn. (5.4) must be modified to include the time delay of the plug flow section before sampling. Eqn. (5.4) remains true if we recognize a residence time in the stirred section of τ_s, and write t* to indicate a real time scale referring only to behavior of the P.S.R. section. For this we therefore have

$$(c/c_o) = \exp(-t^*/\tau_s) \qquad (5.5)$$

This is the equation that would be obeyed by sampling at the junction of the P.S.R. and plug flow section. If therefore we move the sampling point to the end of the plug flow section we merely transpose the time scale, t^*, to a scale, t, which differ only by the time delay in the plug flow section, τ_p. Hence

$$t = t^* + \tau_p \qquad (5.6)$$

Eliminating t^* between Eqns. (5.5) and (5.6) we obtain

$$(c/c_o) = \exp[-(t - \tau_p)/\tau_s] \qquad (5.7)$$

However, since it is convenient to normalize the time scale using τ_t, since this is known (from Eqn. (5.1)), and τ_p and τ_s are initially unknown, we may do this by multiplying by (τ_t/τ_t) and also using

$$\tau_t = \tau_s + \tau_p \qquad (5.8)$$

Eliminating τ_p between Eqns. (5.7) and (5.8), and writing $y = \ln(c/c_o)$, we obtain

$$y = \ln(c/c_o) = [1 - (t/\tau_t)](\tau_t/\tau_s) - 1 \qquad (5.9)$$

This is the equation of a straight line between y and (t/τ_t) (which also has physically unreal values for y when $t < \tau_p$, which is the delay time before information about changes in the P.S.R. section reach the sampling point). When $t = \tau_p$, $c = c_o$, and $y = 0$. (For $t < \tau_p$, y is positive.) When $t = \tau_t$, $y = -1$; this should therefore be a common point for all lines, independently of the size of the reactor section (i.e., τ_s) although it is only a necessary but not a sufficient condition since the well stirred system also shows this same result (see below). The size of the P.S.R. section is also given by Eqn. (5.9) (and the plug flow by Eqn. (5.8)) since the slope of the line on the normalized plot is (τ_t/τ_s). Since τ_t is known, τ_s can be calculated.

(iii) Consider now the condition that the whole of the volume is well stirred. This is a modification of case (i). As described before we propose to represent this by a plug flow section (mixing delay section) followed by a P.S.R. section; so this case parallels the Bragg ideal model, except in that the plug flow section now precedes the P.S.R. section instead of following it. (We should also remember that it represents, schematically, a different physical condition.) Therefore, replacing τ_p in the Bragg model equations by τ_d, we have immediately the equations for the well stirred reactor

$$y = \ln(c/c_o) = [1 - (t/\tau_t)](\tau_t/\tau_s) - 1 \qquad (5.10)$$

which is, of course, identical with Eqn. (5.9), but where

$$\tau_t = \tau_s + \tau_d \qquad (5.11)$$

Eqn. (5.10) is again the equation of a straight line between y and (t/τ_t) (which again has physically unreal values for y when $t < \tau_d$). Paralleling the previous case, when $t = \tau_d$, $c = c_o$ and $y = 0$. When $t = \tau_t$, $y = -1$; so we have again the same common point for all the lines, independent of the size of the stirred section (i.e., τ_s), as we had in case (ii) above. The size of the P.S.R. section can be calculated by the slope since τ_t is known.

We may now consider the introduction of some theoretical stirring factor, using some suitable definition, that will--if suitably chosen--be a reasonable criterion of the effectiveness or completeness of mixing, and that can be measured experimentally. From inspection of our model, we propose that a natural ratio exists, namely τ_s/τ_t, which intuitively satisfies our requirements and expectations. Essenhigh (6) defines a stirring factor, W, as

$$W = \tau_s/\tau_t \tag{5.12}$$

where τ_t must be read as the total residence time of the well stirred section, and only in this case τ_t is assumed to equate to the total residence time of the total volume. The modification involved if the stirred section is followed by a plug flow (as in case (ii)) will be considered below.

Some substantiation for this choice in defining W can be provided by considering limits. If there is no mixing delay then τ_d in Eqn. (5.11) is zero, and $\tau_s = \tau_t$ so $W = 1$. If, at the other limit, there is no mixing whatever, $\tau_s = 0$ (with $\tau_t \neq 0$) so $W = 0$. Therefore we have a factor that ranges from zero to unity as the degree of mixing rises from nothing to complete (or perfect).

Substituting for (τ_s/τ_t) in Eqn. (5.10), using Eqn. (5.12) we obtain the tracer-decay equation now including the stirring factor, W:

$$y = [1 - (t/\tau_t)]/W - 1 \tag{5.13}$$

The stirring factor, W, can then be determined from the slope of the straight line obeying Eqn. (5.13) obtained experimentally. As W increases, the slope decreases.

(iv) Consider now the further modification indicated in the paragraph above of the combination of a well stirred flow followed by plug flow. This again can be treated as an extension of the Bragg model combined with case (iii) described above. Eqn. (5.5) still holds; Eqn. (5.6) only requires the addition of the mixing delay time, τ_d.

Therefore

$$t = t^* + \tau_p + \tau_d \tag{5.14}$$

and

$$\tau_t = \tau_s + \tau_d + \tau_p \tag{5.15}$$

Therefore Eqn. (5.7) becomes

$$y = \ln(c/c_o) = - (t - \tau_p - \tau_d)/\tau_s \tag{5.16}$$

Eliminating $(\tau_p + \tau_d)$ in Eqn. (5.16), using Eqn. (5.15), and writing as before $y = \ln(c/c_o)$ we obtain as before

$$y = [1 - (t/\tau_t)](\tau_t/\tau_s) - 1 \tag{5.17}$$

The stirring factor may be introduced again, but remembering for this case that we have to redefine τ_t in Eqn. (5.12) as the total residence time in the well stirred section, i.e.,

$$W = \tau_s/(\tau_s + \tau_d) \tag{5.18a}$$

or

$$\tau_s/\tau_d = W/(1 - W) \tag{5.18b}$$

This equation in conjection with Eqn. (5.17) defines the joint theoretical and experimental problem involved in specifying W experimentally. We have two equations and three unknowns. However, inspection of Eqn. (5.15) in conjunction with our schematic physical representation of Fig. 9, suggests that the problem may be solvable in principle if the boundary of the stirred section is either reasonably well defined physically, or can be conceptually defined by some appropriate method of extrapolation. For, if it is physically well defined, clearly sampling inside the model at different points moving successively upstream should progressively reduce τ_p (see Eqn. (5.15)), to the point where we may be able to make a decision that it is zero. This would be at the boundary of the stirred reactor section (if physically well defined). Given that, then the residual plug flow time is τ_d and all terms, including W, are calculable. This is the theoretical reason for the internal sampling already indicated, with the results outlined in Sec. 6.

6. RESULTS

The purpose of this section is to compare the results with the theory outlined in Sec. 5 and show the variation of stirring factors with design and operational variables like offset angles, Reynolds numbers, etc. The results of the incinerator model tests are tabulated in Appendix B; and that of the tests on straight and swirling jets are tabulated in Appendix C.

6.1. General Behavior

A typical decay profile of helium concentration with time, for virtually all the configurations and probe stations examined, is indicated in Fig. 10. The chief characteristics are: (i) an initial period through which the concentration remains constant, representing the sum of all plug flow times ($\tau_d + \tau_p$, see Fig. 10), hereafter called combined plug flow time, between the inlet and the sampling point; (ii) a decay period well approximated by an exponential and is in broad agreement with theory (as discussed later). Additionally, between the two primary regions, of constant concentration and exponential decay, there is a transition region providing continuity of slopes of the two sections of the curve. This is due to a real physical behavior representing a departure from the idealized model; but it was found to be very small and therefore it has been neglected; and (iii) the combined plug flow time goes on shortening as the probe is moved upstream and this behavior is again in agreement with expectation, as described in Secs. 4 and 5 and discussed later in this section.

Fig. 10. Typical Experimental Curve for the Decay of the Tracer with Time after Helium is Cut-Off at the Injection Point. (Note: Counting of the time scale is started at the end of the transit time after cut-off.)

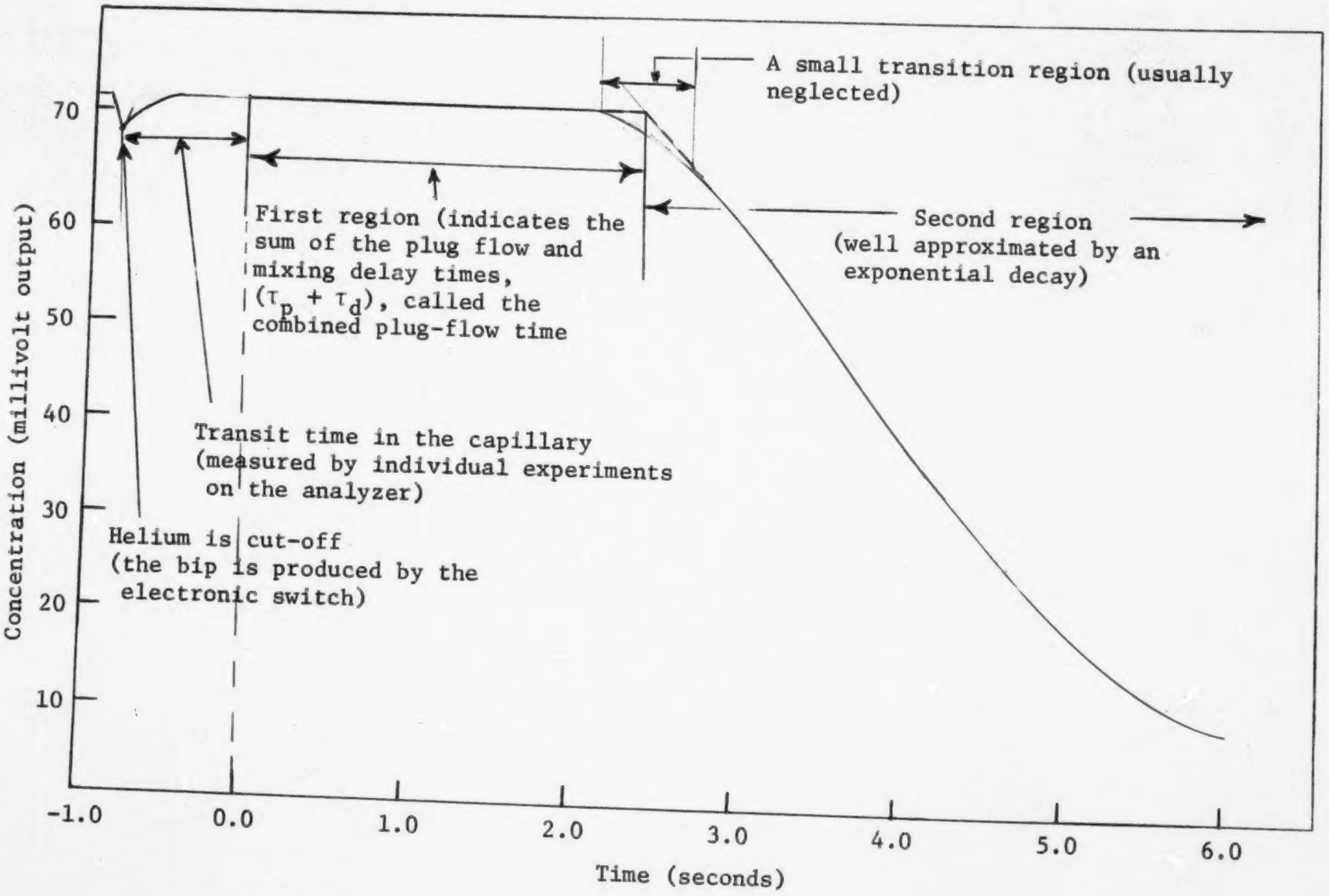
A small transition region (usually neglected)
70
60
50
40
30
20
10
Concentration (millivolt output)
First region (indicates the sum of the plug flow and mixing delay times, $(\tau_p + \tau_d)$, called the combined plug-flow time
Second region (well approximated by an exponential decay)
Transit time in the capillary (measured by individual experiments on the analyzer)
Helium is cut-off (the bip is produced by the electronic switch)
-1.0
0.0
1.0
2.0
3.0
4.0
5.0
6.0
Time (seconds)

6.1.1. Instrument Effect on the General Behavior

Only the decay portions were slightly affected by the "instrument effect," as described in Sec. 4, which was finally traced, after many experimental runs to elucidate the effect, to the behavior of the analyzer itself. The analyzer was found to behave as an effective "stirred reactor," so the net output recorded was the combined effect of the two systems, the model itself and the analyzer. A satisfactory method of correcting the net results for the instrumental effect was worked out and the details of the method of correction are described in Appendix A. Essentially the method uses the experimental finding that the response of the instrument, for a step cut-off at the inlet, is close to that of a P.S.R., an exponential response with a measurable decay constant. The effect of this on the response from the model is to change a sloping straight line that would obey Eqn. (5.16) into curve 1, as illustrated in Fig. 11. The data are supplied in Table 1, which shows the response both before correcting and after correcting for the instrument effect. This graph corresponds to a jet Reynolds number of 41250 with a straight jet (4 in. dia.). In it, the curve is the normalized plot of the raw data as they are recorded by the instrument. The sloping straight line is then obtained if the raw data are corrected for the perturbation introduced by the instrument. The correction is made by the following equation derived in Appendix A.

$$(c/c_o) = (1 - \tau_i/\tau_s)(c'/c'_o) + (\tau_i/\tau_s)\ \exp(-t^*/\tau_i) \qquad (6.1)$$

where c is the concentration after correcting for the instrument effect $c_o(+c'_o)$ is the initial (steady state) concentration, c is the

Fig. 11. Variation of the Uncorrected and the Corrected Concentrations with Three Instrument Factors for a Straight Jet (4 in. dia.) Flowing Into the Box at $Re_j = 41250$.

Curve 1 - uncorrected data with $\tau_i = 2.88$ sec.
Curve 2 - uncorrected data with $\tau_i = 1.95$ sec.
Curve 3 - uncorrected data with $\tau_i = 0.75$ sec.
Curve 4 - corrected data for all the three uncorrected curves.

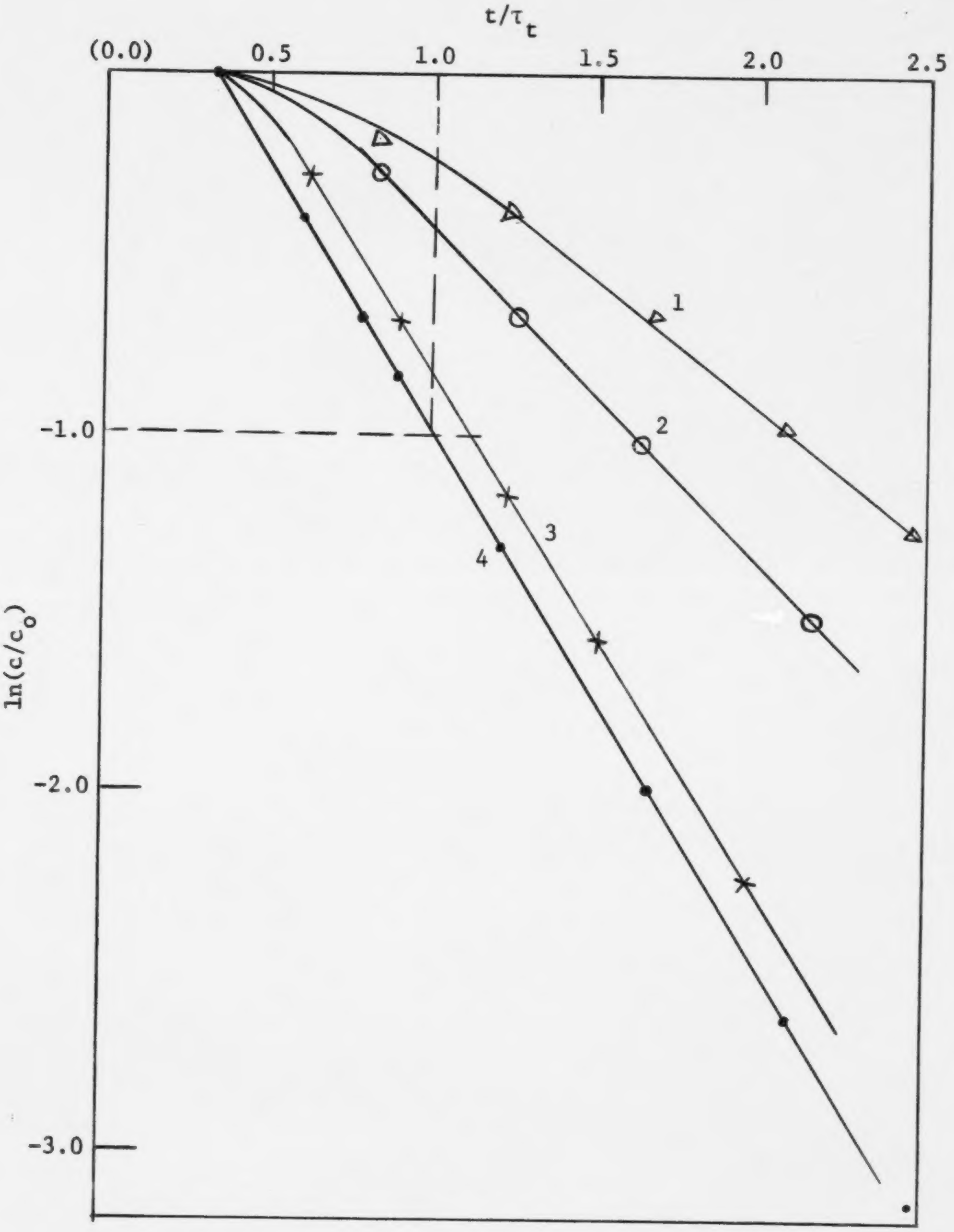
t/τ_t
(0.0)
0.5
1.0
1.5
2.0
2.5
ln(c/c_o)
-1.0
-2.0
-3.0
1
2
3
4

TABLE 1

Raw and Corrected Data for a Straight Jet[a]

τ_i (sec.)		2.88		1.95		0.75	
t (sec.)	t/τ_t	c'/c'_o	c/c_o	c'/c'_o	c/c_o	c'/c'_o	c/c_o
0-1-32	0.359	1.000	1.000	1.000	1.000	1.000	1.000
2	0.545	0.940	0.693	0.916	0.693	0.860	0.693
3	0.818	0.840	0.479	0.760	0.479	0.550	0.479
4	1.090	0.730	0.313	0.603	0.313	0.375	0.313
5	1.361	0.620	0.210	0.450	0.210	0.250	0.210
6	1.636	0.530	0.135	0.350	0.135	0.170	0.1350
7	1.910	0.420	0.096	0.275	0.096	0.115	0.096

[a] note: Jet dia. = 4 in.; $Re_j = 26400$; $\tau_t = 3.67$ sec.; $c_o = 91.0$.

raw concentration, τ_s is the residence time in the P.S.R. section in the box; $t^* = t - (\tau_d + \tau_p)$; and τ_i is an "instrument factor" that is in fact the characteristic decay time for the analyzer operating as a P.S.R. and it is measured by independent experiments on the analyzer, using exactly the same tracer "cut-off" technique that is used for the main model experiments. The value of τ_i under the actual conditions of use was found to be 2.88 sec. (at a sample flow rate of 15 cc/min. and bridge current of 4 ma and τ_s is calculated by subtracting the intercept quantity $(\tau_d + \tau_p)$ from the (calculable) value of τ_t. The intercept quantity $(\tau_d + \tau_p)$ is not affected by the instrument, and so can be obtained from the plot of the raw data.

The value of $\tau_i = 2.88$ sec. was used only in the initial stages of this thesis study. However, after further consultations with the instrument manufacturer, it was found that further increase in bridge current to 8 ma and flow rates to 50 cc/min. could be used safely with the instrument although the suggested maximum values were 4 ma and 15 cc/min. By using a bridge current of 8 ma and flow rate of 50 cc/min. τ_i was reduced to 0.8 sec. and with this reduced value of τ_i, the distortion between the raw data and the corrected value was further reduced. In fact, this observation indicates that it is really the instrument effect that produces the distortion. To substantiate this idea further, two additional experiments varying only τ_i were performed and plots of raw data are given in Fig. 11, with corresponding data in Table 1 for different values of τ_i. It can be noted that when correction was applied using Eqn. (6.1), the behavior reduces to one single coincident plot for all three cases in Fig. 11, which shows that as τ_i increases the distortion also increases. This shows that the instrument is the real source of perturbation.

6.1.2. Transit Time Determination and Allowance for Its Effects

Before passing on to the comparison of the corrected results with theory in Sec. 5, a necessary point to be noted is the counting of time ($t = 0$) after the pip produced on the recorder trace by the cut-off of the helium to the model. The time ($t = 0$) was counted after allowing a certain transit time for the gases in the capillary tubes to the analyzer. This transit time was measured by the cut-off experiments on the analyzer and also checked (within 5% error) with calculated values dividing the capillary lengths (5 ft.) into the velocity of the gases through the capillary tubes. This transit time was much larger (of the order of 5 to 6 sec.) when 1/16 in. dia. rubber tubing was used for gas suction from the box to the analyzer. To bring this time down, capillary steel tubes of 0.03 in. I.D. were used, as discussed in Sec. 4.2.3 and in these tubes the transit time was 0.8 sec. at 50 cc/min. and checked with the calculated value of 0.78 sec. at a tube Reynolds number of 150 (based on capillary I.D.) and tube velocity of 3.12 ft./sec. The effect of increasing the flow velocity was found to decrease the transit time, according to our expectations. A recorder trace produced due to the cut-off experiment on the analyzer is reproduced in Fig. 12. The pip is produced at the time of helium cut-off to the instrument, which is achieved by pulling abruptly the sampling probe out of a helium plus air mixture in the model and placing it in pure atmospheric air, out of the box. The transit time is shown marked in the figure and the decay is exponential with an

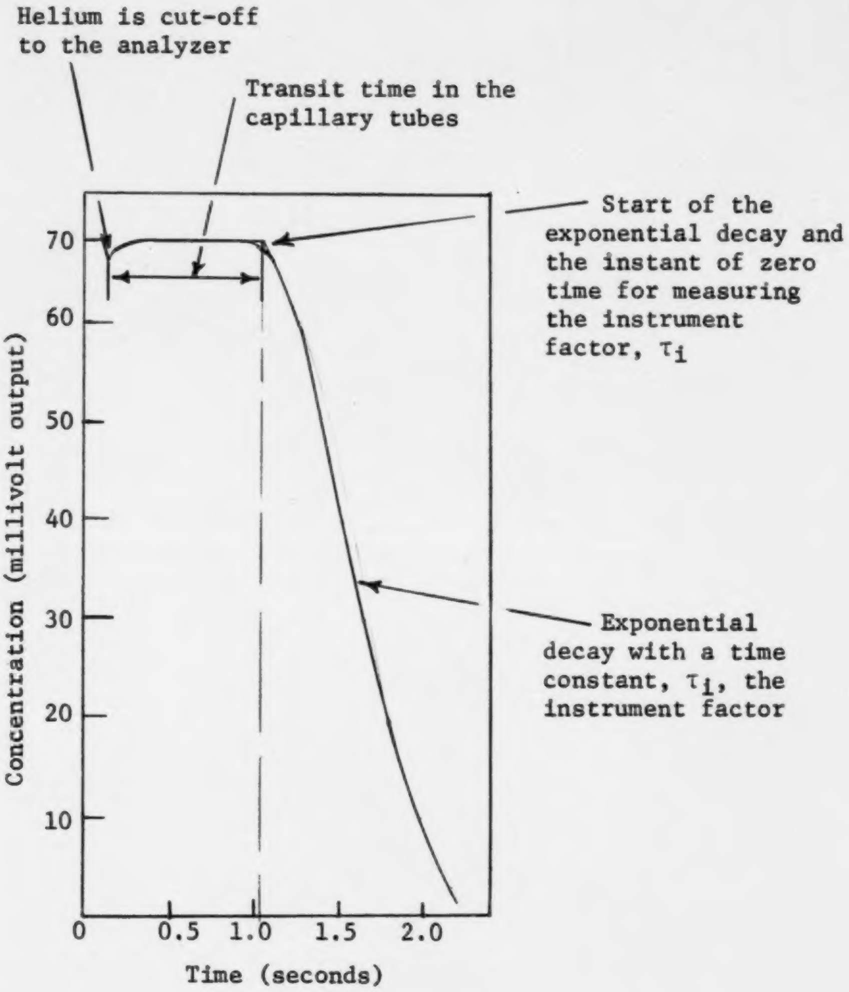

Fig. 12. Tracer Cut-Off Experiment on the Analyzer to Determine the Instrument Factor, τ_i, and the Transit Time in the Capillary Tube.

instrument factor τ_i. These experiments to determine the transit time and the τ_i, were repeated every fifteen minutes during experimental runs and found that the variation was negligible.

6.2. Summary of the Behavior of the Opposed Vortex Flow

As has already been shown in Sec. 4, two layers of jets, generating countervortex and shear, were found to be effective in stabilizing flames in smoke columns. However, the effectiveness of mixing produced and how closely the flow approaches the Bragg model was not known. To measure the effectiveness of mixing produced and to test the idea whether this can be optimized, model experiments, as discussed in Sec. 4, were undertaken and the results of these experiments showed that the effectiveness of mixing (75) was optimized at an intermediate offset angle (described in greater detail below) and that the boundary separating the plug flow and the stirred regions is physically well defined whereas there was no real physical boundary separating the mixing delay section and the P.S.R. section as shown in the schematic model of Fig. 9. The results also showed that there is good control over the size of the W.S.R. if the spacing (distance) between the two jet arrays was varied; however, W went down as the size of W.S.R. was increased by increasing the spacing. The effect of increasing underfire air flow through the back-up plate at constant overfire jet flow was found to decrease W. Additional experiments injecting tracer downstream of the pick-up probe showed that the amount of backmix increases with the stirring factor and in the stirred section escape probability of the tracer increases as the boundary separating the W.S.R. section and the plug flow section is approached. More information on the backmix process was also obtained in the straight and swirled jets (discussed later) which enabled us to study the backmix process experimentally and compare the mixing behavior. The above summary is amplified below, with comparison with the theory outlined.

6.2.1. Exit Sampling with Variation of the Offset Angles

The results are shown in Fig. 13, for five offset angles and the data included in Appendix B as Runs B.1 to B.5. (The results plotted in Fig. 13 are corrected for the instrument effect according to Eqn. (6.1) and the tables contain both the corrected data and the raw data. The data are tabulated in mv since the concentration is found linearly proportional to mv. For comparison with Eqn. (5.16) the plots in Fig. 13 are plotted with ln (c/c_o) versus (t/τ_t). The exit was at a distance of 46 in. from the back-up plate and the above experiments were performed at a box Reynolds number of 8830 giving a momentum ratio, between that through the overfire jets to that through the plate, of 695, and at a spacing of 8 in. between the jet arrays. It can be seen that all the curves pass through the (+1, -1) point and this checks with the Eqn. (5.16). Since the curves pass very close to the (+1, -1) point within the limits of small experimental error, it means that dead spaces are either negligibly small or non-existent. Notice that from these curves (τ_s/τ_t) and $(\tau_d + \tau_p)/\tau_t$ values can be read according to Eqn. (5.16) and then it can be seen that (τ_s/τ_t) values increase first as the angle increases and then start decreasing again. The intercept values $(\tau_d + \tau_p)$ and τ_s are known from the above and in isothermal models where density is constant these times also correspond to actual volumes or volume fractions occupied by a plug

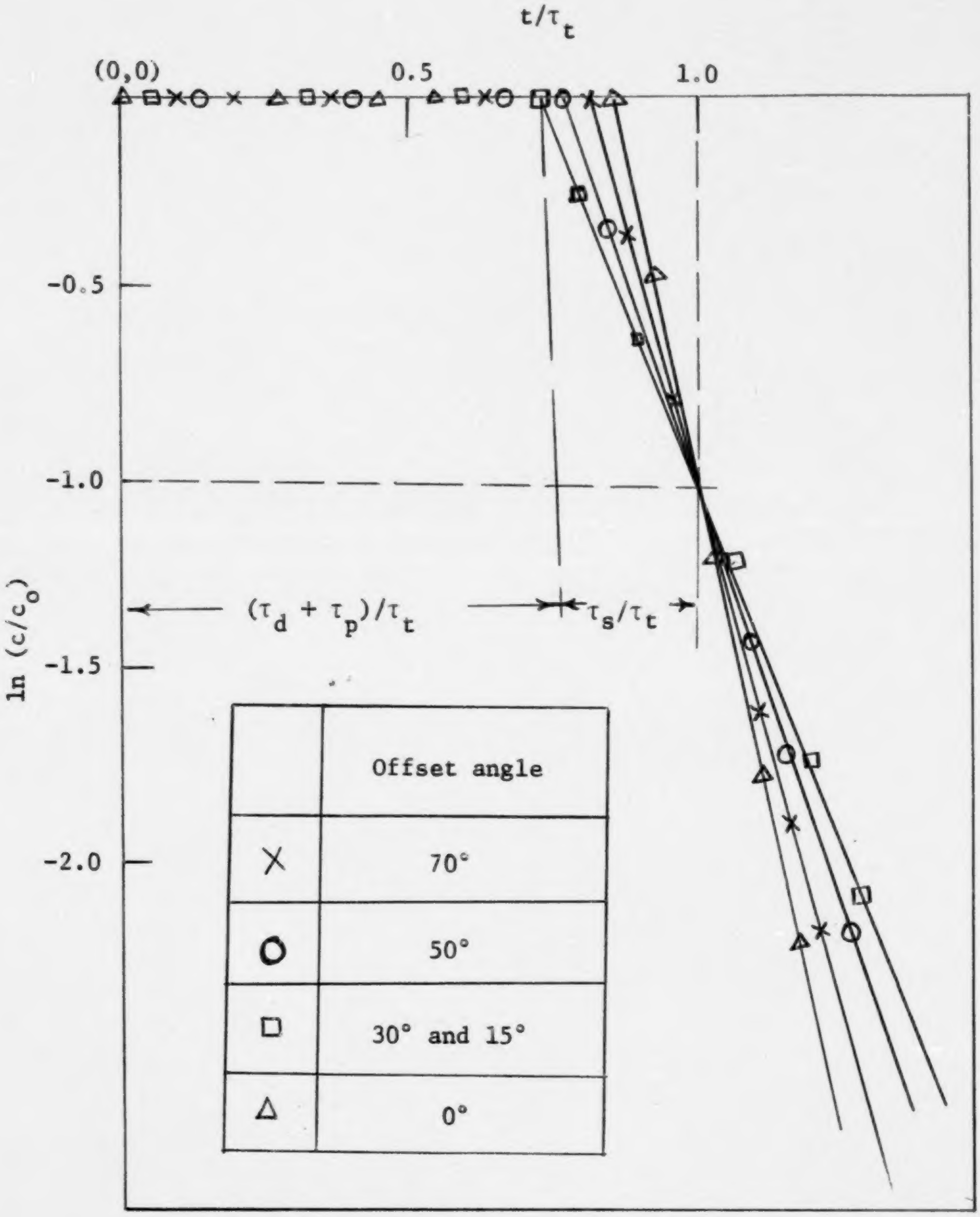

Fig. 13. Tracer Concentration Decay in the Exit Stream of the Air Model as a Function of Time Plotted for Various Offset Angles. (Spacing 8 in., Re_b = 8830, τ_t = 3.01 sec.)

flow and stirred regions. Identification of the different physical regions needs internal sampling.

6.2.2. Internal Sampling

To test the idea whether the stirred section is a compact one followed by a plug flow region with a determinable boundary between them as assumed in the development of Eqn. (5.16) and a mixing delay time (τ_d) can be measured, internal sampling as described in Sec. 4.1 was performed. The results shown in Fig. 14, in the form of variation of combined plug-flow time with distance from the inlet (back-up plate) substantiate the idea very well. As the probe station is moved up the axis of the model, reducing the distance from the inlet, the combined plug flow time ($\tau_d + \tau_p$) falls steadily as expected, but suddenly becoming constant about 12 inches from the inlet (back-up plate) and then remaining so. This is in agreement with the concept of moving from a plug flow into a stirred region, and the residual plug flow time is, therefore, identified as the mixing delay time, τ_d.

As additional substantiation of this interpretation a few check measurements were made off the axis with, mostly, no significant deviation from the axial results. This indicated that the observed behavior was substantially uniform across any horizontal. In addition, the slope of the linear part of the rise in Fig. 14 corresponds to an average plug flow velocity of 1.25 ft./sec. This agrees quite well with the value of 1.35 ft./sec. calculated from the volume rate of air supply and the model dimensions. Near the exit the slope changes, implying increased velocity. This corresponds to a convergence of the stream lines towards the exit (of 6 in. diameter compared with the

Fig. 14. Variation of the Combined Plug Flow Time with Distance from the Inlet. (Spacing = 8 in., Re_b = 8830, Momentum ratio = 695, τ_t = 3.01 sec.)

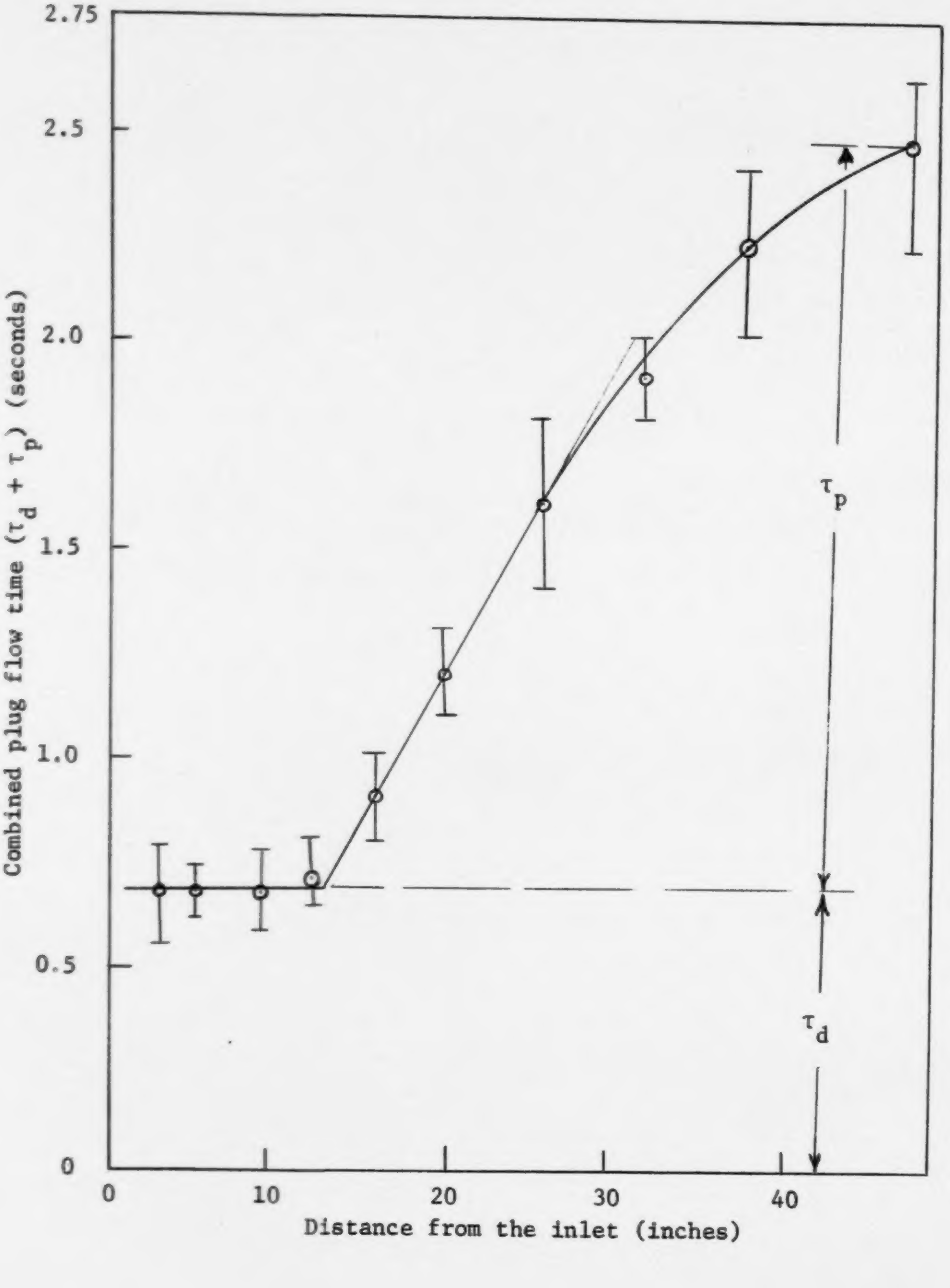
2.75
2.5
2.0
1.5
1.0
0.5
0
Combined plug flow time ($\tau_d + \tau_p$) (seconds)
0
10
20
30
40
Distance from the inlet (inches)
τ_p
τ_d

model width of 12 in.). Since dead space did not seem to show up in the Fig. 13 plots, it is to be presumed that corner recirculations exist outside the converging flow region rather than dead spaces indicated in Fig. 9. Plots similar to that shown in Fig. 14 were obtained with all the five offset angles of 0°, 15°, 30°, 50°, 70° with, of course, different values for τ_d and τ_p shown in Fig. 14 under similar values of Reynolds number, momentum ratio and spacing reported in Sec. 6.2.1. The data of these experiments are included as Runs B.6 to B.10 in Appendix B.

The variation of (τ_s/τ_t), (τ_d/τ_t), (τ_p/τ_t) and $(\tau_s + \tau_d)/\tau_t$ obtained from exit and internal sampling are shown in Fig. 15. Notice that this shows that (τ_p/τ_t) and $(\tau_s + \tau_d)/\tau_t$ values remain unchanged even though the offset angle is varied. This means the physical boundary separating the well-stirred and plug flow regions remains unchanged. However, although the size of the W.S.R. section remains unchanged, inside the W.S.R. the values of τ_s and τ_d have changed and this effects the stirring effectiveness in the W.S.R., as discussed in the next section.

Discussions on error analysis for the spread of the data in Fig. 14 are given in Sec. 6.5.

6.2.3. Stirring Factor Variation with Offset Angle

From Fig. 15, we can see that, although the physical size of the well-stirred section remains unaffected by changes in the offset angle of the jets [constant value $(\tau_s + \tau_d/\tau_t)$], the residence time in the P.S.R. and the mixing delay times change. At first as the offset angle increases τ_d decreases and τ_s increases correspondingly, until

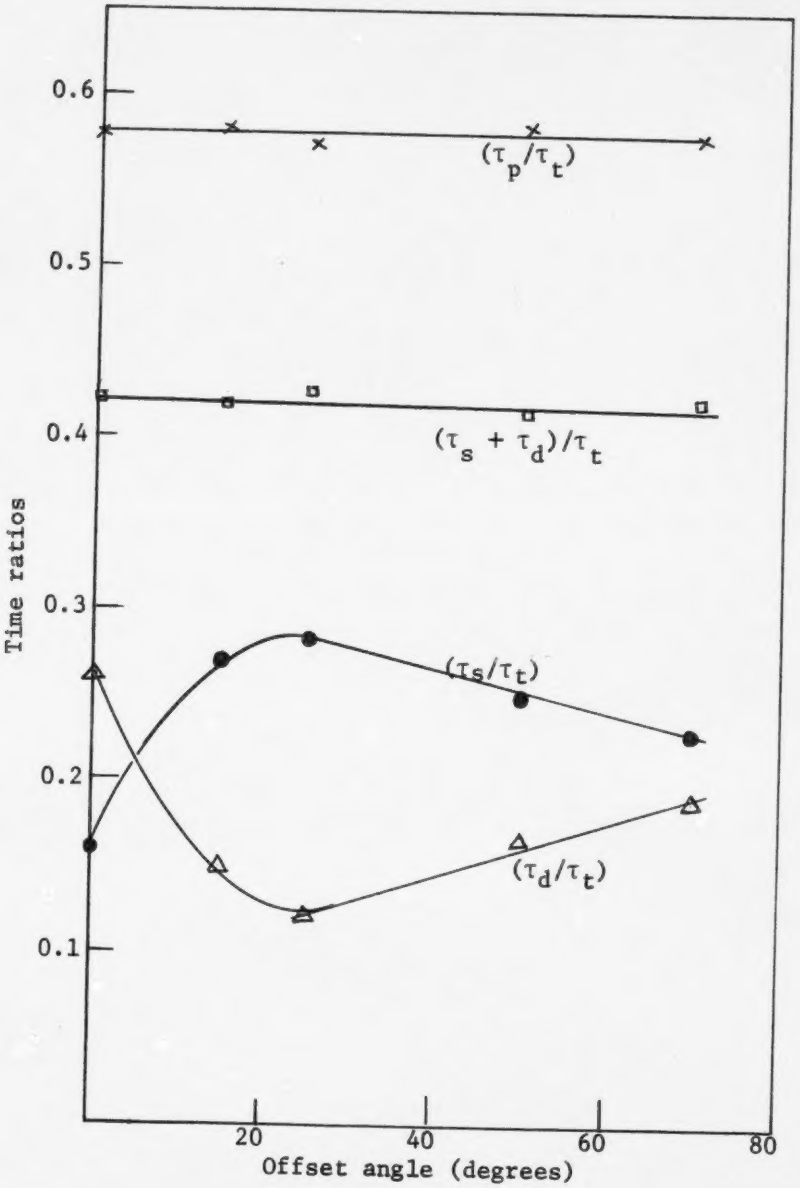

Fig. 15. Variation of Various Time Ratios with the Offset Angles for the Opposed Vortex Flow. (Spacing = 8 in., Re_b = 8830, Momentum ratio = 695)

about a value of 30° is reached. After this angle the τ_d value starts to increase slowly and τ_s starts to decrease correspondingly. When W values are calculated according to the Eqn. (5.18) and plotted as function of offset angle, the plot of Fig. 16 results. This plot shows very clearly an optimizing effect of jet offset angle. As the jets swing away from each other, increasing the diameter of the imaginary circle they are tangent to, the stirring factor (W) rises sharply. Between 20° and 30° the stirring factor peaks, and then drops again. The lowest value measured was at zero offset angle when the jets were directly opposed. This supports the intuitive idea that shear between counter rotating fluid sections might promote backmixing.

6.2.4. Variation of Stirring Factor with Jet Array Spacing

One of the problems to be solved in optimizing ignition conditions is matching the size of, or period in the stirred section, to the reaction time (6). It is obviously desirable, therefore, to know to what extent the physical dimensions of the stirred section can be controlled by adjustment of the jet array spacing. Intuitively, one would also imagine that the shear between the two vortices would diminish as the jet planes move apart so that the stirring factor would also drop. The results of exit sampling generated plots as in Fig. 13, in agreement with Eqn. (5.16) and internal sampling produced results which followed the trend shown in Fig. 14. The data of internal and exit sampling are included in Appendix B as Runs B.11 to B.22. For convenience these results are summed up in Fig. 17 as the variation of τ_d, τ_s, τ_p, and $(\tau_s + \tau_d)$ with spacing. From these results W values, following Eqn. (5.18), were calculated and the variation of W with

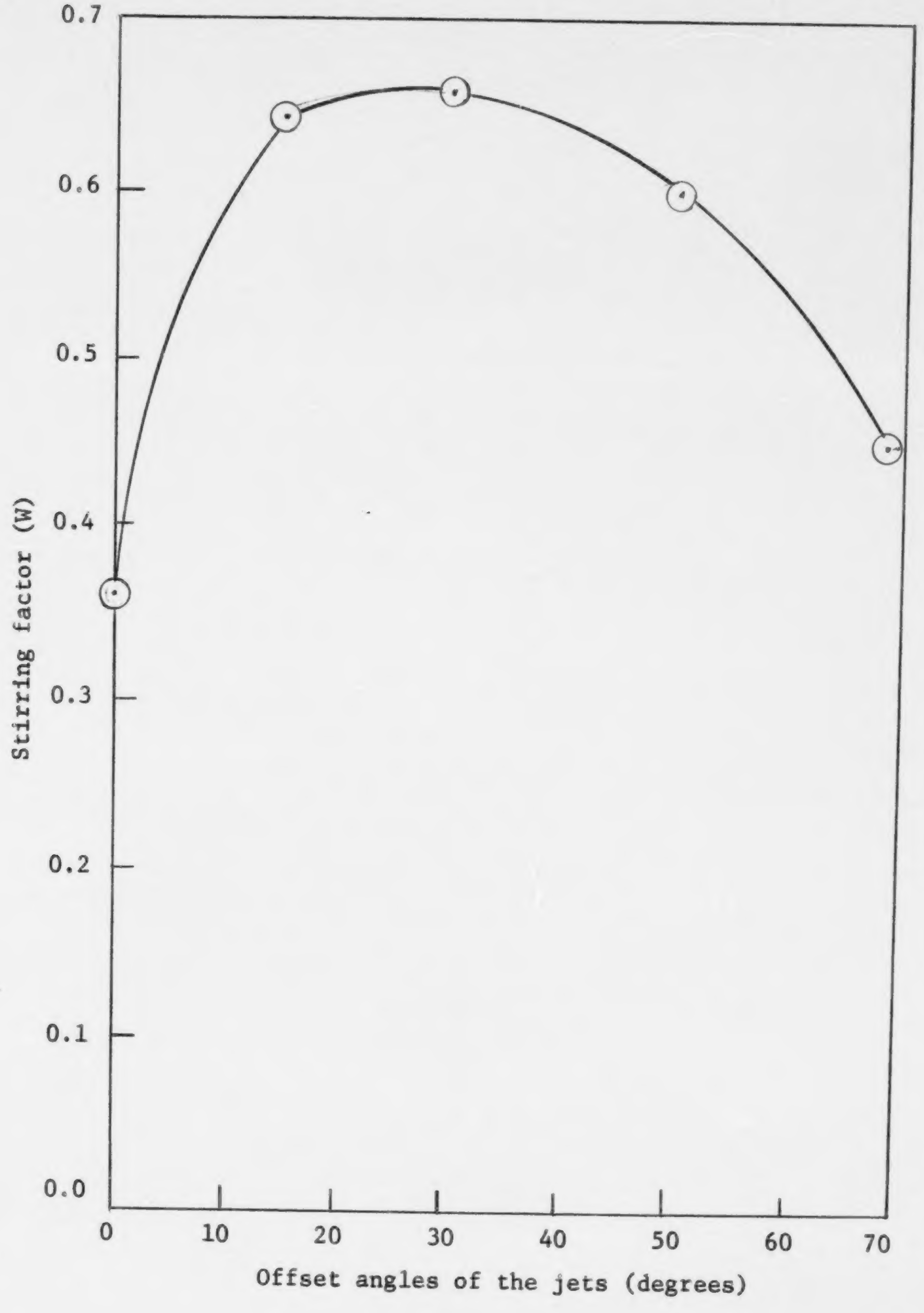

Fig. 16. Variation of the Stirring Factor with the Offset Angle of the Jets. (Spacing = 8 in., Re_b = 8830, τ_t = 3.01 sec., Momentum ratio = 695)

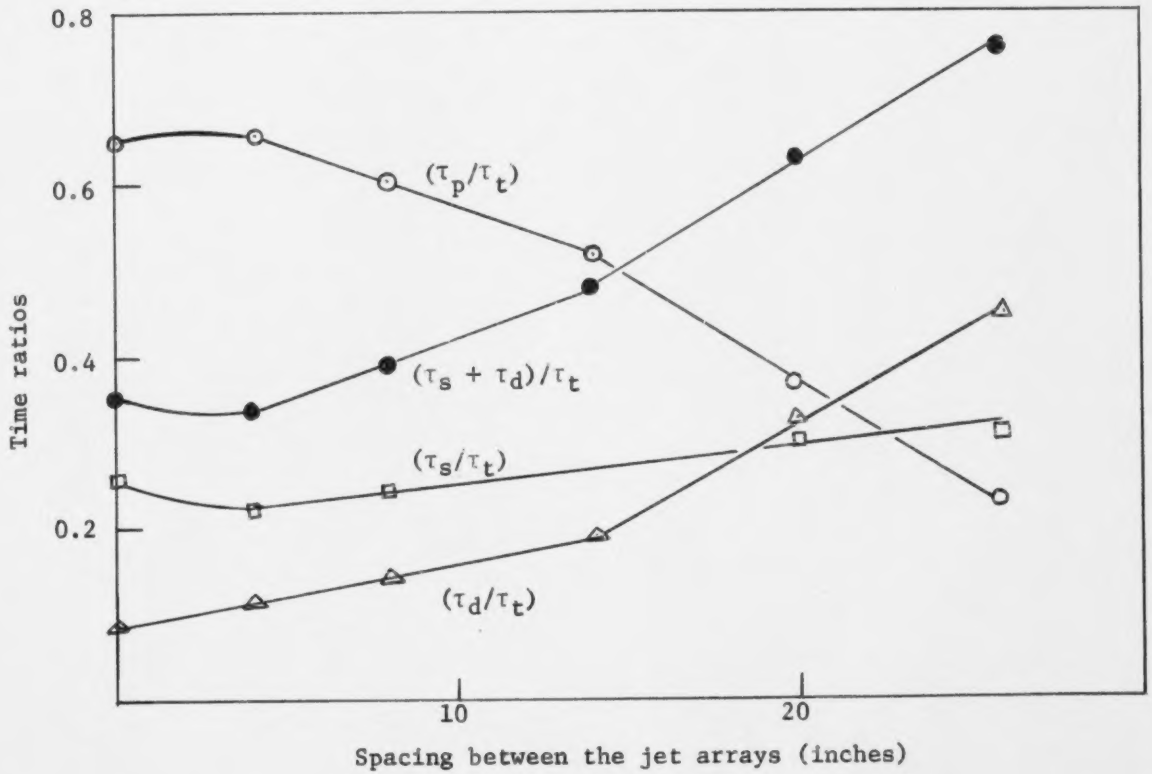

Fig. 17. Variation of Various Time Ratios with the Spacing Between the Jet Arrays. (Offset angle = 30°, Momentum ratio = 695, Re_b = 8830)

spacing has been plotted in Fig. 18 (for momentum ratio 695, offset angle 30°, and $Re_b = 8830$). In general, the stirring factor falls with jet array spacing, as expected. In particular, the coupling between the vortices vanished, almost discontinuously, with a spacing in excess of 14 in. Beyond that spacing, the equivalent plot to Fig. 14 indicated separate stirred reactor zones individually associated with each jet array (Fig. 19). With spacing less than 14 in. the two stirred regions merged, with substantially greater stirring factors than existed for the individual zones.

An unexpected result, however, was the maximum stirring factor at zero spacing. The zero spacing was simulated by a specially built jet array using two exits at the proper angle from each of the four jets at a single level. This apparent anomaly is discussed further below.

6.2.5. Variation of Stirring Factor with Momentum Ratio

The stirring factor was also found to be strongly affected by the relative magnitude of the initial axial flow. This is the air coming through the back-up plate and it corresponds to the mass flow of volatiles and gasification products coming through the top of the refuse bed. The results so far obtained depend on increasing the axial flow rate whilst maintaining the horizontal supply rate through the overfire ports constant. Consequently, the total flow rate, and Reynolds number increase, whilst the residence time decreases. The offset angle in these experiments was 70°. The results are summarized in Table 2 and data included as Runs B.23 to B.29 in Appendix B.

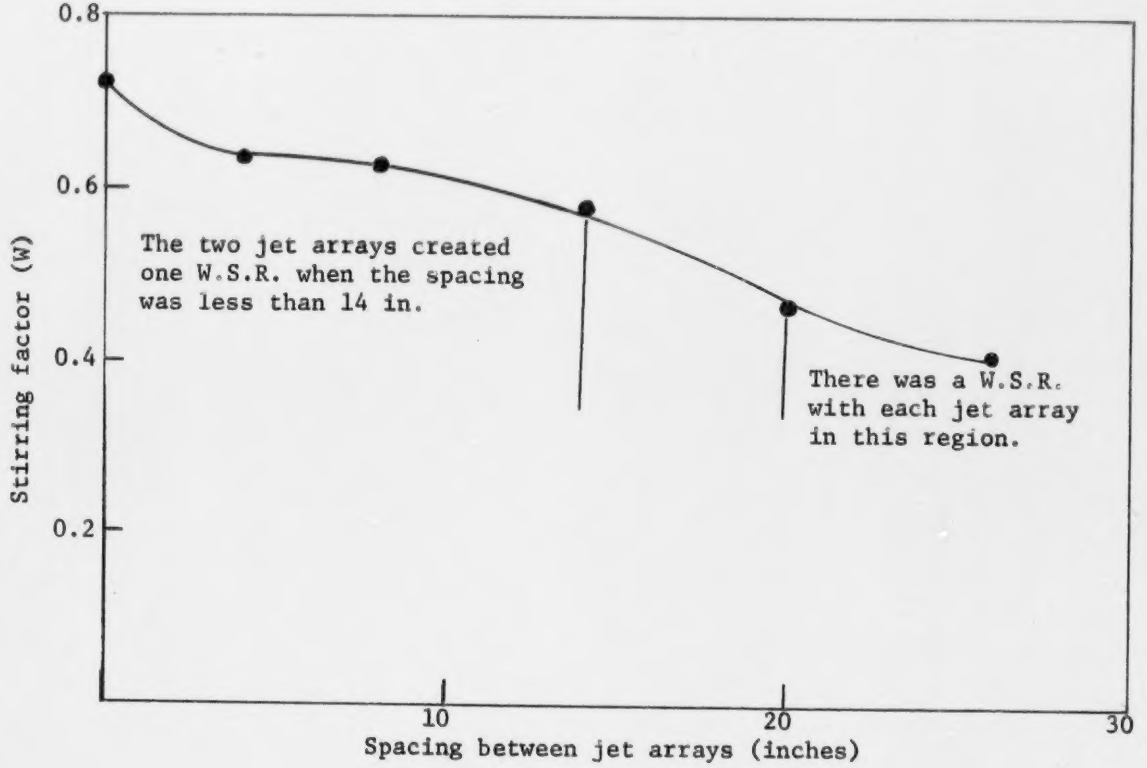

Fig. 18. Variation of the Stirring Factor with the Spacing. (Offset angle = 30°, Momentum ratio = 695, Re_b = 8830)

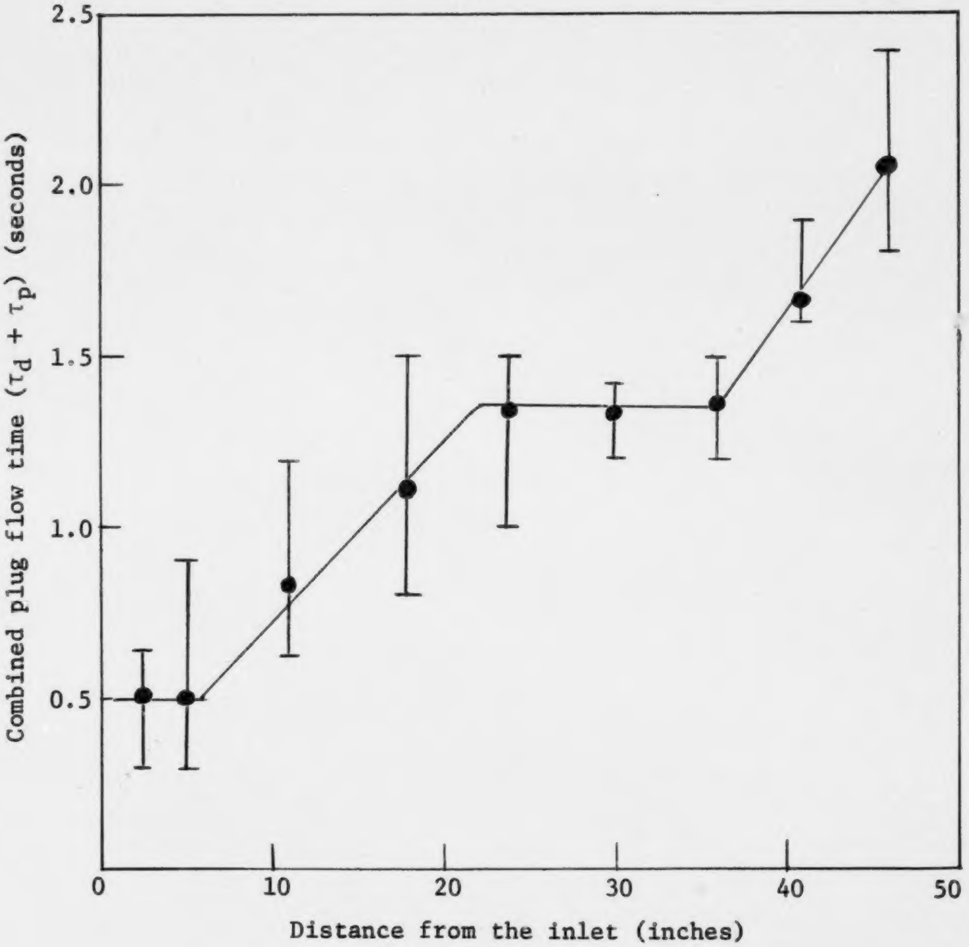

Fig. 19. Variation of the Combined Plug Flow Time with Distance at a Spacing of 26 Inches. (Offset angle = 30°, Momentum ratio = 695, Re_b = 8830)

TABLE 2

Variation of Stirring Factor with Momentum Ratio at an Offset Angle, 20°

Momentum Ratio	W Stirring Factor	Ratio of Flows	τ_t (sec.)	Re_b
6100.0	0.625	12.5	4.26	6250
695.0	0.453	3.0	3.01	8830
20.0	0.000	0.7	1.91	13900

The most striking result here is the evidence that too high an initial axial flow rate can eliminate the stirring altogether. The flow ratios correspond to 7.5 percent, 25 percent, and 60 percent of the total air being supplied through the back-up plate (fuel bed simulator). In terms of an individual jet in the overbed array the axial flow or momentum is even more heavily weighted against penetration by the jet across the stream than even these numbers suggest.

6.2.6. Other Results

(i) Plug flow volume: Since the plots typified by Fig. 14 all indicated a remarkably distinct boundary between the stirred section and the plug flow section, with relatively or trivially narrow transition zones in all cases, these results demonstrate that the conceptual representation of Fig. 9 with regard to the plug flow section also represents physical reality. The magnitude of the ratio (τ_p/τ_t) also therefore represents the fraction of the volume that is in plug flow, and the method of determining τ_p also determines the physical location of the boundary between the two sections in terms of inches from one end or the other. It is, therefore, of interest and significance to find that, for a fixed set of total flow conditions with only the offset angle being changed, the margin between the stirred and the plug flow sections remained constant. The stirred region was about 43 percent of the total volume, and the plug flow region 57 percent. This indicates that with this particular jet configuration the size of the stirred region is dominated by the jet array spacing. This is partially substantiated by the experiments on the effect of the jet array spacing where, apart from the anomaly of an initial increase in

τ_p between 0 and 4 in., it then declines more or less linearly over the next 10 in. At 4 in. spacing about 64 percent of the volume is in plug flow; at 14 in. this has dropped to about 53 percent. At the same time the volume between the jet arrays has increased by over 20 percent, so evidently as the jet arrays move apart the plane between the stirred and plug flow regions moves relatively closer to the lower jet array.

(ii) Delayed mixing region: Unlike the physically real separation between the stirred section and the plug flow section, the parallel concept illustrated in Fig. 9 of a real physical separation between a delayed mixing section and a true P.S.R. is not substantiated. This conclusion is supported by a number of reasons, one being the failure to detect the real existence of physically separate, delayed mixing sections by internal probing; another reason was the behavior of the direct backmixing experiments, which also indicated a delayed mixing time. The conceptual model predicting the results actually obtained is not, therefore, to be taken literally. An adequate alternative model that predicts the same result, but is physically real, has yet to be developed; however, there is now evidence that the magnitude of the backmixing effect plays a significant part in determining the stirring factor and τ_d.

(iii) Backmixing experiments: In these, helium was injected downstream of the sampling point. With the sampling point near the back-up plate, more helium was picked up as the injection point was moved upstream. In a true P.S.R. the injection point should make no difference. The actual probability of helium escape from the stirred region into the plug flow region increases as the injection point moves closer to the junction between the two regions (Fig. 20). In a second set of experiments where the sampling and injection stations were the same, but the offset angle was changed, the "strength" of the backmix flow as measured by the concentration of helium pickup was greatest at 30° offset, less at 70°, and least at 0°. This agrees with the results of Fig. 16. A somewhat different picture emerged, however, during experiments to determine the maximum margin of backmix, i.e., the furthest distance downstream that helium could be injected and still picked up upstream. For this it was least at 70° offset, but a maximum at 0° offset (opposed jets). The explanation seems to be that, as the jets move more into opposition with decreasing offset after passing the 30° optimum offset, the fluid rotation is diminished and the jets tend to coalesce on the axis to form an approximation to an axially-centered, single jet with corner recirculation. This also seems to be the explanation for the otherwise anomalously high stirring factor with zero spacing between jet arrays. The whole physical flow pattern has changed from the opposed vortices otherwise examined.

6.3. Mixing Behavior of Straight and Swirling Jets

As has been explained earlier, straight and swirling jets have been included for studies to provide a comparative standard for the effectiveness of mixing created by the opposed vortex flow used in the incinerator. Experiments, as set out in Sec. 4, were then carried out to develop some standard of effectiveness against which the performance of the incinerator system can be judged and also to test the validity of applicability of Bragg's criterion to these systems. It was found that, again, the physical boundary separating a stirred region and plug

Fig. 20. Helium Concentrations (Output) Reached at Three Inches from the Inlet Due to the Injection of Equal Helium Flows at Various Distances from the Inlet.

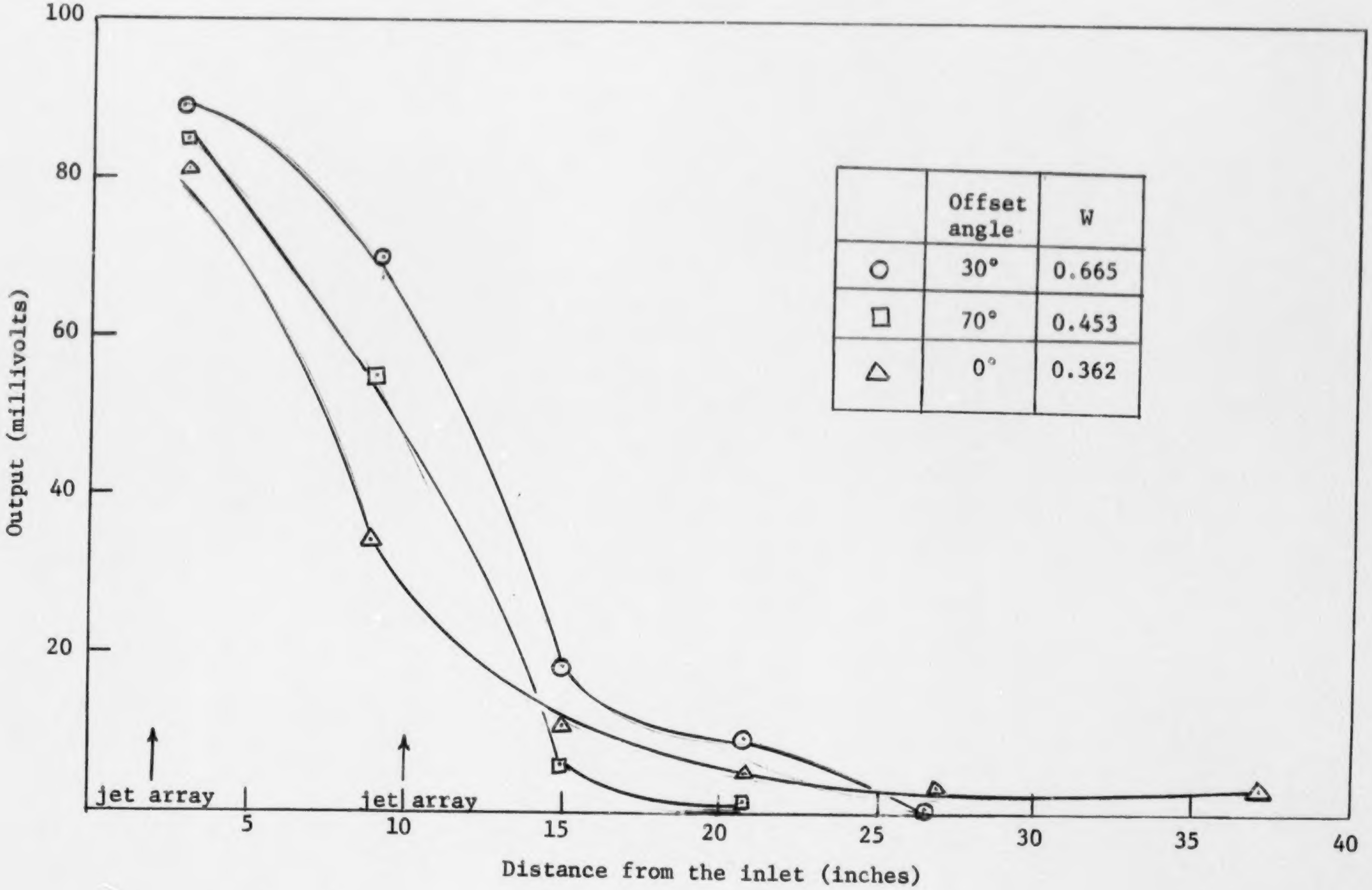
100
80
60
40
20
Output (millivolts)
5
10
15
20
25
30
35
40
Distance from the inlet (inches)
jet array
jet array
Offset angle
W
○ 30° 0.665
□ 70° 0.453
△ 0° 0.362

flow modified by corner recirculation region was precise and only highly swirled jets created a W.S.R. for which W values can be calculated. Poorly swirled and unswirled straight jets created a stirred region which was only nominally stirred. Further experiments on the level of backmixing established two different mixing characteristics (discussed in detail below). As will also be discussed, studies on jets developed further information on the nature and heterogeneity of the backmix process, required for mixing, that was unanticipated, and non-existent in the incinerator counter-vortex system. In addition, therefore, to developing the comparative data sought, these studies then stand in their own right adding additional useful information on the behavior of typical jet burners found in many industrial furnaces and combustors.

6.3.1. General Behavior with Straight and Swirled Jets

As already mentioned in Sec. 6.1, virtually all the tracer response curves obtained by sampling either inside the model or at the exit showed the common characteristics of: (i) an initial period, following cut-off, during which the tracer concentration remained unchanged; followed by (ii) an exponential decay of the tracer concentration with time. Between these two dominant periods a small transition region was in evidence allowing a smooth transition from the constant period to the exponential decay. The exponential nature of the decay in all instances was substantiated by log/linear plots designed to test the applicability of Eqn. (5.16) and the result as already mentioned was a set of straight lines of negative slope with varying intercepts on the time axis, but all passing through the normalized point (1,-1). This latter point indicated negligible or zero volume of dead space. At the intercept on the time axis, the transition region between the two decay periods was also negligible, thus enabling determination of fairly precise values of the sum of the plug flow times ($\tau_d + \tau_p$). The plots to check the applicability of Eqn. (5-16) are not reproduced here but are identical in form to Fig. 13. However, it was found: (i) As the diameter of the straight jets increased, the τ_s value decreased; (ii) With the vane swirled jet, as the secondary vane angle was increased, the τ_s value decreased; and (iii) With tangential entry jet, as the tangential flow increased, the τ_s value decreased. Reduction in τ_s value can generally be interpreted to mean the size of the stirred section decreased making the stirring more intense or effective. We will discuss more about this below. The data of the exit sampling are included in Appendix C as Runs C.1 to C.10.

6.3.2. Variation of Combined Plug Flow Time with Distance

Since the intercept of the concentration decay lines on the time axis described above gives an estimate of the sum of the mixing delay and plug flow periods, a plot of this combined plug flow time with distance through the model gives us a picture of the gross mixing behavior in the model. Figs. 21, 22, and 23 are selected plots of typical data for each of the three burners. Fig. 21 is for the vane swirled jet; Fig. 22 for the tangential entry jet; and Fig. 23 for the straight jet. The curves show some expected and some unexpected characteristics. In all cases, the curves show a clear cut "break" that is interpreted, as discussed below, as the expected demarkation

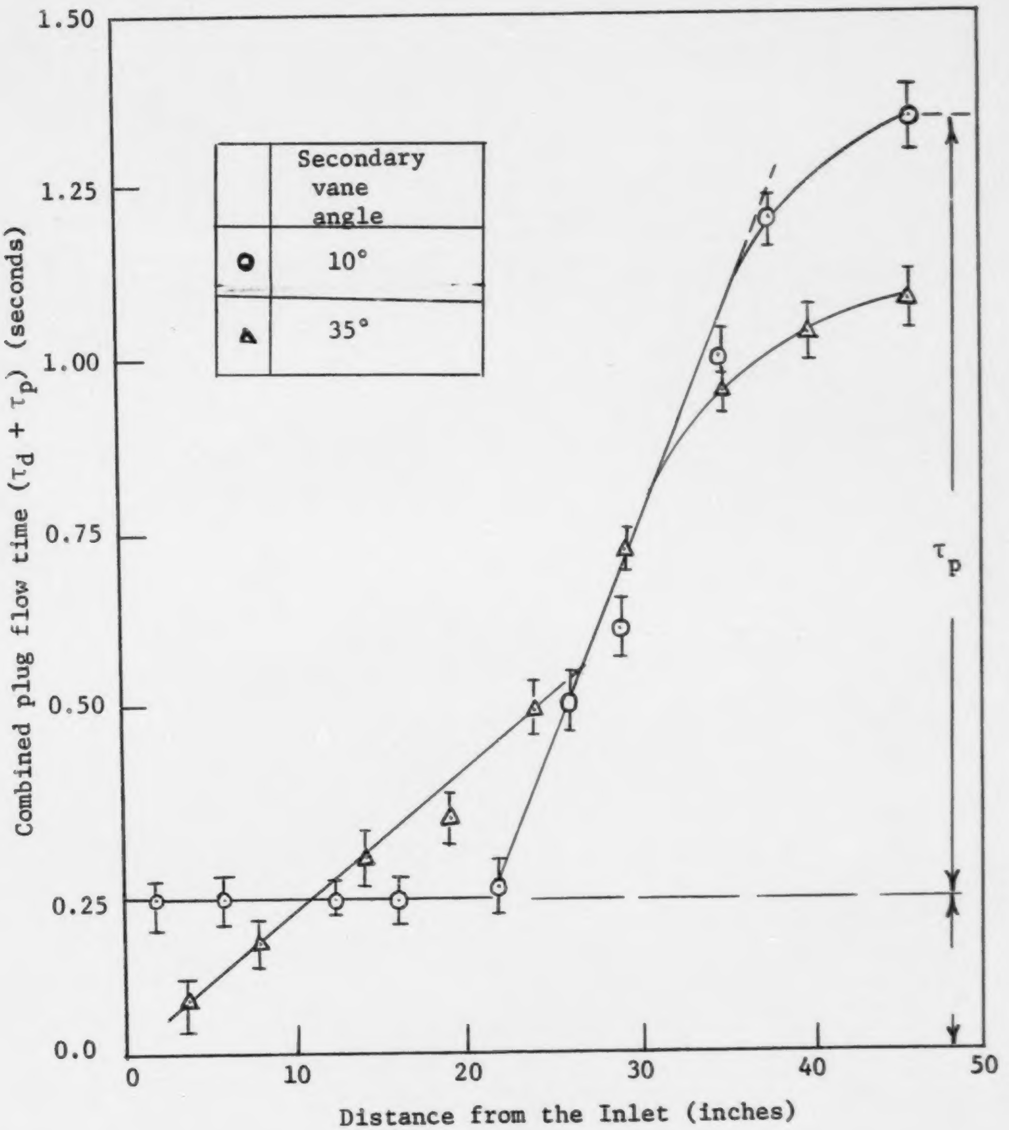

Fig. 21. Variation of the Combined Plug Flow Time with Distance from the Inlet for Two Levels of Secondary Vane Angles. (Flow rate = 100 cu. ft./min., Re_b = 11200, Slope of plug flow = 1.49 ft./sec., Theoretical plug flow slope = 1.67 ft./sec. The spread shown is the range of the data.)

Fig. 22. Variation of the Combined Plug Flow Time with Distance from the Inlet for the Tangential Entry Jet. (Re_b = 8000, flow rate = 72.75 cu.ft./min. The range of the spread of data is not shown for two plots because of the eventual crowding. However, the spreads have similar range as that shown in the figure. Note all the plotted points are averages of one to ten measurements.

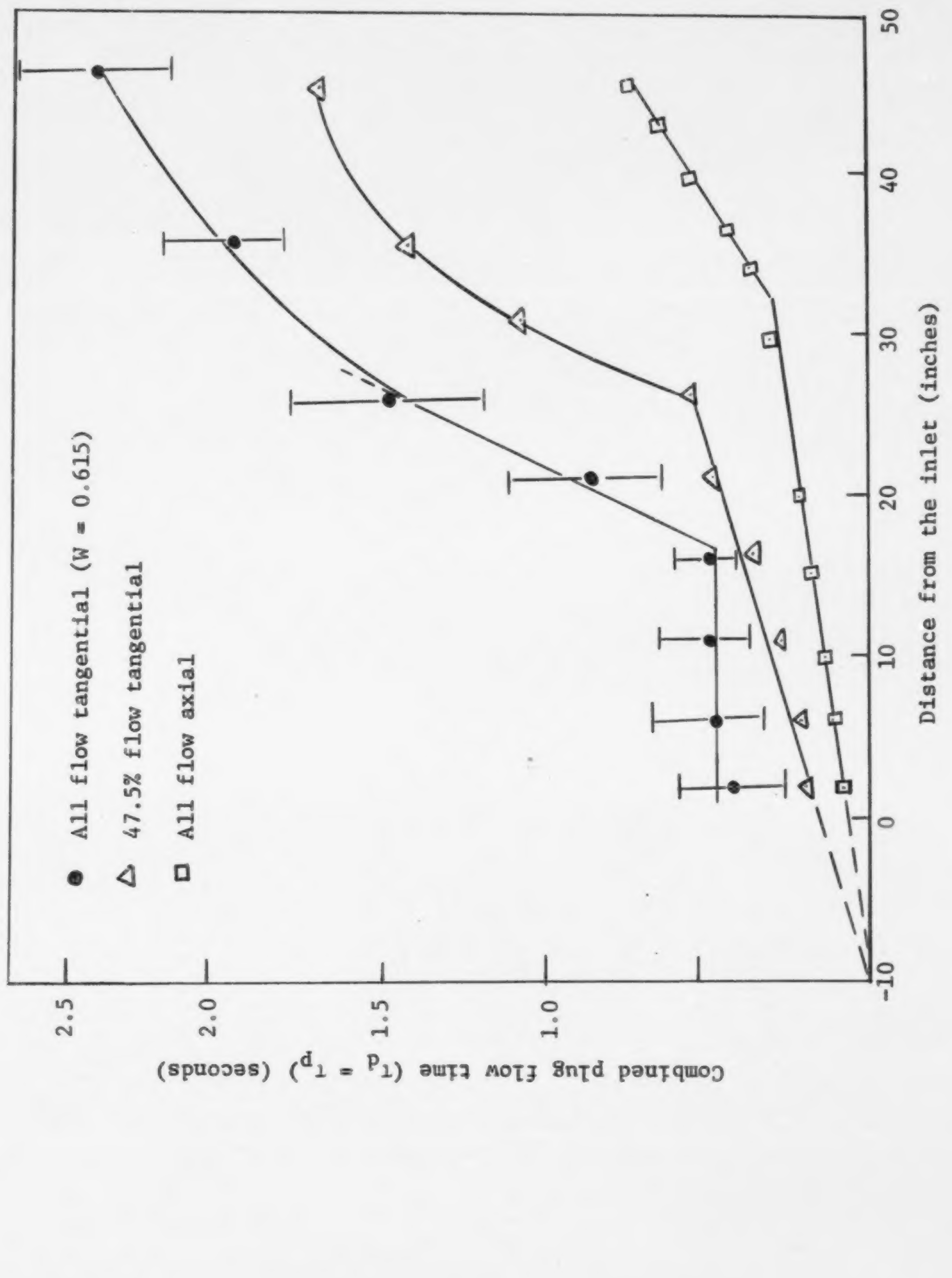
● All flow tangential (W = 0.615)
△ 47.5% flow tangential
□ All flow axial
Combined plug flow time ($\tau_d = \tau_p$) (seconds)
2.5
2.0
1.5
1.0
Distance from the inlet (inches)
-10
0
10
20
30
40
50

Fig. 23. Variation of the Combined Plug Flow Time with Distance from the Inlet for a Straight Jet (4 in. dia.). (Flow rate = 1.871 cu. ft./sec. Re_b = 12530, Theoretical slope of plug flow time = 1.84 ft./sec., Experimental slope = 2 ft./sec., Slope of the stirred region (near the inlet) = 10 ft./sec., Velocity of the jet at the inlet = 14.5 ft./sec.)

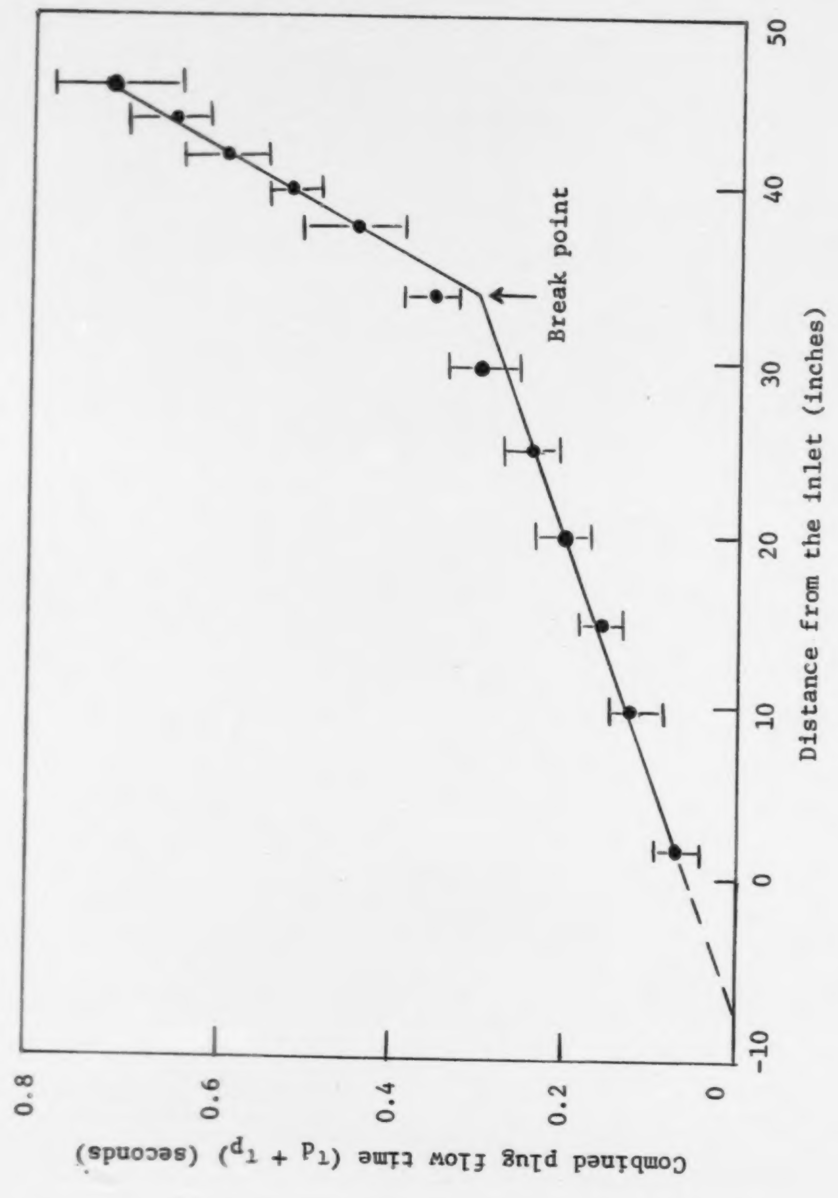
Combined plug flow time (t_d + t_p) (seconds)
0.8
0.6
0.4
0.2
0
-10
0
10
20
30
40
50
Distance from the inlet (inches)
Break point

between the stirred region and the following plug flow region. The data are tabulated in Appendix C as Runs C.11 to C.18.

In the plug flow region, the qualitative behavior is much as found before (c.f., Fig. 14) with all curves approximating to straight lines just beyond the break point, and then declining in slope. The significance of these lines is that their slope is the reciprocal of the flow velocity at the plane of the model indicated, if the flow is true plug flow. By calculation, good agreement near the break point was obtained: for example, in Fig. 22 the calculated plug flow velocity is 1.21 ft./sec., whilst that calculated from the slope of the curve is 1.175 ft./sec. Similar magnitude of agreement is obtained in most other cases. Near the exit, the slope decreases, implying that the velocity increases. This is due to convergence of the stream lines (as discussed in Sec. 6.2.2) for the flow to leave through a narrower opening. Between the converging stream lines and the wall there is then a space with the fluid in corner recirculation so it does not show up as dead space.

In the stirred region, however, the results varied somewhat unexpectedly, with some of the curves showing a constant plug flow or mixing delay time and others showing a declining decay time. These differences are amplified below.

6.3.3. Stirring Factors at High Swirl

From examination of the plots in the "stirred" region between the burner and the break, it is evident that some of the curves show behavior in agreement with expectation, with a constant residual plug-flow time, identified as the mixing delay time. This occurred with only two of the burners, and both only at high swirl. For the vane burner this was at a setting of 10°, so the vanes were barely open; for the tangential entry jet, this was at 100 percent tangential admission and no axial admission. The relevant lines on these plots then show, overall, similar characteristics to those obtained from the incinerator model (see Fig. 14).

With τ_d measured by these means, stirring factors can be calculated. For the vane swirled jet with the vanes at 10°, W had a value of 0.815 and this was found to be independent of the box Reynolds number over the range 7000 to 11500. (A wider Re_b range would have been desirable, but this was not possible without higher fan power because of the pressure loss across the burner at the close vane setting.) This value of 0.815 can be compared with: the theoretical value of unity for Perfect Stirring (zero for zero mixing); 0.675 as the maximum for the incinerator model (and dropping to 0.36)(75); and 0.615 for the tangential-entry jet at a box Reynolds number of 8000.

Although the variation in range of Reynolds number for the vane swirled jet was fairly small, significant changes did nevertheless occur in the absolute values of τ_s and τ_d before their ratio was calculated in forming W. Both were found to fall roughly in proportion to the increasing box Reynolds number, as in Fig. 24. Since the value of (τ_d/τ_t) and (τ_s/τ_t), shown in Fig. 25, are also estimates of the volumes occupied by the mixing delay region and equivalent P.S.R. region, the inference is that the physical size of these regions is unchanged by increased flow; only the velocity through the regions

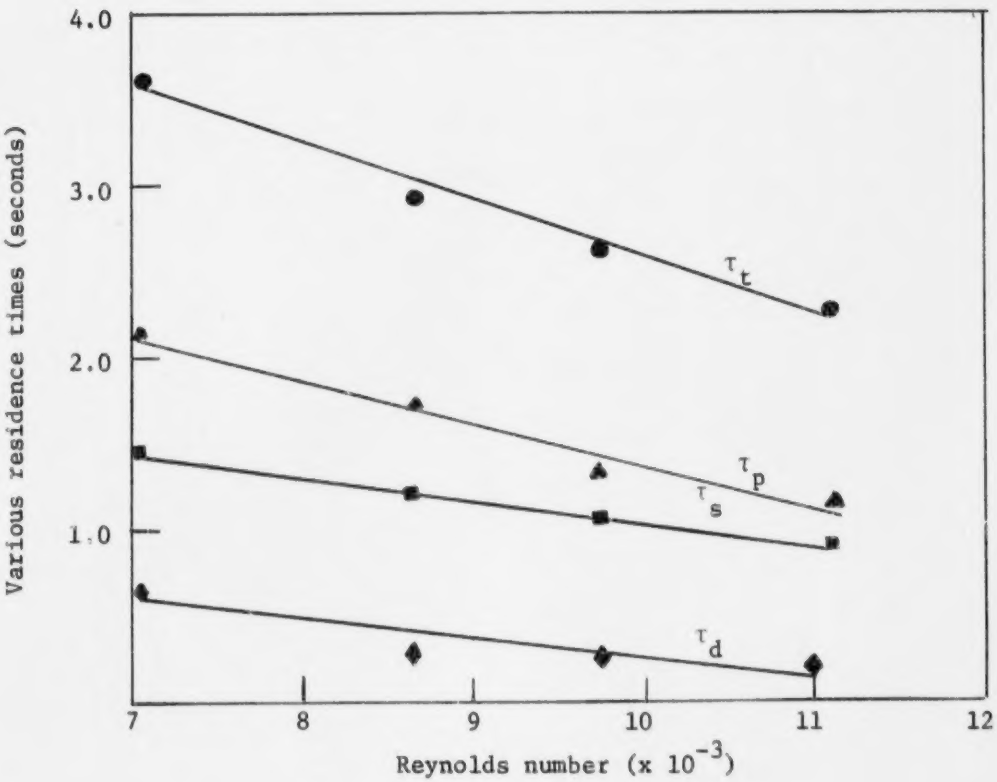

Fig. 24. Variation of Various Residence Times with Reynolds Number for the Vane Swirled Jet.

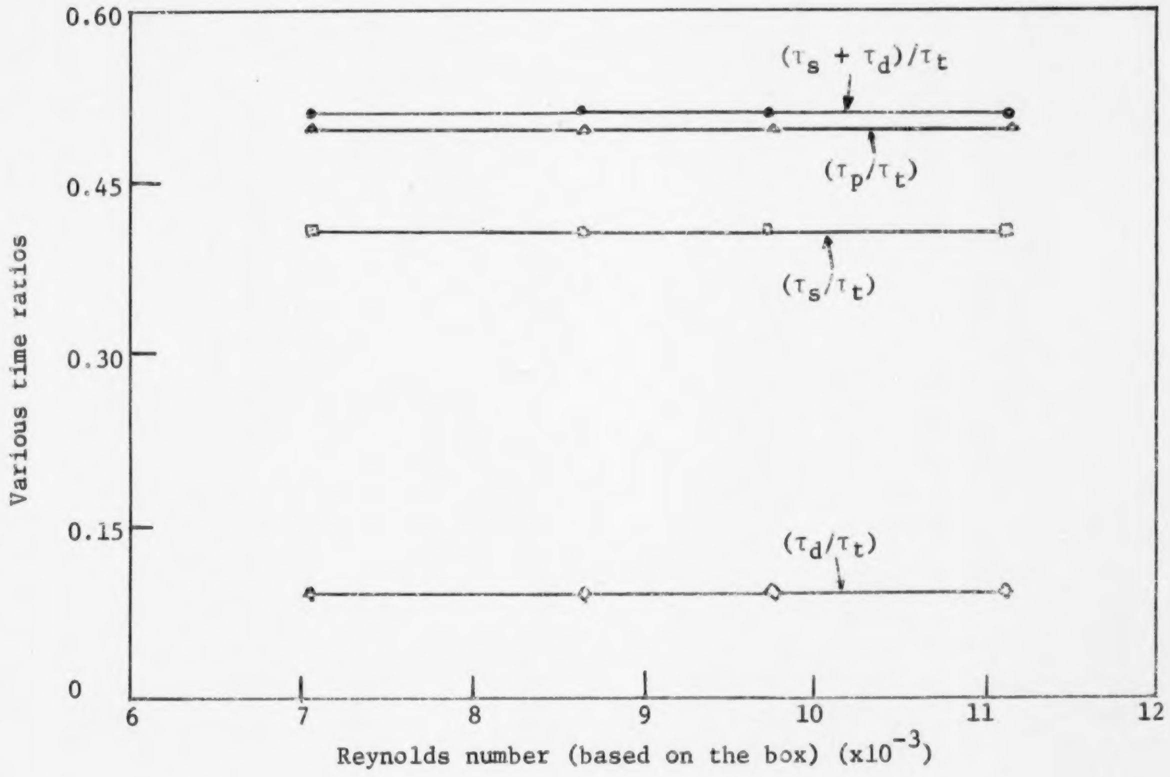

Fig. 25. Variation of Various Time Ratios with Reynolds Number for the Vane Swirled Jet.

changes. Because τ_s/τ_t and τ_d/τ_t remain constant, W also remains constant, although flow rate is increased.

6.3.4. Behavior at Zero Swirl

We can best understand the behavior at the low swirl conditions by concentrating first on the straight jet. The characteristics of Fig. 23 are then very much self-evident. The classic behavior of a straight confined jet is a flow system containing an expanding jet, with corner recirculation flow between the jet boundaries and the confining walls. Exchange of mass then takes place between the expanding jet and the recirculation flows all along the jet boundary between the two flows. At the simplest approximation, we can assume that exchange only occurs from the jet to the recirculation flow as the jet nears the model wall, and back from the recirculation flow to the root of the jet at the burner exit. This corresponds to a recycle reactor, and such a system has been reanalyzed recently by Rippin (79). He showed that the residence time distribution function (R.T.D.) obtained consisted of an infinite series of impulses or delta functions of magnitude decreasing as a geometric series. In the limit, as the intervals between impulses become very small, the series tended to an exponential decay. In our system, with the unswirled jet, we can think of the recirculation flow as a set of recycle systems all superimposed to take into account the effect of exchange all along the jet boundary and not just confined to the ends.

Rippin's analysis accounts, at least in general terms, for the nominal P.S.R. behavior indicated by the exponential decay in concentration at points on the jet axis, once the signal that the tracer flow has been cut off has reached the sampling station. The time taken for the cut-off signal to reach the sampling station obviously increases with distance from the inlet, in general qualitative agreement with the initial slopes of the no-swirl lines (Figs. 22 and 23). Quantitatively, however, there are some puzzling points. In a free jet, the velocity on the axis normally decays in inverse proportion to the distance from the nozzle exit and enclosed jets often have substantial regions where the free jet behavior is obeyed. On this account we should expect to find curves of rising slope, not straight lines for the initial portion of each curve. It may be, however, that this is a result specific to the systems studied in view of the relatively large ratio of burner diameter to model diameter; this ratio is 1/3, and it could be that the free jet behavior never develops. This is normally said to require about eight nozzle diameters or 32 in. As the result of radial probing we are satisfied that the break in the lines occurs where the jet has expanded to the walls, which coincidentally is about eight diameters downstream from the burner for the 4 in. dia. jet.

Other behavior, however, is more nearly consistent with results of other investigations. Knowing the point of expansion to the wall, the jet half angle can be calculated. The figure obtained is about 6.7° which is in the middle of the range of values listed by Field, et al. (34) for 15 different investigations of the concentration half angle. Likewise, the extrapolated point of origin of the jet is about two diameters behind the nozzle exit in accordance with Davis' results (33). When Reynolds number (Re_b) was varied from 2010 to 19200 in ten steps for a 4 in. dia. straight jet, the half-angle remained constant at 6.7°.

6.3.5. Effect of Increasing Swirl

At low and medium levels of swirl we evidently have some sort of superimposed mix of a well-stirred reactor and unswirled jet with recirculation. Attempts to treat the system as an uncoupled combination of the two mixing systems operating independently have not been too successful so far, partly because of the complexity of the equations obtained. A more promising model is one based on a concept of homogeneous and heterogeneous or discrete backmix streams. This is still incomplete quantitatively (but see Sec. 6.3.6), but qualitatively it has already been usefully informative for interpretation of the results.

For all jets, whether swirled or unswirled, backmixing or the motion of tracer against the net resultant flow takes place. In recirculation generated by an unswirled jet, we can identify, locally, large regions with a dominant flow in a particular direction. In general, we can find a small number of physically large backmix streams that are nonuniformly distributed. This can be described as discrete or heterogeneous backmix.

If now we suppose that these large backmix streams are progressively reduced in size, increased in number, and more uniformly distributed, the discrete nature of the central jet will be progressively eliminated till we have, finally, the other limit of homogeneous backmix. This corresponds to a well stirred condition with reasonably uniform concentration and residence time distribution at all points in the stirred volume.

The qualitative behavior illustrated by increasing swirl in Figs. 21 and 22 is certainly in accord with this description. In addition we may note that the size of the stirred section (i.e., distance downstream to the "break") decreases with increasing swirl.

6.3.6. Backmix Measurements

Pending completion of a theoretical analysis of the backmix behavior, this has been partially investigated by direct measurement. In a number of experiments, tracer was injected at a constant rate downstream of the sampling point, and measurements were then made of: (i) the steady state concentration reached as a function of injection distance from the sampling point (Fig. 26); (ii) the mixing delay time (τ_d) and P.S.R. time (τ_s) after cutoff; and (iii) the influence of stirring factor on the upstream steady-state concentration for fixed injection and sampling points.

In these experiments it was found that τ_d was independent of injection or sampling point, and so was τ_s for a given stirring factor. As the stirring factor was increased, the upstream steady-state concentration rose more or less linearly with W (Fig. 27). Finally, in Fig. 26 it can be seen that the closer the injection point to the junction between the stirred and plug flow regions, the greater the probability of tracer escape from the stirred region. Fig. 26 also illustrates the comparative behavior of different levels of swirl. We can analyze this situation at steady state very roughly in the following way. If multiple streams generating homogeneous backmix exist, we can introduce a "convective" diffusion coefficient, D_c, to account for the net transport in both directions due to the backmix streams. Superimposed on this is a paraxial flow of velocity V due to the overall supply of fluid at one end of the model and its removal at the

Fig. 26. Variation of the Amount of Backmix with the Distance of the Tracer Injection Point from the Inlet for Tangential Entry Jet at Three Levels of Swirl. (Re_j = 45000).

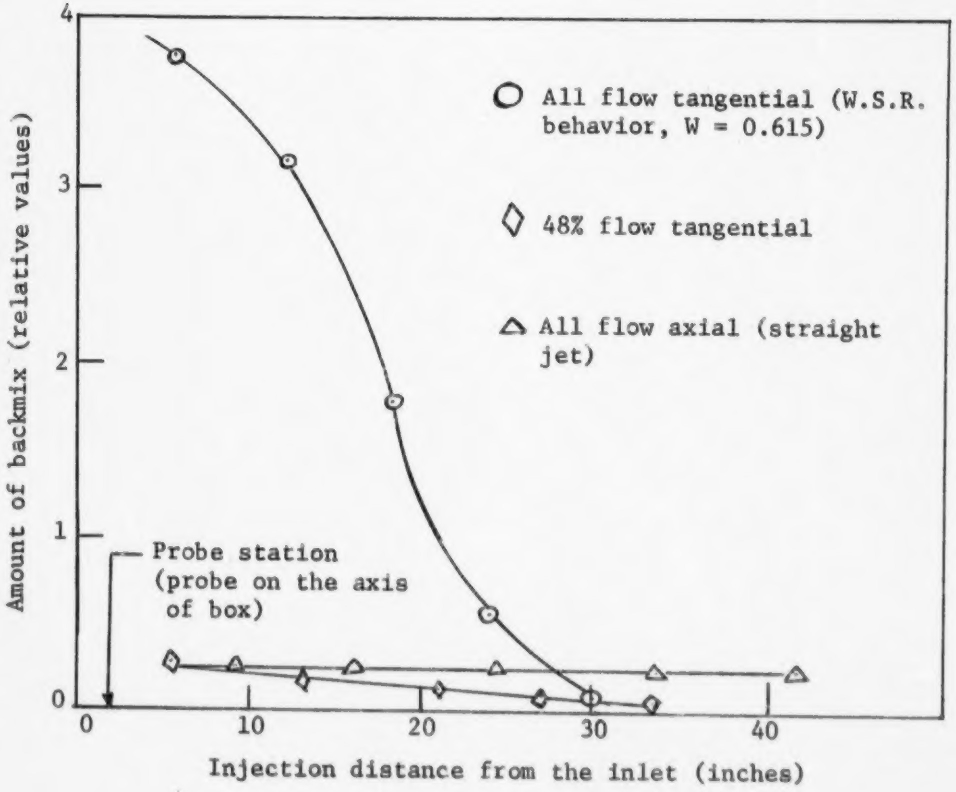

4
3
2
1
0
Amount of backmix (relative values)
0
10
20
30
40
Injection distance from the inlet (inches)
Probe station (probe on the axis of box)
O All flow tangential (W.S.R. behavior, W = 0.615)
◊ 48% flow tangential
△ All flow axial (straight jet)

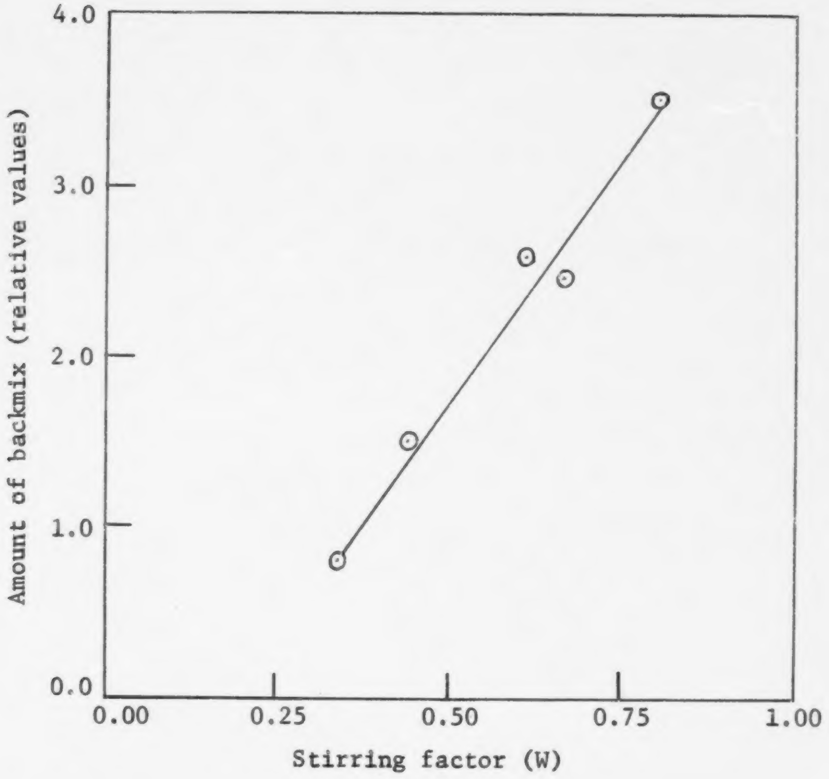

Fig. 27. Variation of the Amount of Backmix with the Stirring Factor.

other end. At steady state the convective upstream diffusion (the backmix) balances the overall convective flow so we have

$$D_c(dc/dx) + V_c = 0 \qquad (6.2)$$

whence

$$c_o = c_o^m \cdot \exp(-V/D_c)x \qquad (6.3)$$

where c_o is the steady state concentration at some distance x upstream from the point of injection, and c_o^m is the concentration maintained at the injection point. If the stirring factor increases we may assume that D_c increases. In the limit, for D_c very large, c_o tends to c_o^m. On the other hand, increasing V will quite reasonably diminish c_o.

6.4. Tracer Jet Dissipation and Turbulence Effects

In addition to measuring stirring factors, it becomes necessary to experiment to find out whether there is some correlation between stirring factors measured and the microturbulence that is produced by the various mixing methods. It is forgotten at times, however, that a high level of turbulence does not by itself necessarily generate any degree of backmix (6). We have no precise information at present on the relation between the homogeneity of backmix and microturbulence levels for local mixing once the backmix stream has reached its destination; nevertheless, it does seem not unreasonable to suppose that the homogeneity of backmix and microturbulence levels do in fact correlate with the stirring factor. Support for this was obtained by some gross experiments on sampling the tracer right across the model almost at the plane of inlet, about 2 in. from the inlet. The results are plotted in Fig. 28. With the straight jet the high peak was obtained across the exit of the tracer injector. However, it can be seen that as the swirl and the stirring level increase, the coherent tracer jet was progressively dissipated till, at high swirl levels, concentration was appreciably uniform right across the chamber.

6.5. Error Analysis

Notice that in Fig. 14 there is some spread in the value of combined plug flow time at each sampling point. The spread shown is the range of the data, for five to ten observations; from these observations, average values were calculated and these are indicated as circles for plotting the curve. (It is of interest to notice when only one sample reading was taken at each probing station, no particular trend of data could be seen on a graph similar to Fig. 14; however, by plotting the averages of five to ten observations, the trend is clear.) Another point of interest is when statistics of small number of observations, as suggested by Dean and Dixon (81), was used to calculate the percentage error of the mean, confidence limits for the mean value lying inside the range 95 percent of the time, and to test for extraneous values so that any data can be rejected, it was found that the error of the mean varied from 3 percent to 10 percent. The larger value was found in the stirred section; however, the error seems to be larger because of the smaller times (τ_d) in the stirred region and the percentage error as defined is inversely proportional to the average values. The range of the data is the most significant for small number of observations according to Dean and Dixon (81) and thus the range of the data has been included on Fig. 14. This spread of the

Fig. 28. Variation of the Steady State Concentration of Helium Across the Box at a Distance of Two Inches From the Inlet. (Notice each curve is for a different burner configuration. Only the right halves of the curves are shown; the left halves are exactly similar. The output was 3000 millivolts when only helium was injected into the box.)

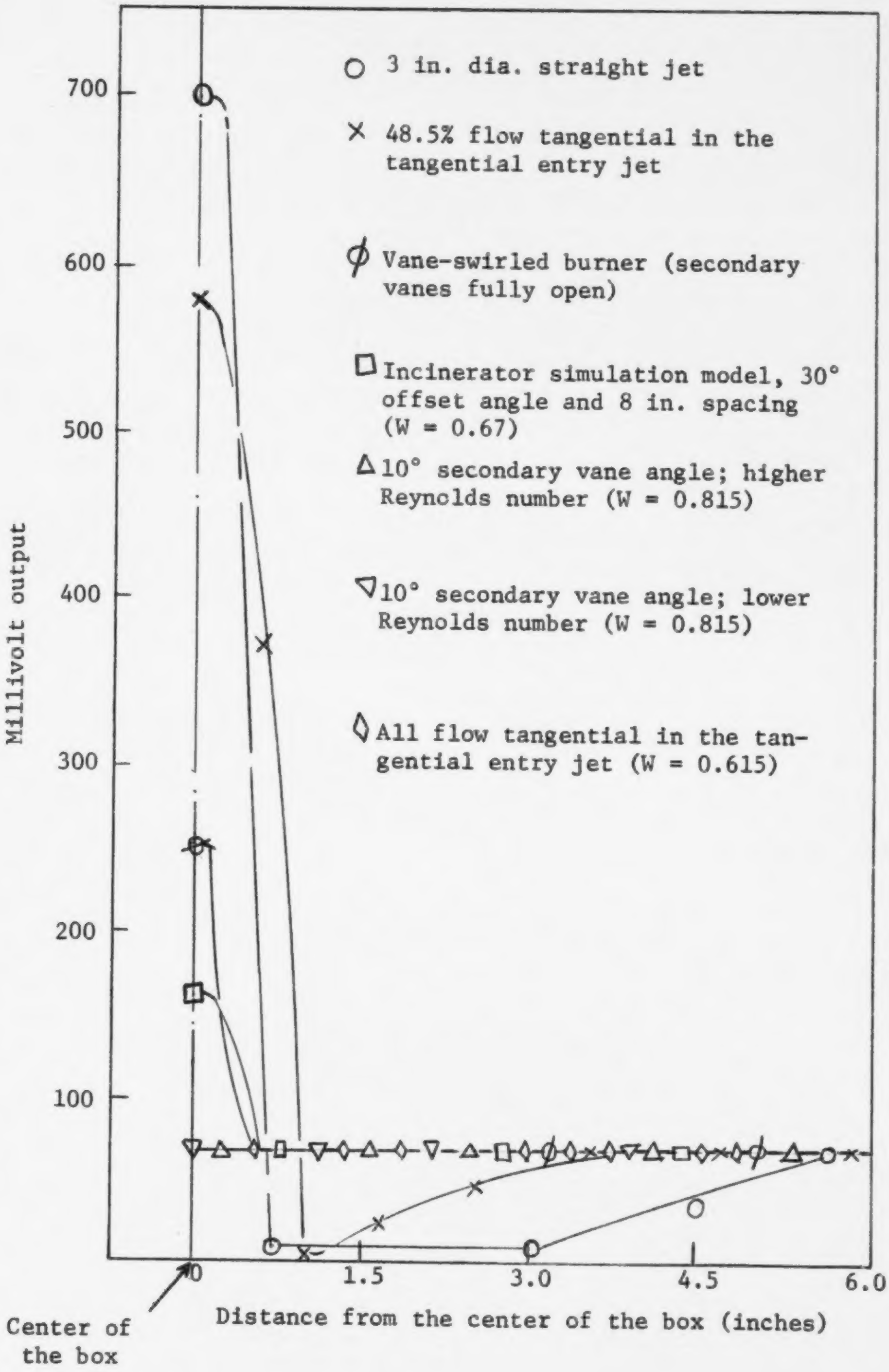
○ 3 in. dia. straight jet
× 48.5% flow tangential in the tangential entry jet
ϕ Vane-swirled burner (secondary vanes fully open)
□ Incinerator simulation model, 30° offset angle and 8 in. spacing (W = 0.67)
△ 10° secondary vane angle; higher Reynolds number (W = 0.815)
▽ 10° secondary vane angle; lower Reynolds number (W = 0.815)
◊ All flow tangential in the tangential entry jet (W = 0.615)
Millivolt output
700
600
500
400
300
200
100
0
1.5
3.0
4.5
6.0
Distance from the center of the box (inches)
Center of the box

data does not seem to be due to the instrumental error, because when similar spread was studied for the instrument (see Appendix A), the range is appreciably smaller than that in Fig. 14. However, it seems that concentration fluctuations over a mean value as found inside the box seem to be the source of spread of the data. Also, no extraneous values were found that could be rejected because they did not lie beyond a certain statistically expected range. Because of the above reasons the confidence in the data obtained was very good.

Another point which was checked is the accuracy of reading the combined plug flow times from the recorder traces. Theoretically, one would expect the output of the instrument would stay constant for some time and then decay exponentially. In this case the combined plug flow time would be read as the time beginning at cut-off until the time of the end of constant output or the beginning of exponential decay. In our experiments where there was a slight transition period connecting the two regions, decision had to be made of the time at which the period of constant concentration ended and the decay started. For this purpose two tangents for the two regions were drawn and the intersection of the tangents was taken as the time. Some small difficulties arose, sometimes due to the reason that in the initial region the output of instrument was not very constant but changed by one or two percent; then also the above method and also the method of extrapolating the initial region to meet the tangent to the second faster decaying region gave almost the same results for the time. This is due to the small transition region and, therefore, the accuracy of the data was found to be not affected by personal errors.

7. DISCUSSION, CONCLUSIONS, AND SUGGESTIONS FOR FUTURE WORK

7.1. Incinerator Model Results

To summarize the model results, it is evident that the method of experiment is indeed able to identify the boundary between a stirred section and a plug flow section, which therefore enables us to measure definable stirring factors. These results also show that the boundary between the two zones is unexpectedly precise: we had anticipated something much more diffuse. The results also indicate that the counter-vortex pattern provides good mixing, with stirring factors ranging from 0.4 to 0.7. There also seems to be good mechanical control over the physical size of the stirred region by altering the spacing between the burner arrays.

What is less certain is the precise mechanistic reason for the residual flow time described as the mixing delay time. There is reason to believe that this is a parameter inversely measuring the "strength" of the backmix flow, but this requires further investigation. A second point of uncertainty concerns the relation between stirring factor and the homogeneity of the mix. There is reason to believe that the high stirring factors obtained with the zero-spaced jet arrays are more probably due to recirculation (which is a discretely identifiable backmix stream), and though recirculation can be a prime factor in stabilizing flames it is not necessarily the optimum method. There is, therefore, the intuitive feeling that stirring factor by itself may be insufficient as a total determinator of mixing quality for maintenance of ignition. An additional parameter of significance could be the microturbulence level in the stirred region and the turbulence frequency distribution. Investigation of this, however, will have to be left for the future. In the mean time the stirring factor, and stirred volume ratio are major parameters of importance that can now be measured.

7.2. Application of the Incinerator Model Results

To apply these results to an incinerator there are first certain qualitative and semi-quantitative results that can be applied directly. In the first place it is obvious that the underfire air rate through the bed should always be kept as low as possible consistent with gasifying the solid waste at the rate required (see (82)). This is to keep the axial flow rate down to avoid disrupting the overbed backmix process. Alternatively, if the flow rate through the bed must be substantial, then the axial momentum must be matched by one means or another to avoid the disruption. One method is to reduce the size of the overfire air ports so that, for the same mass flow, the velocities and momenta are increased and the jets have greater penetration. The penalty here, of course, is the increased fan pressure required though, other things being equal, this can aid combustion rates by increasing the combustion intensity as indicated by Fig. 4 in (1). Another method of countering the axial momentum of the flow through the bed could be to tilt the overfire jets down towards the bed, so providing an appropriate matching component of momentum. This indeed suggests that several problems could be met simultaneously by having the overfire air jets able to swivel horizontally and to tilt vertically at the same time. This would allow for matching the axial flows through the bed as mentioned, but also would allow opportunity to change the effective jet array spacing to change the size of the stirred section, to match operating conditions as they changed.

Quantitatively, these model results are also potentially applicable to real systems by use of appropriate scaling methods (e.g., Thring-Newby criterion (15)).

7.3. Swirling and Straight Jets

The results described above show that the conceptual picture of a stirred section followed by a plug flow section being generated by swirled and unswirled jets is broadly supported. This is not entirely unexpected in view of the exit sampling results of previous investigators (e.g., (3,4)), but what is new in this and the incinerator model investigation, as discussed above, is the demonstration that the physical demarkation between the two main regions is quite sharply defined; and that the stirred section can then be characterized by a determinable stirring factor (W): a possible correlation between the stirring factor and flame holding ability has yet to be demonstrated, but its existence is not unreasonable. What also is new in the tests on swirling and straight jets that did not appear in the incinerator model tests is the importance of high swirl on a single jet if reasonably homogeneous backmix streams are to be created. Behavior of the unswirled jet is quite reasonably explicable qualitatively, and to some extent quantitatively, by Rippin's (79) recycle-reactor analysis; and general behavior of zero, low, and medium swirled jets is reasonably explicable, at least qualitatively, in terms of increasing number and homogeneity of backmix streams.

(i) On the other hand, the conceptual picture of a discrete mixing delay region is not an accurate physical picture. Such discrete regions were looked for but not found. Moreover, if they did exist physically, the rest of the overall well stirred section should be perfectly stirred in accordance with the conceptual picture, but the experiments involving tracer injection at different points inside the model showed no evidence of such perfect stirring. In developing a more accurate physical explanation for the "mixing delay" time we have to account for its uniform distribution throughout the mixing volume; as the direct backmix experiments also showed, we also have to account for the inverse relation between τ_d and W, the strength of the backmix streams. This suggests that τ_d really represents the consequence of less-than-infinite speed of mixing throughout the volume. Perhaps more accurately it depends on the difference between the backmix diffusional velocity indicated by D_c in Eqn. (6.2) and the bulk forward flow velocity, V, for we get the same net result by decreasing V as by increasing D_c. Mixing delay time is still, therefore, a reasonable name for the parameter since it is an index of the time delay involved in backmixing upstream or maybe across a reactor.

(ii) In comparing one mixing system with another it does then seem reasonable to use the stirring factor as a comparative unit, at least to start with. On that basis, we find that the order of effectiveness is: vane swirled jet (0.815); countervortex flow (incinerator experiments) (0.675); and tangential entry jet (0.615). On this basis it would seem that: (1) multiple jets generating a single vortex are superior in mixing to a few jets; and (2) that countervortex flow generated by a few jets is superior to a single vortex generated by a few jets. On this basis, therefore, it would seem to imply - at least as a tentative conclusion worthy of experimental test - that the systems so far studied can be improved on still further by countervortex flow using multiple ports or vanes to generate each individual vortex. This is in fact the system approximated by the oil burner we have tested qualitatively, and although no instrumental measurements have been made on the system, from visual inspection it seems to burn very evenly (and possibly with rather low noise).

(iii) We are still not certain, however, that the stirring factor alone is adequate to characterize the total mixing characteristics. In the first place, the stirring factor can only be defined for homogeneous backmix systems, and in such systems we have no information at present on the relation between homogeneity or "grain" of the backmix and microturbulence levels for local mixing once the backmix stream has reached its destination; it is sometimes forgotten that a high level of turbulence does not, by itself, necessarily imply any significant degree of backmix. Nevertheless, it does seem not unreasonable to suppose that the homogeneity of the backmix and the local microturbulence levels do in fact correlate with the stirring factor. Some support for this was obtained by some fairly gross experiments on sampling the tracer right across the model almost at the plane of the burner exit. With the straight jet the usual high peak was obtained across the exit of the tracer injector. However, as swirl and the stirring level increased, the coherent tracer jet was progressively dissipated till, at high swirl levels, the concentration was appreciably uniform right across the chamber.

(iv) Since a mixing factor cannot be defined for an unswirled or low swirl-level jet this presents a different, and new, problem altogether. What we now require for these systems is an index for specifying the degree of homogeneity or heterogeneity of the backmix streams, together with some method of measuring such an index. A theoretical specification must wait upon theoretical development of some satisfactory representation of the nonhomogeneous backmix process but, as an empirical index for immediate purposes, perhaps a ratio based on the distance of the break point from the inlet in the time delay curves would be satisfactory. Our original thought was that the slopes of the initial region of the time delay curves would be adequate, but on more detailed examination this was ruled out. The distance to the break point, however, seems to increase with backmix heterogeneity.

(v) In all this, relatively little has been said so far about the application to an actual combustion process, other than a few references in passing. Detailed discussion is, of course, quite out of place here; however, a few observations on the mixing of fuel and oxidant streams may be pertinent. Discussions on mixing in the general literature frequently fail to distinguish explicitly between mixing of incoming fuel and oxidant streams with each other on the one hand, and mixing of the fuel/oxidant streams with the partially reacted mixture already in the chamber on the other hand. When nonpremixed, turbulent diffusion flames are being described it is the first consideration that is relevant; but if Braggs criterion is being applied, either to premixed or nonpremixed fuel/oxidant streams, then it is the second consideration that is relevant. If the region of injection in the combustion chamber is perfectly stirred in the ideal sense, we have a distinction without a difference. The points of injection can then be widely separated, and the combustion behavior, theoretically, is insensitive to the location and velocity of injection. However, as the stirring factor drops below unity the distinction becomes real and important. In particular, increasing attention must then be given to the interaction of the jets themselves, and the relative importance of the microscopic point of view in analysis also then increases. According to Essenhigh (76), this in effect partially parallels the view given, for example, by Herbert (83) in considering flame stabilization by baffles and cans. According to this view, a high dependence of stability correlation on Reynolds number implied rather poor mixing, and low dependence implied good mixing. In our terms, we would say that a high stirring factor probably implies good flameholding; and, if W is already high, an increased injection velocity has progressively less significance, with diminishing increase in improvement with further increase in injection velocity as W approaches unity. In this connection it is of interest that W was substantially independent of velocity at the highest level of swirling for the vane-swirled jet (Sec. 6.3).

Finally, in conclusion, it does seem that this fairly simple method of investigation is capable of elucidating gross mixing behavior, at least in outline and with some useful detail. It parallels and complements the more microscopic and mechanistic views of, for example, Herbert (83). The additional value of our approach is that it is not confined to jet cans and baffles.

7.4. Suggestions for Future Work

What is now required is (1) quantitative development of the concept of homogeneous and heterogeneous backmixing; and (2) comparative combustion stability tests to determine a correlation, if any, between combustion stability and stirring factor; and, (3) tests to study the correlation, if any, between stirring factor and turbulence parameters like intensity and scale.

In heterogeneous backmixing, the amount of recirculation flow to the inlet flow and the distance of the break point (Sec. 7.3.4) can be measured and used as an effective indicator of heterogeneity in mixing. Recirculation has been measured by Barchillon and Curtet (48). The amount of recirculation can be predicted by theories of Thring and Newby (15), and Curtet and Craya (47). The concept of homogeneous backmixing as outlined in Sec. 6.3.6 needs further development. A much simpler method of measuring heterogeneity may be devised from the observations of Fig. 28. We can notice that the central peak is the highest with a straight jet and zero for the W.S.R. Therefore a scale of heterogeneity can be assigned with a value of one to a straight jet and a value of zero for the homogeneous W.S.R. case. In between these two extremes can lie partially swirled jet mixing. These values can be easily measured although prediction, based on theory, may be very difficult.

NOMENCLATURE

c	Concentration of the tracer gas after correcting for instrument effect (volume per volume)
c'	Uncorrected concentration of the tracer gas as measured by the instrument
c_m	Concentration of the jet fluid at distance, x
c_o	Concentration of the tracer at the time of cut-off
G	Momentum of the jet
M	Mass of the jet flow at a distance, x, from the nozzle mouth
Re_b	Reynolds number, based on the box
Re_j	Reynolds number, based on the jet dia.
t	Time in seconds measured from the instant of cut-off
u	Velocity parallel to the main flow of the jet
u_o	Velocity of the jet as it emerges from the nozzle
V	Volumetric flow rate (ft.^{3}/sec.)
V_o	Total volume of the model (ft.^{3})
W	Stirring factor
x	Distance from the jet mouth
y	Distance from the jet axis
τ_d	Turbulent mixing delay time (sec.)
τ_i	Instrument factor (sec.)
τ_p	Transit time in the plug flow volume (sec.)
τ_s	Residence time in the perfectly stirred volume (sec.)
τ_t	Residence time in the plexiglass box (sec.)

REFERENCES

1. Essenhigh, R.H., and Kuo, T.J., "Development of Fundamental Basis for Incinerator Design Equations and Specifications," Rep. No. FS/PhS-8/69-4, Prepared for the Department of Health, Education, and Welfare under Contract No. 5R01/AP00391, Department of Materials Science, The Pennsylvania State University (1969).

2. Bragg, S.L., Aero. Res. Council, Paper No. 16170, C.F. 272 (Sept., 1953).

3. Beer, J.M., and Lee, K.B., "Tenth Symposium (International) on Combustion," P1187, The Combustion Institute, Pittsburgh (1965).

4. Drake, P.F., and Hubbard, E.H., J. Inst. Fuel, 39, p98 (Mar., 1966).

5. Vulis, L.A., "Thermal Regimes of Combustion," McGraw-Hill Book Co., New York (1961).

6. Essenhigh, R.H., "A New Application of Perfectly Stirred Reactor (P.S.R.) Theory to Design of Combustion Chambers," Tech. Rep. FS67-1(u), Office of Naval Research, Power Branch, Contract Nonr 656(29) (Mar., 1967).

7. Biswas, B., and Essenhigh, R.H., Mech. Engr., 91, P68 (1969).

8. Biswas, B., and Essenhigh, R.H., "Stabilization of Flames in Smoke," Paper accepted for publication, Combust. Flame (1970).

9. Shieh, W.S., Kuo, T.J., and Essenhigh, R.H., "Combustion and Emission Phenomena in Incinerators: Development of Physical and Mathematical Models of Incinerators, Part II, Initial testing of a Real System," Paper accepted for publication in the 4th National Incinerator Conference, A.S.M.E., Cincinnatti (May, 1970).

10. Langhaar, H.L., "Dimensional Analysis and Theory of Models," 7th Printing, John Wiley and Sons, Inc., New York (1965).

11. Johnstone, R.E., and Thring, M.W., "Pilot Plants, Models, and Scale-up Methods in Chemical Engineering," McGraw-Hill Book Company, New York (1957).

12. Fryling, G.R., "Combustion Engineering," Revised Edition, Combustion Engineering, Inc., New York (1967).

13. Anson, D., "Proceedings of the Third Symposium on Flames and Industry," J. Inst. Fuel (1966).

14. Beer, J.M., J. Inst. Fuel, P466 (Nov., 1966).

15. Thring, M.W., and Newby, M.P., "Fourth Symposium (International) on Combustion," P789, William and Wilkins, Baltimore (1953).

16. Hottel, H.C., "Fourth Symposium (International) on Combustion," P97, William and Wilkins, Baltimore (1953).

17. Groume-Grijimailo, W.E., "The Flow of Gases in Furnaces," John Wiley and Sons, Inc., New York (1923).

18. Rosin, P.O., J. Inst. Fuel, 9, P287 (1936).

19. Chesters, J.H., et al., J. Iron Steel Inst., 162, P385 (1949).

20. Newby, M.P., J. Iron Steel Inst., 162, P452 (1949).

21. Watson, E.A., and Clarke, J.S., J. Inst. Fuel, 21, P2 (Oct., 1947).

22. Inman, C., J. Inst. Fuel, P60 (Dec., 1969).

23. Beer, J.M., Chigier, N., and Lee, K.B., "Ninth Symposium (International) on Combustion," P892, Cornell University, New York (1962).

24. Pai, S.I., "Fluid Dynamics of Jets," D. Von Nostrand Co., Inc., New York (1954).

25. Abramovich, A., "The Theory of Turbulent Jets," The M.I.T. Press, Cambridge (1965).

26. Thring, M.W., "The Science of Flames and Furnaces," Second Edition, John Wiley and Sons, New York (1962).

27. Reichardt, H., Gesetzmassigkeiten der freien Turbulenz, V.D.I., Forschungsheft, No. 414 (1942).

28. Corrsin, S., Nat. Adv. Comm. Aeron., Adv. Conf. Rep. 3L29 (1943).

29. Tollmien, W., Birechung Turbulenter Ausbreitungsvorgange, Z.f. agnew, Math. U. Mech., 6, P468 (1926).

30. Howarth, L., Proc. Cambridge Phil. Soc., 34, P185 (1938).

31. Hinze, J.O., and Van der Hegge Zingen, B.G., Appl. Sci. Res., Al, P435 (Hague, 1949).

32. Ricou, F.P., and Spalding, D.B., J. Fluid. Mech., 11, P21 (1961).

33. Davis, R.F., Proc. Inst. Mech. Eng., 137 P11 (1937).

34. Field, M.A., et al., "Combustion of Pulverized Coal," Ch. 2, P25, The British Coal Utilization Association, Surrey (England) (1967).

35. Hawthorne, W.R., Weddell, D.S., and Hottel, H.C., "3rd Symposium (International) on Combustion," P266, Williams and Wilkins Co., Baltimore (1951).

36. Sunavala, P.D., Hulse, C., and Thring, M.W., Combust. Flame, 1, P179 (June, 1957).

37. Forstall, W., and Shapiro, A.H., J. of Applied Mechanics (Dec., 1950).

38. Squire, H.B., and Trouncer, J., "Round Jets in a General Stream," Aero. Res. Council, Tech. Rep. L. and M. No. 1974 (1944).

39. Sherman, R.A., "An Experimental Study of the Burning Characteristics of Pulverized Fuels," International Conference on Bituminous coals (1931).

40. Longwell, J.P., Frost, E.F., and Weiss, M.A., Industr. Eng. Chem., 45, No. 8, P1629 (1953).

41. Hedley, A.B., and Jackson, E.W., J. Inst. Fuel, P290 (July, 1965).

42. Karr, C., and Putnam, A.A., "Influence of Recirculated Combustion Products on Burning VElocity," ASHARE, P43 (Sept., 1962).

43. Longwell, J.P., and Weiss, M.A., Industr. Eng. Chem., 47, P1635 (1955).

44. Beer, J.M., and Thring, M.W., "Proceedings of the Anthracite Conference," The Pennsylvania State University (Sept., 1961).

45. Beer, J.M., "2nd Symposium on Flames and Industry," J. Inst. Fuel, London (1962).

46. Essenhigh, R.H., and Csaba, J., "Ninth Symposium (International) on Combustion," P111, Academic Press, New York (1962).

47. Curtet, R., and Craya, J., Combust. Flame, 2, P383 (1958).

48. Barchillon, M., and Curtet, R.J., Basic Eng., Trans. A.S.M.E., P777 (Dec., 1964).

49. Becker, H.A., Hottel, H.C., and Williams, G.C., "Ninth Symposium (International) on Combustion," P7, Academic Press, New York (1962).

50. Kerr, N.M., and Fraser, D., J. Inst. Fuel, 37, P519 (1965).

51. Kerr, N.M., J. Inst. Fuel, 37, P526 (1965).

52. Loitsyanskii, L.A., Prikl, Mat. i. Mech., 17, P3 (1953).

53. Gortler, H., Revisita Matematica Hispano Americano, 14, P3 (1953).

54. Cude, A.L., J. Iron Steel Inst., 175, P304 (Nov., 1953).

55. Hottel, H.C., and Pearson, R.A., "Fourth Symposium (International) on Combustion," Williams and Wilkins, Baltimore (1953).

56. Chigier, N.A., and Beer, J.M., Trans. A.S.M.E., 86, Series D, J. Basic Eng., P788 (Dec., 1964).

57. Mathur, M.L., and Maccalum, N.R.L., J. Inst. Fuel (May, 1967).

58. Levenspiel, O., "Chemical Reaction Engineering," John Wiley and Sons, Inc., New York (1967).

59. Hottel, H.C., Williams, A.C., and Baker, M.L., "Sixth Symposium (International) on Combustion," P398, The Reinhold Publishing Corporation, New York (1955).

60. Clarke, A.F., Harrison, A.J., and Odgers, J., "Seventh Symposium (International) on Combustion," P664, Butterworths Scientific Publications, London (1959).

61. Bragg, S.L., and Holiday, J.B., "Selected Combustion Problems," P470, Butterworths Scientific Publications, London (1956).

62. Hottel, H.C., Williams, G.C., and Bonnel, A.H., Combustion Flame, 2, P13 (1958).

63. Spalding, D.B., Aero. Res. Council, C.F. 19181 (1957).

64. Thring, M.W., and Masdin, E.A., Combust. Flame, 3, P125 (1959).

65. Avery, W.H., "Fifth Symposium (International) on Combustion," P86, Reinhold Publishing Corporation (1955).

66. Essenhigh, R.H., "Application of P.S.R. Theory to Analysis of One Dimensional Flames," Tech. Rep. No. FS66=3(u), Office of Naval Research, Department of Fuel Science, The Pennsylvania State University (Oct., 1966).

67. Danckwerts, P.V., Chem. Eng. Sci., 2, P1 (1953).

68. Hottel, H.C., Williams, G.C., and Miles, G.A., "Eleventh Symposium (International) on Combustion," The Combustion Institute, Pittsburgh (1967).

69. Engdahl, R.B., "B.C.R. Aid to Industry--Application of Overfire Air Jets to Prevent Smoke from Stationary Power Plants," Bituminous Coal Research, Inc., Pittsburgh (1951).

70. Woodruff, P.H., and Larson, A.P., "Proceedings of the Third National Incinerator Conference," P327 A.S.M.E., New York (May, 1968).

71. Sternitzke, R.F., and Dvirka, M., "Proceedings of the Third National Incinerator Conference," P295, A.S.M.E., New York (May, 1968).

72. Essenhigh, R.H., "Proceedings of the Third National Incinerator Conference," P87, A.S.M.E., New York (May, 1968).

73. Essenhigh, R.H., Environmental Science and Technology, 2, P524 (1968).

74. Essenhigh, R.H., and Kuo, T.J., "Combustion and Emission Phenomena in Incinerators: Development of Physical and Mathematical Models, Part I," Tech. Rep. No. FS/PHS-9/69-5, Prepared for the Department of Health, Education, and Welfare, Contract No. 5R01 AP00397, Paper accepted for Publication in the 4th National Incinerator Conference, A.S.M.E. (May, 1970).

75. Rao, S.T.R., Kuo, T.J., and Essenhigh, R.H., "Combustion and Emission Phenomena in Incinerators: Characterization of Stirring Factors by Cold Model Simulation," Tech. Rep. No. FS/PHS-9/69-9, Prepared for the Dept. of Health, Education, and Welfare, Contract No. 5R01 AP00397, Paper accepted for publication in the 4th National Incinerator Conference, A.S.M.E. (May, 1970).

76. Rao, S.T.R., and Essenhigh, R.H., "Experimental Determination of Stirring Factors Generated by Straight and Swirling Jets in Isothermal Combustion Chamber Models," Tech. Rep. No. FS/PHS-(2)69-11, prepared for the Department of Health, Education, and Welfare, Contract No. 5R01 AP00397, Paper accepted for publication in "13th Symposium (International) on Combustion," The Combustion Institute, Pittsburgh (Aug., 1970).

77. Aris, R., "Introduction to the Analysis of Chemical Reactors," Prentice-Hall, New Jersey, P208 (1965).

78. Villalobos, R., Chem. Engr. Progress, 65, P55 (April 1968).

79. Rippin, D.W.T., Ind. Eng. Chem. Fundamentals, 6, P488 (1967).

80. Gillespie, G.M., and Carberry, J.J., Ind. Eng. Chem. Fundamentals, 5, P164 (1966b)

81. Dean, R.B., and Dixon, W.J., Analytical Chem., 23, P636 (1951).

82. Kuwaka, M., Kuo, T.J., and Essenhigh, R.H., "Combustion and Emission Phenomena in Incinerators: Burning Rates and Extinction Limits in a Solid Fuel Bed," Rep. No. FS/PHS9/69-6, Prepared for the Department of Health, Education and Welfare under contract No. 5R01 AP00397, Paper accepted for publication at the A.S.M.E. 4th National Incinerator Conference, Cincinnati (May, 1970).

83. Herbert, M.V., "Progress in Combustion Science and Technology," 1, P61, Pergamon Press (Oxford) (1960).

APPENDIX A

DERIVATION OF THE EQUATION FOR THE CORRECTION OF THE INSTRUMENT EFFECT

A.1. Derivation

Because the Gow-Mac analyzer behaves as a stirred reactor, as explained in the main text, the expected output signal due to actual changes in tracer concentration is distorted. This distortion is the "Instrument Effect," and to determine the real changes in concentration at the model exit, a correction to the raw output data is required. In this Appendix, the derivation of the required correction equation is given as indicated in Sec. 6.1 [see Eqn. (6.1)].

The basis of the analysis is to treat the analyzer as a perfectly stirred reactor in series with the model. Consider an instant of time t during which the sample gases are flowing at a rate V_i through the instrument. Let the concentration at the inlet to the instrument be c and at the outlet be c'. Then the rate of tracer flow into the instrument = $V_i c$; and the rate of tracer flow out of the instrument = $V_i c'$. Then the net difference in tracer flow rate between the inlet and outlet of the instrument = $(V_i c - V_i c')$. Since the instrument cell is a perfectly stirred reactor, the concentration in the outgoing stream is the same as the concentration inside the instrument cell. Therefore, the rate of change of tracer in the instrument = $V_a(dc'/dt)$ where V_a is the volume of the instrument cell. By a mass balance we can write the following:

$$V_a(dc'/dt) = V_i c - V_i c' \qquad (A.1)$$

Also we define:

$$\tau_i = V_a/V_i \qquad (A.2)$$

where τ_i is the "Instrument Factor," which is the residence time of the sample gases. Eqn. (A.1) can be simplified using Eqn. (A.2) and by transposing as follows.

$$(dc'/dt) + c'/\tau_i = c/\tau_i \qquad (A.3)$$

In Eqn. (A.3), the rate of decay of concentration c at the model exit is unknown, but is given by Eqn. (5.16) as:

$$\ln(c/c_o) = -[t - (\tau_d + \tau_p)]/\tau_s \qquad (5.16)(A.4)$$

In any experiment, the quantity $(\tau_p + \tau_d)$ is unaffected by the "Instrument Effect" and so it is a determinable quantity, even without correction for the instrument distortion. Therefore, Eqn. (A.4) becomes

$$c = Rc_o \exp(-t/\tau_s) \qquad (A.5)$$

where $R = \exp[(\tau_d + \tau_p)/\tau_s]$. Substituting for c by Eqn. (A.5) in Eqn. (A.3) we obtain:

$$(dc'/dt) + c'/\tau_i = R(c_o/\tau_i) \exp(-t/\tau_s) \qquad (A.6)$$

Eqn. (A.6) is a first order differential equation between c' and t which can be solved using the integrating factor $\exp(t/\tau_i)$. Integrating, with the initial condition: $c' = c'_o$ at $t = \tau_d + \tau_p$ gives us

$$(c/c_o) = (1 - \tau_i/\tau_s)(c'/c'_o) + (\tau_i/\tau_s)/\exp[-\{t-(\tau_d + \tau_p)\}/\tau_i] \qquad (A.7)$$

where $(\tau_d + \tau_p) < t < \infty$. This Eqn. (A.7) has physically real values only after a time $(\tau_d + \tau_p)$. A shift of time coordinate by

$t^* = t - (\tau_d + \tau_p)$ gives the equation real values from $t^* = 0$. Therefore, we obtain:

$$(c/c_o) = (1 - \tau_i/\tau_s)(c'/c_o') + (\tau_i/\tau_s) \exp(-t^*/\tau_i) \qquad (6.1)(A.8)$$

where $0 < t^* < \infty$. This is the equation used in Sec. 6.1 [Eqn. (6.1)] for correcting the raw data to obtain the real changes in concentration at the model exit.

A.2. Additional Instrument--Tests

In the main text (Sec. 6.1) some of the tests on the instrument response were given. In Sec. 6.4 it was concluded that the instrument cannot be the source of the spread in data given in Fig. 15. This is concluded from the results in Fig. 14 which show the small spread of the data and also the variation of τ_i with increased bridge current at a constant cell-flow rate of 35 cc/min. It can be noticed that there is almost no spread in the data, indicating that the instrument is not erratic and not the source of the spread of the data in Fig. 14. Also, the instrument factor, τ_i, goes down linearly at first with increasing bridge current; but the rate of decrease of τ_i with further increase in current becomes almost negligible at higher currents. This was the reason that in most of the experiments currents greater than 8 ma were not used.

Fig. 30 shows the linear relationship between the millivolt output of the instrument and the sample gas concentration of helium. Usually the output at zero concentration was compensated by feeding in a negative voltage of equal magnitude and then the millivolt output is linearly proportional to the sample gas concentration, and hence

Fig. 29. Variation of the Instrument Factor with the Instrument (Bridge) Current at a Fixed Flow Rate. (Flow rate = 35 cc/min. τ_i is the time to change over to 36.8% of the change in output for a step change over from 2% helium in air to pure air.)

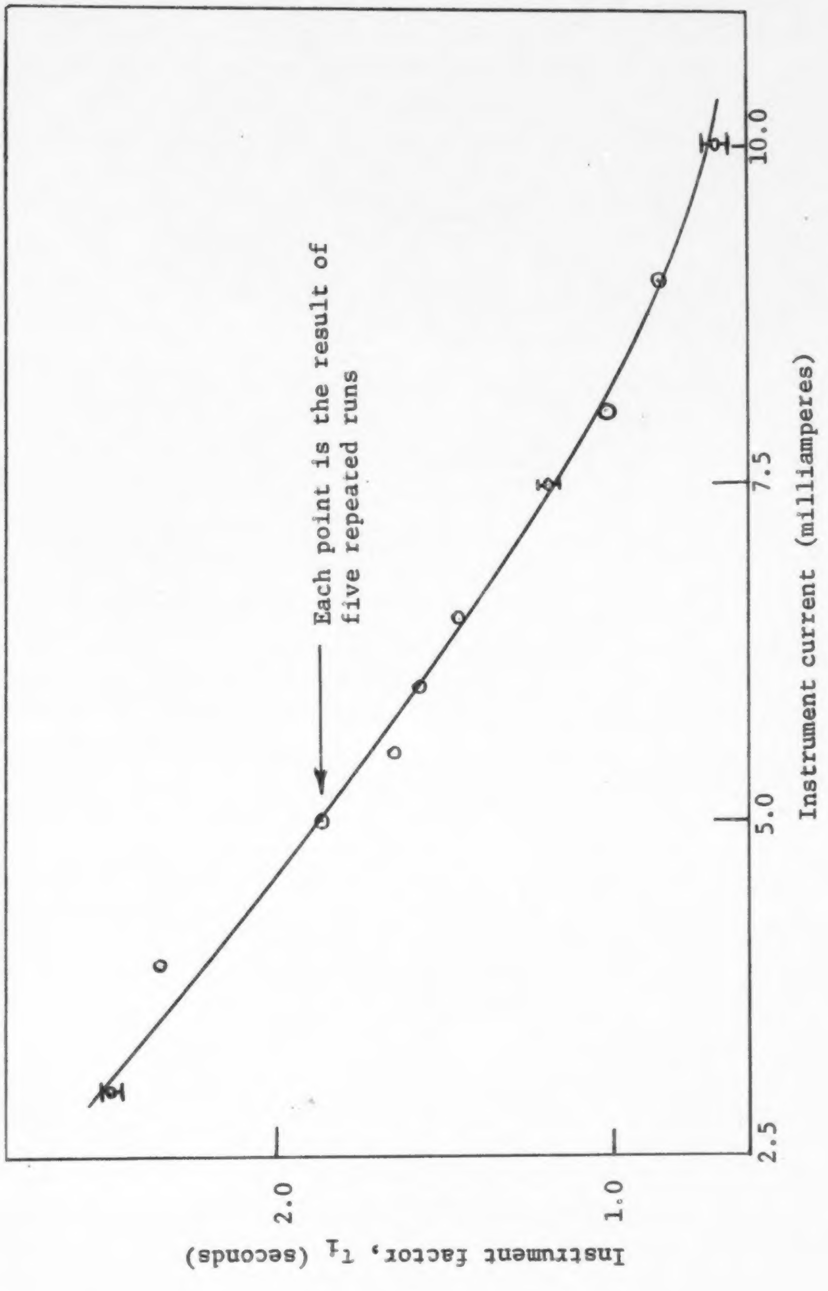
Each point is the result of five repeated runs
Instrument factor, t_1 (seconds)
2.0
1.0
2.5
5.0
7.5
10.0
Instrument current (milliamperes)

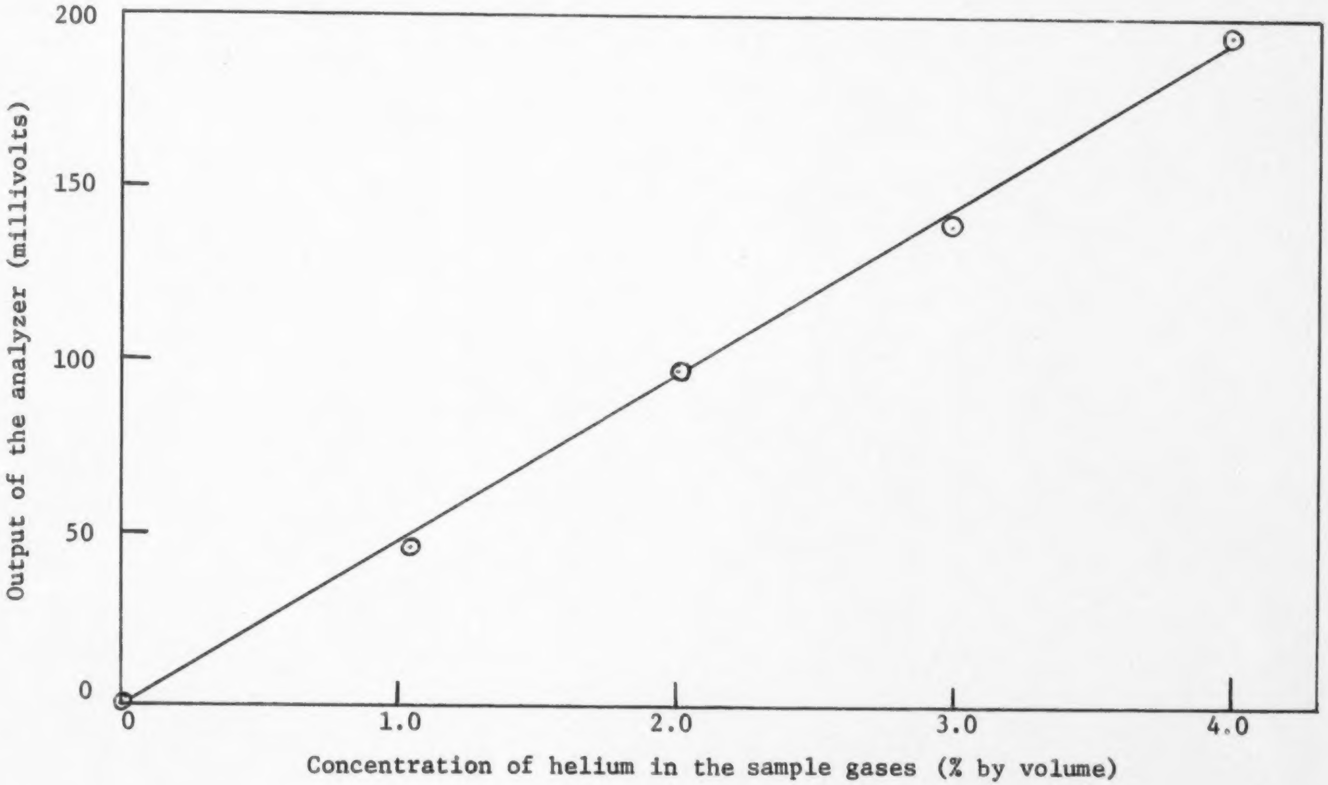

Fig. 30. Variation of the Instrument (Gow-Mac Analyzer) Output with Helium Concentration in the Sample Gases. (Change of flow rate of the sample gases is found to have no effect on the linearity of the curve but changes the slope of the line, only slightly. Flow rate = 50 cc/min, Instrument current = 8 ma.)

millivolts can be used as a direct measure of concentrations. This is the reason why most of the concentrations (both raw and corrected) in Appendicies B and C are tabulated in mv.

APPENDIX B

DATA FOR THE INCINERATOR-MODEL TESTS

Run B.1

Exit sampling with the opposed vortex system

Distance of the exit from the inlet = 46 in.

Reynolds number, Re_b = 8830

Residence time, τ_t = 3.02 sec.

Instrument factor, τ_i = 0.73 sec.

Spacing between the jet arrays = 8 in.

Offset angle = 0°

Momentum ratio = 695

$(\tau_d + \tau_p) = 2.55$ sec., $\tau_s = 0.47$ sec.

time, t (sec.)	t/τ_t	c'	c'/c'_o	c/c_o
0 - 2.55	0.845	73	1.000	1.00
2.80	0.930	69	0.930	0.60
3.00	0.999	67	0.917	0.32
3.50	1.160	61	0.835	-
4.00	1.325	47	0.645	-

Run B.2

Exit sampling with the opposed vortex system

Distance of the exit from the inlet = 46 in.

Reynolds number, Re_b = 8830

Residence time, τ_t = 3.02 sec.

Instrument factor, τ_i = 0.73 sec.

Spacing between the jet arrays = 8 in.

Offset angle = 15°

Momentum ratio = 695

$(\tau_d + \tau_p)$ = 2.2 sec., τ_s = 0.82 sec.

(corrected data is not shown)

time, t (sec.)	t/τ_t	c'	c'/c'_o
0 - 2.2	0 - 0.73	70	1.0
2.7	0.894	65	0.93
3.2	1.06	55	0.785
3.7	1.23	44.5	0.635
4.2	1.39	33	0.47
4.7	1.555	23	0.328
5.2	1.72	15	0.214
5.7	1.89	9	0.0128
6.2	2.05	5.5	0.0785

Run B.3

Exit sampling with the opposed vortex system

Distance of the exit from the inlet = 46 in.

Reynolds number, Re_b = 8830

Residence time, τ_t = 3.02 sec.

Instrument factor, τ_i = 0.73 sec.

Spacing between the jet arrays = 8 in.

Offset angle = 30°

Momentum ratio = 695

$(\tau_d + \tau_p) = 2.224$ sec., $\tau_s = 0.796$ sec.

time, t (sec.)	t/τ_t	c'	c'/c'_o	c/c_o
0 - 2.226	0 - 0.716	84.0	1.000	1.0000
2.700	0.898	81.0	0.965	0.5525
3.200	1.060	71.0	0.845	0.3095
3.700	1.230	56.5	0.6725	0.2350
4.2	1.395	44.0	0.524	-
4.7	1.560	36.0	0.405	-

Run B.4

Exit sampling with the opposed vortex system

Distance of the exit from the inlet = 46 in.

Reynolds number, Re_b = 8530

Residence time, τ_t = 3.02 sec.

Instrument factor, τ_i = 0.72 sec.

Spacing between the jet arrays = 8 in.

Offset angle = 50°

Momentum ratio = 695

$(\tau_d + \tau_p)$ = 2.3 sec., τ_s = 0.72 sec.

time, t (sec.)	t/τ_t	c'	c'/c'_o	c/c_o
0 - 2.3	0 - 0.762	80	1.00	1.000
2.8	0.927	73	0.91	0.500
3.3	1.091	64	0.80	0.249
3.8	1.260	48	0.60	0.124

Run B.5

Exit sampling with the opposed vortex system

Distance of the exit from the inlet = 46 in.

Reynolds number, Re_b = 8830

Residence time, τ_t = 3.02 sec.

Instrument factor, τ_i = 0.73 sec.

Spacing between the jet arrays = 8 in.

Offset angle = 70°

Momentum ratio = 695

$(\tau_d + \tau_p) = 2.44$ sec., $\tau_s = 0.58$ sec.

time, t (sec.)	t/τ_t	c'	c'/c'_o	c/c_o
0 - 2.44	0 - 0.81	85	1.000	1.0
2.50	0.83	83	0.976	0.948
2.80	0.93	81	0.954	0.514
3.00	0.997	79	0.920	0.336
4.00	1.330	51	0.600	-

Run B.6

Internal sampling with the opposed vortex system

Reynolds number, Re_b = 8830

Residence time, τ_t = 3.02 sec.

Spacing = 8 in.

Offset angle = 0°

Momentum ratio = 695

τ_d = 0.81 sec., τ_p = 1.74 sec., W = 0.362

Distance from the inlet (in.)	Average ($\tau_d + \tau_p$) (sec.)	Run No. Combined plug flow time (sec.) 1	2	3	4	5	6
48	2.55	2.2	2.4	2.6	2.6	2.7	2.9
36	2.26	2.1	2.2	2.5	-	-	-
27	1.57	1.9	1.5	1.6	1.55	1.5	1.50
18	1.10	0.9	1.0	1.2	1.3	-	-
9	0.80	0.6	0.85	0.95	-	-	-
4	0.82	0.8	0.6	0.9	0.9	0.9	-

Run B.7

Internal sampling with the opposed vortex system

Reynolds number, Re_b = 8830

Residence time, τ_t = 3.02 sec.

Spacing = 8 in.

Offset angle = 15°

Momentum ratio = 695

τ_d = 0.45 sec., τ_p = 1.75 sec., W = 0.644 sec.

Distance from the inlet (in.)	Average $(\tau_d + \tau_p)$ (sec.)	Run No. 1	2	3	4	5	6	7	8	9	10	11
		Combined plug flow time (sec.)										
46	2.2	2.0	2.0	2.05	2.15	2.10	2.18	2.25	2.25	2.35	2.3	2.5
34	1.74	1.2	1.45	1.63	1.7	1.85	1.9	1.95	2.0	2.0	-	-
22	1.12	0.85	0.90	0.9	0.90	0.95	1.00	1.10	1.15	1.15	1.3	-
11	0.62	0.5	0.5	0.5	0.6	0.6	0.6	0.6	0.7	0.75	0.8	-
8	0.46	0.25	0.3	0.4	0.4	0.4	0.42	0.45	0.48	0.55	0.6	0.06
4	0.45	0.3	0.32	0.35	0.4	0.45	0.45	0.5	0.60	0.60	-	-

Run B.8

Internal sampling with the opposed vortex system

Reynolds number, Re_b	=	8830
Residence time, τ_t	=	3.02 sec.
Spacing	=	8 in.
Offset angle	=	30°
Momentum ratio	=	695

τ_d = 0.44 sec., τ_p = 1.684 sec., W = 0.665

Distance from the inlet (in.)	Average ($\tau_d + \tau_p$) (sec.)	Run No. 1	2	3	4	5	6	7	8
		Combined plug flow time (sec.)							
48	2.16	2.13	2.15	2.15	2.21	-	-	-	-
38	1.90	2.00	1.80	1.90	-	-	-	-	-
32	1.51	1.70	1.70	1.40	1.35	1.5	-	-	-
26	1.36	1.20	1.20	1.30	1.50	1.60	-	-	-
20	1.07	0.90	1.05	1.10	1.10	1.10	1.2	-	-
14	0.72	0.7	0.7	0.7	0.7	0.7	0.8	-	-
11	0.47	0.4	0.4	0.43	0.43	0.5	0.6	0.7	-
8	0.47	0.2	0.2	0.5	0.55	0.6	0.6	0.7	0.7
5	0.45	0.2	0.4	0.4	0.4	0.6	0.7	-	-
3	0.41	0.2	0.2	0.45	0.6	0.6	-	-	-

Run B.9

Internal sampling with the opposed vortex system

Reynolds number, Re_b = 8830

Residence time, τ_t = 3.02 sec.

Spacing = 8 in.

Offset angle = 50°

Momentum ratio = 695

τ_d = 0.508 sec., τ_p = 1.722 sec., W = 0.599

Distance from the inlet (in.)	Average $(\tau_d + \tau_p)$ (sec.)	Run No.							
		1	2	3	4	5	6	7	8
		Combined plug flow time (sec.)							
46	2.23	2.2	2.3	2.5	2.11	2.13	2.17	-	-
40	2.07	2.0	2.0	2.2	-	-	-	-	-
27	1.42	1.30	1.35	1.5	1.55	-	-	-	-
21	1.08	0.8	0.95	1.15	1.20	1.30	-	-	-
15	0.73	0.69	0.69	0.85	-	-	-	-	-
9	0.52	0.30	0.45	0.45	0.6	0.6	0.6	0.6	0.6
7	0.5	0.30	0.4	0.55	0.6	0.6	-	-	-
4	0.5	0.3	0.5	0.55	0.6	0.6	-	-	-

Run B.10

Internal sampling with the opposed vortex system

Reynolds number, Re_b = 8830

Residence time, τ_t = 3.02 sec.

Spacing = 8 in.

Offset angle = 70°

Momentum ratio = 695

τ_d = 0.69 sec., τ_p = 1.75 sec., W = 0.453

Distance from the inlet (in.)	Average ($\tau_d + \tau_p$) (sec.)	Run No.							
		1	2	3	4	5	6	7	8
		Combined plug flow time (sec.)							
48	2.44	2.6	2.6	2.5	2.4	2.4	2.35	2.35	2.2
38	2.17	2.15	2.2	2.17	2.17	2.16	2.18	2.2	-
32	1.90	1.80	2.0	1.9	2.1	1.7	2.2	1.6	-
26	1.60	1.4	1.45	1.7	1.8	1.7	1.5	-	-
20	1.20	1.10	1.30	1.20	1.15	1.25	1.2	1.1	1.2
16	0.9	0.80	0.90	0.90	0.90	0.80	1.0	0.80	-
12	0.71	0.65	0.70	0.80	0.70	0.9	0.5	-	-
9	0.69	0.6	0.7	0.8	0.71	0.69	-	-	-
5	0.69	0.6	0.65	0.7	0.75	0.69	0.72	0.65	-
3	0.69	0.55	0.60	0.60	0.70	0.75	0.80	-	-

Run B.11

Exit sampling with the opposed vortex system

Distance of the exit from the inlet = 46 in.

Reynolds number, Re_b = 8350

Residence time, τ_t = 3.22 sec.

Instrument factor, τ_i = 0.73 sec.

Spacing = 0 in.

Offset angle = 30°

Momentum ratio = 695

$(\tau_d + \tau_p)$ = 1.98 sec., τ_s = 1.23 sec.

time, t (sec.)	t/τ_t	c'	c'/c'_o	c/c_o
0 - 1.98	0 - 0.616	81	1.0	1.0
2.8	0.874	72	0.89	0.554
3.3	1.030	61	0.755	0.4038
3.8	1.18	50	0.617	0.2988
4.3	1.34	39	0.482	-

Run B.12

Exit sampling with the opposed vortex system

Distance of the exit from the inlet = 46 in.

Reynolds number, Re_b = 8830

Residence time, τ_t = 3.02 sec.

Instrument factor, τ_i = 0.73 sec.

Spacing = 4 in.

Offset angle = 30°

Momentum ratio = 695

$(\tau_d + \tau_p) = 2.33$ sec., $\tau_s = 0.68$ sec.

time, t (sec.)	t/τ_t	c'	c'/c'_o	c/c_o
0 - 2.33	0 - 0.774	84	1.0	1.0000
2.8	0.930	78	0.929	0.5000
3.3	1.096	62	0.738	0.2316
3.8	1.260	39	0.464	0.1115

Run B.13

Exit sampling with the opposed vortex system

Distance of the exit from the inlet = 46 in.

Reynolds number, Re_b = 8830

Residence time, τ_t = 3.02 sec.

Instrument factor, τ_i = 0.73 sec.

Spacing = 8 in.

Offset angle = 30°

Momentum ratio = 695

time, t (sec.)	t/τ_t	c'	c'/c'_o	c/c_o
0 - 2.224	0 - 0.716	84.0	1.000	1.000
2.700	0.898	81.0	0.965	0.5525
3.200	1.060	71.0	0.845	0.3095
3.700	1.230	56.6	0.6725	0.2350
4.20	1.395	44.0	0.524	-
4.70	1.560	34.0	0.405	-

Run B.14

Exit sampling with the opposed vortex system

Distance of the exit from the inlet = 46 in.

Reynolds number, Re_b = 8830

Residence time, τ_t = 3.02 sec.

Instrument factor, τ_i = 0.73 sec.

Spacing = 14 in.

Offset angle = 30°

Momentum ratio = 695

$(\tau_d + \tau_p)$ = 2.2 sec., τ_s = 0.82 sec.

time, t (sec.)	t/τ_t	c'	c'/c'_o	c/c_o
0 - 2.2	0 - 0.731	88	1.0	1.0000
2.7	0.898	82	0.931	0.5470
3.2	1.06	75	0.853	0.3135
3.7	1.23	63	0.715	0.1862
4.2	1.395	46	0.522	-

Run B.15

Exit sampling with the opposed vortex system

Distance of the exit from the inlet = 46 in.

Reynolds number, Re_b = 8830

Residence time, τ_t = 3.02 sec.

Instrument factor, τ_i = 0.73 sec.

Spacing = 20 in.

Offset angle = 30°

Momentum ratio = 695

$(\tau_d + \tau_p) = 2.11$ sec., $\tau_s = 0.91$ sec.

time, t (sec.)	t/τ_t	c'	c'/c'_o	c/c_o
0 - 2.11	0 - 0.700	84	1.000	1.000
3.0	0.996	76	0.905	0.412
3.5	1.160	63	0.750	0.263
4.0	1.330	40	0.476	0.152

Run B.16

Exit sampling with the opposed vortex system

Distance of the exit from the inlet = 46 in.

Reynolds number, Re_b = 8830

Residence time, τ_t = 3.02 sec.

Instrument factor, τ_i = 0.73 sec.

Spacing = 26 in.

Offset angle = 30°

Momentum ratio = 695

time, t (sec.)	t/τ_t	c'	c'_o	c/c_o
0 - 2.06	0.685	80	1.0	1.0
3.0	0.996	69	0.863	0.4105
3.8	1.26	47	0.587	0.185
5.0	1.66	29	0.362	-

Run B.17

Internal sampling with the opposed vortex system

Reynolds number, Re_b = 8830

Residence time, τ_t = 3.02 sec.

Spacing = 0 in.

Offset angle = 30°

Momentum ratio = 695

τ_d = 0.41 sec., τ_p = 1.57 sec., W = 0.75

Distance from the inlet (in.)	Average ($\tau_d + \tau_p$) (sec.)	Run No. Combined plug flow time (sec.) 1	2	3	4	5	6	7	8	9
46	1.98	1.5	1.8	2.02	2.1	2.35	2.1	2.1	2.1	2.05
36	1.71	1.55	1.8	1.52	1.78	1.6	1.6	1.95	1.7	1.8
21	1.46	1.0	1.2	1.25	1.65	1.3	1.3	1.45	1.45	1.6
9	0.57	0.42	0.43	0.43	0.49	0.55	0.6	0.61	0.65	0.73
5	0.41	0.20	0.30	0.4	0.40	0.45	0.45	0.45	0.5	0.5
2	0.41	0.2	0.30	0.35	0.38	0.40	0.41	0.45	0.45	0.5

Run B.18

Internal sampling with the opposed vortex system

Reynolds number, Re_b = 8830

Residence time, τ_t = 3.01 sec.

Spacing = 4 in.

Offset angle = 30°

Momentum ratio = 695

τ_d = 0.38 sec., τ_p = 1.95 sec.

Distance from from inlet (in.)	Average $(\tau_d + \tau_p)$ (sec.)	Run No. 1	2	3	4	5	6	7	8	9	10
		Combined plug flow time (sec.)									
46	2.33	2.25	2.30	2.30	2.40	2.40	2.3	2.4	2.32	2.34	2.32
38	1.90	1.70	1.80	2.0	2.1	2.0	1.8	1.9	1.9	2.0	1.8
28	1.46	1.8	1.7	1.5	1.41	1.35	1.31	1.25	-	-	-
18	0.88	1.1	1.0	0.92	0.9	0.9	0.8	0.7	0.7	-	-
11	0.53	0.7	0.7	0.65	0.52	0.5	0.48	0.4	0.3	-	-
7	0.42	0.50	0.45	0.45	0.45	0.45	0.45	0.45	0.45	0.2	0.35
5	0.34	0.55	0.45	0.42	0.4	0.35	0.35	0.33	0.25	0.25	0.15
2	0.38	0.5	0.5	0.45	0.45	0.3	0.25	0.2	-	-	-

Run B.19

Internal sampling with the opposed vortex system

Reynolds number, Re_b = 8830

Residence time, τ_t = 3.01 sec.

Spacing = 8 in.

Offset angle = 30°

Momentum ratio = 695

τ_d = 0.44 sec., τ_p = 1.684 sec., W = 0.665

Distance from the inlet (in.)	Average ($\tau_d + \tau_p$) (sec.)	Run No. 1	2	3	4	5	6	7	8
		Combined plug flow time (sec.)							
48	2.16	2.13	2.15	2.15	2.21	-	-	-	-
38	1.90	2.00	1.80	1.90	-	-	-	-	-
32	1.51	1.70	1.70	1.40	1.35	1.50	-	-	-
26	1.36	1.20	1.20	1.30	1.50	1.60	-	-	-
20	1.07	0.90	1.05	1.10	1.10	1.10	1.20	-	-
14	0.72	0.70	0.70	0.70	0.70	0.80	-	-	-
11	0.47	0.40	0.40	0.43	0.43	0.50	0.60	0.70	-
8	0.47	0.20	0.20	0.50	0.55	0.60	0.60	0.70	0.70
5	0.45	0.20	0.40	0.40	0.40	0.60	0.70	-	-
3	0.41	0.20	0.20	0.45	0.60	0.60	-	-	-

Run B.20

Internal sampling with the opposed vortex system

Reynolds number, Re_b	= 8830
Residence time, τ_t	= 3.01 sec.
Spacing	= 14 in.
Offset angle	= 30°
Momentum ratio	= 695

τ_d = 0.59 sec. , τ_p = 1.61 sec., W = 0.580

(Note: When probed across the box, at 9 in. from inlet the tracer was found to be uniformly mixed.)

Distance from the inlet (in.)	Average $(\tau_d + \tau_p)$ (sec.)	Run No. 1	2	3	4	5	6
		Combined plug flow time (sec.)					
46	2.14	2.05	2.05	2.45	2.25	2.1	2.05
38	1.8	1.68	1.74	1.95	1.8	1.7	1.9
26	1.16	0.8	1.2	1.5	1.2	1.1	1.16
20	0.72	0.7	0.7	0.78	0.75	0.7	-
14	0.54	0.2	0.35	0.5	0.6	0.7	0.85
8	0.62	0.4	0.5	0.6	0.7	0.9	-
6	0.60	0.4	0.55	0.6	0.7	0.75	0.6
4	0.60	0.4	0.55	0.6	0.7	0.75	0.6

Run B.21

Internal sampling with the opposed vortex system

Reynolds number, Re_b = 8830
Residence time, τ_t = 3.01 sec.
Spacing = 20 in.
Offset angle = 30°
Momentum ratio = 695

(Note: Internal sampling showed each jet array was associated with a stirred section.)

τ_d (top array) = 1.025 sec., τ_s = 0.9 sec.
τ_d (bottom array) = 0.51 sec., W = 0.468

Distance from the inlet (in.)	Average $(\tau_d + \tau_p)$ (sec.)	Run No. 1	2	3	4	5	6	7	8	9	10
		Combined plug flow time (sec.)									
46	2.11	1.75	1.8	1.9	1.92	2.2	2.25	2.25	2.3	2.3	2.4
38	1.75	1.6	1.65	1.7	1.7	1.75	1.75	1.75	1.95	2.0	-
32	1.45	1.2	1.3	1.4	1.4	1.4	1.5	1.5	1.55	1.8	-
26	1.08	0.9	0.9	1.0	1.1	1.15	1.2	1.15	1.15	1.2	1.15
20	1.04	0.85	0.9	1.0	1.0	1.1	1.1	1.15	1.18	1.2	1.2
14	1.03	0.76	0.82	1.0	1.0	1.0	1.1	1.10	1.2	1.3	-
8	0.94	0.55	0.7	0.8	0.9	0.9	0.95	1.25	1.15	1.10	1.15
3	0.50	0.3	0.4	0.55	0.55	0.65	0.7	-	-	-	-
1	0.50	0.3	0.4	0.5	0.55	0.6	0.7	-	-	-	-

Run B.22

Internal sampling with the opposed vortex system

Reynolds number, Re_b = 8830

Residence time, τ_t = 3.01 sec.

Spacing = 26 in.

Offset angle = 30°

Momentum ratio = 695

(Note: Internal sampling showed each jet array was associated with a stirred section. In between these two a plug flow section existed).

τ_d (top array) = 1.35 sec., τ_s = 0.95 sec.
τ_d (bottom array) = 0.51 sec., W = 0.414

Distance from the inlet (in.)	Average ($\tau_d + \tau_p$) (sec.)	Run No. Combined plug flow time (sec.)									
		1	2	3	4	5	6	7	8	9	10
46	2.06	1.8	1.8	1.9	2.0	2.0	2.1	2.15	2.2	2.3	2.4
41	1.67	1.6	1.5	1.5	1.7	1.8	1.9	1.82	1.7	1.75	-
36	1.37	1.2	1.2	1.25	1.3	1.4	1.4	1.4	1.5	-	-
30	1.34	1.2	1.3	1.3	1.2	1.3	1.3	1.35	1.4	1.4	1.35
24	1.35	1.0	1.4	1.15	1.15	1.2	1.2	1.3	1.3	1.4	1.5
18	1.15	0.8	0.95	1.0	1.0	1.1	1.5	1.1	1.15	1.2	1.4
11	0.83	0.9	0.7	0.65	0.8	0.85	0.85	0.9	1.0	1.0	1.2
5	0.51	0.5	0.55	0.45	0.8	0.3	0.9	0.4	0.4	0.8	0.4
2	0.51	0.3	0.4	0.4	0.5	0.6	0.6	0.65	0.55	0.49	0.51

Run B.23

Exit sampling with the opposed vortex system

Momentum ratio = 20.3

Spacing = 80 in.

Residence time, τ_t = 1.91 sec.

Instrument factor, τ_i = 0.7 sec.

Offset angle = 70°

Reynolds number, Re_b = 13900

time, t (sec.)	t/τ_t	c'	c'/c'_o	c/c_o
0 - 1.4	0 - 0.735	65	1.0	1.0
1.6	0.838	62	0.955	0.677
1.9	0.995	55	0.845	0.360
2.2	1.150	45	0.695	0.181
2.4	1.255	35	0.54	0.128
2.6	1.36	25	0.384	-
2.9	1.52	13.5	0.208	-

Run B.24

Exit sampling with the opposed vortex system

Momentum ratio = 695

Spacing = 8 in.

Offset angle = 70°

Instrument factor, τ_i = 0.73 sec.

$(\tau_d + \tau_p)$ = 2.44 sec., τ_s = 0.58 sec.

time, t (sec.)	t/τ_t	c'	c'/c'_o	c/c_o
0 - 2.44	0 - 0.81	85	1.00	1.00
2.50	0.83	83	0.976	0.948
2.80	0.93	81	0.954	0.514
3.00	0.997	79	0.920	0.336
4.00	1.330	51	0.600	-

Run B.25

Exit sampling with the opposed vortex system

Momentum ratio = 6100

Spacing = 8 in.

Residence time, τ_t = 4.26 sec.

Reynolds number, Re_b = 6250

Instrument factor, τ_i = 0.75 sec.

$(\tau_d + \tau_p)$ = 2.7 sec., τ_s = 1.56 sec.

time, t (sec.)	t/τ_t	c'	c'/c'_o	c/c_o
0 - 2.7	0 - 0.575	80	1.0	1.0
2.9	-	79	-	-
3.4	0.798	75	0.939	0.622
3.9	-	70	-	-
4.4	1.03	60.5	0.755	0.3925
4.9	-	47	-	-
5.4	1.27	40	0.463	0.249
5.9	-	29	-	-

Run B.26

Internal sampling with the opposed vortex system

Momentum ratio = 20.3
Reynolds number, Re_b = 13900
Residence time, τ_t = 1.91 sec.
Spacing = 8 in.
Offset angle = 70°

It was found that the helium jet flew through the top level of the box without any well stirred conditions (concentration not uniformly distributed across the box). However, lower in the box the jet mixed uniformly across the box. Here we have shown that, although exit sampling Run B.23 showed well-stirred and plug flow combination [following Equation (5.16)] internal sampling can show that the well-stirred condition does not exist.

Run B.27

Internal sampling with the opposed vortex system

Reynolds number, Re_b = 8830

Residence time, τ_t = 3.02 sec.

Spacing = 8 in.

Offset angle = 70°

Momentum ratio = 695

τ_d = 0.69 sec., τ_p = 1.75 sec., W = 0.453

Distance from the inlet (in.)	Average $(\tau_d + \tau_p)$ (sec.)	Run No. 1	2	3	4	5	6	7	8
		Combined plug flow time (sec.)							
48	2.44	2.6	2.6	2.5	2.4	2.4	2.35	2.35	2.2
38	2.17	2.15	2.2	2.17	2.17	2.16	2.18	2.2	-
32	1.90	1.80	2.0	1.9	2.1	1.7	2.2	1.6	-
26	1.60	1.4	1.45	1.7	1.8	1.7	1.5	-	-
20	1.20	1.10	1.30	1.20	1.15	1.25	1.2	1.1	1.2
16	0.9	0.80	0.90	0.90	0.90	0.80	1.0	0.80	-
12	0.71	0.65	0.70	0.80	0.70	0.9	0.5	-	-
9	0.69	0.6	0.7	0.8	0.71	0.69	-	-	-
5	0.69	0.6	0.65	0.7	0.75	0.69	0.72	0.65	-
3	0.69	0.55	0.60	0.60	0.70	0.75	0.80	-	-

Run B.28

Internal sampling with the opposed vortex system

Momentum ratio = 6100

Reynolds number, Re_b = 6250

Spacing = 8 in.

Offset angle = 70°

Residence time, τ_t = 4.26 sec.

$\tau_d = 0.64$ sec., $\tau_p = 2.56$ sec., $W = 0.625$

Distance from the inlet (in.)	Average $(\tau_d + \tau_p)$ (sec.)	Run No. 1	2	3	4
		Combined plug flow time (sec.)			
46	3.2	3.2	3.1	3.3	3.2
33	2.75	2.7	2.8	2.75	2.75
27	2.25	2.2	2.3	2.25	2.2
21	1.62	1.6	1.72	1.52	1.61
15	1.05	1.05	1.05	1.95	1.15
7	0.65	0.65	0.68	0.68	0.60
4 1/2	0.65	0.65	0.60	0.68	0.68
1 1/2	0.65	0.65	0.60	0.70	0.65

APPENDIX C

DATA FOR THE TESTS ON THE STRAIGHT, TANGENTIAL ENTRY, AND VANE-SWIRLED JETS

Run C.1

Sampling at 46 in. from the inlet with the vane swirled burner fitted to the box

Angle of the secondary vanes = 10°

Reynolds number, Re_b = 1120

Residence time, τ_t = 2.29 sec.

Instrument factor, τ_i = 0.76 sec.

$(\tau_d + \tau_p)$ = 1.2 sec., τ_s = 0.94 sec.

time, t (sec.)	t/τ_t	c'	c'/c'_o	c/c_o
0 - 1.35	0 - 0,58	76	1.0	1.0
1.85	0.809	65	0.855	0.591
2.35	1.025	51.5	0.678	0.346
2.85	1.242	32.0	0.421	0.196
3.35	1.460	18.5	0.244	0.115
3.85	1.680	11.0	0.145	0.0658

Run C.2

Sampling at 46 in. from the inlet with the vane swirled burner fitted to the box

Secondary vane angle = 35°

Reynolds number, Re_b = 11200

Residence time, τ_t = 2.28 sec.

Instrument factor, τ_i = 0.78 sec.

$(\tau_d + \tau_p)$ = 1.15 sec., τ_s = 1.13 sec.

time, t (sec.)	t/τ_t	c'	c'/c'$_o$	c/c_o
0 - 1.15	0 - 0.505	88	1.0	1.000
1.65	0.125	80	0.910	0.646
2.15	0.945	63	0.716	0.414
2.65	0.160	44	0.5	-
3.15	1.380	28.5	0.324	-

Run C.3

Sampling at 46 in. from the inlet with vane swirled burner fitted to the box

Secondary vane angle (fully open) = 90°

Reynolds number, Re_b = 11900

Residence time, τ_t = 2.14 sec.

Instrument factor, τ_i = 0.70 sec.

$(\tau_d + \tau_p) = 0.4$ sec., $\tau_s = 1.74$ sec.

time, t (sec.)	t/τ_t	c'	c'/c'_o	c/c_o
0 - 0.4	0 - 0.187	77.0	1.0	1.0
0.65	0.304	73.5	0.955	0.876
0.90	0.420	67.5	0.876	-
1.40	0.655	55.0	0.715	0.522
1.90	0.890	43.0	0.559	0.384
2.40	1.120	31.0	0.4025	-
2.90	1.360	23.0	0.298	-

Run C.4

Sampling at 46 in. from the inlet with the tangential entry jet fitted to the box

All flow is introduced tangentially

Reynolds number, Re_b = 8100, Re_j = 31200

Residence time, τ_t = 3.12 sec.

Instrument factor, τ_i = 0.65 sec.

$(\tau_d + \tau_p)$ = 2.3 sec., τ_s = 0.82 sec.

time, t (sec.)	t/τ_t	c'	c'/c'_o	c/c_o
0 - 2.3	0 - 0.737	84	1.0	1.0
2.7	0.865	81	0.965	0.634
3.2	1.022	72	0.860	0.351
3.7	1.185	60	0.715	-
4.2	1.345	50	0.595	0.1507
4.7	1.505	41	0.498	-

Run C.5

Sampling at 46 in. from the inlet with the tangential entry (jet swirled) jet fitted to the box

81.5 percent of flow introduced tangentially

Reynolds number, $Re_b = 8100$, $Re_j = 31200$

Residence time, $\tau_t = 3.12$ sec.

Instrument factor, $\tau_i = 0.75$ sec.

$(\tau_d + \tau_p) = 2.1$ sec., $\tau_s = 1.02$ sec.

time, t (sec.)	t/τ_t	c'	c'/c'_o	c/c_o
0 - 2.1	0 - 0.675	85	1.0	1.0
2.6	0.835	82	0.965	0.634
3.1	0.995	70	0.825	0.412
3.8	1.220	50	0.589	0.2325
4.3	1.38	38	0.446	-
5.8	1.86	17	0.200	-

Run C.6

Sampling at 46 in. from the inlet with the tangential entry (jet swirled) jet fitted to the box

38 percent of the flow introduced tangentially

Reynolds number, Re_b = 8100, Re_j = 31200

Residence time, τ_t = 3.12 sec.

Instrument factor, τ_i = 0.78 sec.

$(\tau_d + \tau_p)$ = 1.55 sec., τ_s = 1.67 sec.

time, t (sec.)	t/τ_t	c'	c'/c'_o	c/c_o
0 - 1.55	0 - 0.496	83.0	1.0	1.0
1.85	0.594	81.5	0.98	0.832
2.35	0.754	74.5	0.9	0.64
2.85	0.914	66.0	0.795	-
3.35	1.071	54.0	0.650	0.3872
3.85	1.230	41.5	0.500	-
4.35	1.395	37.0	0.446	-
4.85	1.560	31.0	0.374	-

Run C.7

Sampling at 46 in. from the inlet with the tangential entry (jet swirled) jet fitted to the box

All the flow is introduced axially
(no flow is introduced tangentially)

Reynolds number, Re_b = 8100, Re_j = 31200

Residence time, τ_t = 3.12 sec.

Instrument factor, τ_i = 0.65 sec.

$(\tau_d + \tau_p)$ = 1.05 sec., τ_s = 2.07 sec.

time, t (sec.)	t/τ_t	c'	c'/c'_o	c/c_o
0 - 1.05	0 - 0.336	86	1.00	1.0
1.5	0.480	79	0.92	0.759
1.7	0.544	73	0.85	0.712
2.3	0.738	55	0.64	0.478
2.8	0.900	43	0.50	0.3796
3.3	1.06	34	0.396	0.2896
4.3	1.38	21	0.244	0.201

Run C.8

Sampling at 46 in. from the inlet with a straight jet fitted to the box

Dia. of jet = 2 in.

Residence time, τ_t = 1.94 sec.

Reynolds number, Re_b = 12700, Re_j = 96600

Instrument factor = 0.65 sec.

$(\tau_d + \tau_p)$ = 0.35 sec., τ_s = 1.59 sec.

time, t (sec.)	t/τ_t	c'	c'/c'_o	c/c_o
0 - 0.35	0 - 0.18	85.0	1.000	1.000
0.80	0.412	78.0	0.917	0.757
1.30	0.670	61.5	0.725	0.534
1.80	0.926	46.0	0.540	0.375
2.80	1.440	27.0	0.318	-
3.30	1.700	21.0	0.247	0.200
4.8	2.48	8.5	0.100	-

Run C.9

Sampling at 46 in. from the inlet with a straight jet fitted to the box

Dia. of jet = 3 in.

Reynolds number, Re_b = 12100, Re_j = 62000

Residence time, τ_t = 2.022 sec.

Instrument factor, τ_t = 0.8 sec.

$(\tau_d + \tau_p)$ = 0.39 sec., τ_s = 1.63 sec.

time, t (sec.)	t/τ_t	c'	c'/c'_o	c/c_o
0 - 0.39	0 - 0.193	83	1.0	1.0
0.90	0.445	75	0.905	0.726
1.40	0.692	63	0.760	
1.90	0.940	47	0.565	0.375
2.3	1.138	34	0.410	0.300
2.8	1.381	25	0.301	0.1881
3.3	1.630	17	0.205	-
3.8	1.880	13	0.157	-
4.3	2.12	9	0.1081	0.0667

Run C.10

Sampling at 46 in. from the inlet with a straight jet fitted to the box

Dia. of the jet = 4 in.

Residence time, τ_t = 2.04 sec.

Reynolds number, Re_b = 12530, Re_j = 48000

Instrument factor, τ_i = 2.6 sec.

$(\tau_d + \tau_p)$ = 0.73 sec., τ_s = 1.31 sec.

time, t (sec.)	t/τ_t	c'	c'/c'$_o$	c/c$_o$
0 - 0.73	0 - 0.358	83	1.0	1.0
1.00	0.490	81.5	0.982	0.833
2.00	0.980	68.5	0.825	0.42
3.00	1.470	51.0	0.615	0.243
4.00	1.960	35.5	0.428	0.159
5.00	2.48	24.0	0.290	0.112
6.00	2.94	16.0	0.193	0.083
7.00	3.44	10.0	0.120	

Run C.11

Internal sampling with the vane swirled jet fitted to the box

Angle of the vane setting = 10°

Reynolds number, Re_b = 1120

Residence time, τ_t = 2.29 sec.

$\tau_d = 0.23$ sec., $\tau_p = 1.12$ sec., $\tau_s = 0.94$ sec.

W = 0.805

Distance from the inlet (in.)	Average $(\tau_d + \tau_p)$ (sec.)	Run No. 1 Combined plug flow time (sec.)	Run No. 2 Combined plug flow time (sec.)	Run No. 3 Combined plug flow time (sec.)
46	1.35	1.35	1.4	1.3
38	1.20	1.23	1.15	1.20
35	1.0	1.0	1.04	0.96
29	0.68	0.65	0.70	0.68
26	0.51	0.51	0.50	0.52
22	0.26	0.25	0.28	0.25
16,11,6,2	0.23	0.23	0.21	0.25

Run C.12

Internal sampling with the vane swirled jet fitted to the box

Secondary vane angle = 35°

Reynolds number, Reb = 11200

Residence time, τ_t = 2.28 sec.

(Note: In this case W was not calculated since the mixing delay is not constant in the stirred region.)

Distance from the inlet (in.)	Average $(\tau_d + \tau_p)$ (sec.)	Run No. 1	2	3	4	5
		Combined plug flow time (sec.)				
46	1.15	1.3	1.05	1.11	1.05	1.1
40	1.03	1.1	1.05	0.98	-	-
35	0.95	0.85	1.0	1.0	-	-
29	0.72	0.8	0.65	0.75	0.7	-
24	0.50	0.35	0.45	0.60	0.60	-
19	0.325	0.25	0.30	0.40	0.40	-
11	0.25	0.20	0.25	0.25	0.3	-
6	0.14	0.125	0.15	0.15	0.15	-
4	0.115	0.10	0.15	0.1	0.1	-

Run C.13

Internal sampling with the tangential entry jet fitted to the box

All the flow is introduced tangentially. (Highly swirled jet)

Reynolds number, $Re_b = 8100$, $Re_j = 30000$

Residence time, $\tau_t = 3.16$ sec.

$\tau_d = 0.475$ sec., $\tau_p = 1.925$ sec.,

$\tau_s = 0.76$ sec., $W = 0.615$

Distance from the inlet (in.)	Average $(\tau_d + \tau_p)$ (sec.)	Run No. 1	2	3	4	5	6
		Combined plug flow time (sec.)					
46	2.4	2.7	2.4	2.5	2.25	2.2	-
36	1.98	2.05	2.1	2.2	1.9	1.9	1.8
26	1.50	1.80	1.55	1.45	1.20	1.50	-
21	0.875	1.00	1.125	0.625	0.75	0.87	-
16	0.507	0.30	0.30	0.85	0.70	0.45	0.6
11	0.505	0.50	0.55	0.65	0.65	0.5	0.5
6,2	0.505	0.50	0.55	0.65	0.65	0.5	0.5

Run C.14

Internal sampling with the tangential entry jet fitted to the box

47.5 percent of the total flow is introduced tangentially with the rest introduced axially (partially swirled jet)

Reynolds number, Re_b = 8100, Re_j = 30000

Residence time, τ_t = 3.16 sec.

(Note: In this case W was not calculated since mixing delay, τ_d, is not constant in the stirred region, near the inlet.)

Distance from the inlet (in.)	Average $(\tau_d + \tau_p)$ (sec.)	Run No.								
		1	2	3	4	5	6	7	8	9
		Combined plug flow time (sec.)								
46	1.7	1.5	1.5	1.6	1.65	1.7	1.95	-	-	-
36	1.425	1.05	1.35	1.35	1.45	1.45	1.5	1.725	-	-
31	1.075	0.80	0.85	0.90	1.05	1.425	1.425	-		
26	0.55	0.35	0.40	0.45	0.675	0.9	-	-	-	-
21	0.50	0.1,2*	0.15	0.25	0.35	0.4	0.5	0.6	0.65,2	0.7,4
16	0.45	0.1	0.3	0.35	0.40	0.55	0.65	0.65	-	-
11	0.225	0.15	0.15	0.175,2	0.2	0.25	0.3	0.35	0.35	
6	0.175	0.15,3	0.2	0.25						
2	0.075	0.05	0.05	0.075	0.1,3					

*The number following the comma indicates the number of repeated appearances of the value.

Run C.15

Internal sampling with the tangential entry jet fitted to the box

All the flow occurs axially with zero flow through the tangential ports.
(zero swirl, straight jet)

Reynolds number, Re_b = 10420, Re_j = 39900

Residence time, τ_t = 2.44 sec.

(Note: In this case W was not calculable since the mixing delay time, τ_d) was not constant in the stirred region.)

Distance from the inlet (in.)	Average $(\tau_d + \tau_p)$ (sec.)	Run No. 1	2	3	4	5
		Combined plug flow time (sec.)				
46	1.32	1.1	1.6	1.25	1.4	1.25
44	1.19	1.2	1.25	1.05	1.2	1.25
40	1.10	1.15	1.0	1.3	1.05	1.0
38	1.02	0.9	0.85	1.1	0.95	1.3
34	0.725	0.8	0.75	0.6	0.75	0.72
25	0.45	0.4	0.5	0.4	0.5	0.45
20	0.625	0.35	0.4	0.5	0.45	-
15	0.325	0.35	0.3	0.35	0.3	-
10	0.30	0.30	0.25	0.35	-	-

Run C.16

Internal sampling with a (2 in. dia.) straight jet fitted to the box

Reynolds number, $Re_b = 12700$, $Re_j = 96600$

Residence time, $\tau_t = 1.94$ sec.

(Note: In this case W was not calculable since the mixing delay time, τ_d, was not constant in the stirred region.)

Distance from the inlet (in.)	Average $(\tau_d + \tau_p)$ (sec.)	Run No. 1	2	3	4	5
		Combined plug flow time (sec.)				
46	0.35	0.35	0.36	0.34	0.35	0.35
39	0.27	0.25	0.25	0.28	0.30	
34	0.22	0.20	0.20	0.3	-	-
24	0.16	0.12	0.15	0.18	0.2	0.16
15	0.092	0.08	0.08	0.1	0.11	0.09
7	0.07	0.04	0.1	0.07	0.6	0.08

Run C.17

Internal sampling with a (3 in. dia.) straight jet fitted to the box

Reynolds number, $Re_b = 12100$, $Re_j = 62000$

Residence time, τ_t = 2022 sec.

(Note: In this case stirring factor was not calculated because the mixing delay time, τ_d, was not constant in the stirred region.)

Distance from the inlet (in.)	Average ($\tau_d + \tau_p$) (sec.)	Run No. 1	2	3	4	5	6
		Combined plug flow time (sec.)					
46	0.38	0.4	0.4	0.4	0.375	0.36	0.4
41	0.30	0.34	0.32	0.3	0.275	0.275	-
36	0.26	0.20	0.25	0.25	0.27	0.3	0.3
31	0.2125	0.25	0.25	0.22	0.15	-	-
26	0.20	0.15	0.15	0.20	0.24	0.24	-
21	0.15	0.162	0.152	0.1375	0.1375	0.13	
16	0.12	0.10	0.10	0.12	0.13	0.14	0.14
5	0.095	0.11	0.1	0.08	0.08	-	-

Run C.18

Internal sampling with a (4 in. dia.) straight jet fitted to the box

Reynolds number, $Re_b = 12530$, $Re_j = 4800$

Residence time, $\tau_t = 2.04$ sec.

(Note: In this case stirring factor was not calculated because the mixing delay time, τ_d, was not constant in the stirred region.)

Distance from the inlet (in.)	Average $(\tau_d + \tau_p)$ (sec.)	Run No. 1	2	3	4	5
		Combined plug flow time (sec.)				
46	0.73	0.74	0.83	0.74	0.74	0.6
44	0.69	0.72	0.55	0.75	0.73	0.7
42	0.60	0.62	0.56	0.58	0.64	0.6
40	0.54	0.6	0.6	0.42	0.54	0.56
38	0.44	0.55	0.44	0.38	0.44	0.37
36	0.44	0.43	0.40	0.46	0.48	0.45
34	0.36	0.34	0.42	0.37	0.35	0.38
32	0.35	0.32	0.32	0.38	0.35	-
30	0.30	0.32	0.30	0.32	0.32	0.29
25	0.24	0.22	0.23	0.26	0.28	0.23
20	0.19	0.28	0.24	0.16	0.15	0.13
15	0.17	0.17	0.21	0.15	0.18	0.15
10	0.12	0.12	0.12	0.12	0.12	0.11

VITA

Satyanarayana T. R. Rao was born in Talya, Mysore State, India and graduated with high honors from the Government High School, Chitradurga, India. He graduated with a first class Bachelor of Engineering (B.E.) degree in Mechanical Engineering from the Mysore University, India, in 1963. Then he studied at the Indian Institute of Science, Bangalore, India, where he obtained a high class Master of Engineering (M.E.) degree in Mechanical Engineering with specialization in Heat Power Engineering in 1965. His Master's thesis problem was, "The Determination of the Coefficients of Discharge in a Rectangular Duct with a Rotating Core." He has also been a graduate student, studying for his Ph.D. degree in Fuel Science, at The Pennsylvania State University from September 1966 to June 1970.

He worked as an Aeronautical Engineer in the Design, Development Department of Aero-Engines, Hindustan Aeronautics Ltd., India, from 1965 to 1966.

He is a member of The Combustion Institute and The American Society of Mechanical Engineers. His publications number six.